MASTER IN ENVIRONMENTAL MANAGEMENT OF MOUNTAIN AREAS

Title Thesis: Hydraulic characteristics of geomorphic units in two Alpine streams.

Student

Florian Lico

Supervisor of the Free University of Bozen-Bolzano
Assoc.-Prof. Dr. Francesco Comiti

Supervisor of the University of Innsbruck
Assoc.-Prof. DI Dr. Bernhard Gems

Co-Supervisor

Dr. Walter Gostner

Dr. Giulia Marchetti

Year Degree Conferred   2021/2022

Exam Date 05/10/2022

Acknowledgements

ABSTRACT

For this master thesis, there were studied two mountain rivers, namely Ova dal Fuorn located in the Swiss National Park, Canton Grisons, Switzerland, and the Rio Carlino a tributary of the Adige River located in South Tyrol, Italy. The core part of the thesis consists of the field measurements of the flow depth and velocity on a reach scale for different geomorphic units. The measurements are taken on different points along cross-sections and are at the same time georeferenced by means of GPS. There are also georeferenced points from the perimeter of the geomorphic units to facilitate their delineation after. The second part of the field survey comprises taking aerial images by means of drone and as a last step sediment analysis applying the line count method and extracting bank material to further analyze in the laboratory. Analysis is accomplished following a few steps. First, the data of the flow depth and velocity are digitized in Excel and calculations of the maximal, minimal, and mean value for both streams are performed. Second, utilizing the SfM algorithm and Agisoft Metashape software, orthophotos and DEM are created employing the aerial images as input data. Third, the geomorphic units, following the georeferenced points are mapped over the orthophoto in the form of polygons by means of GIS. Each unit is also characterized morphologically judging from the field survey and the photos taken in the field.

The major results show a high variability between the two streams, morphologically, sediment wise and hydraulically. The geomorphic units from the streams differ in type and occurrence, the sediment size is also different, and the flow depth and velocity show a high fluctuation. The highest fluctuations occur in the same type of unit of both streams, while it is of a lower scale when two units of the same stream are confronted.

Table of Contents

LIST OF FIGURES

LIST OF TABLES

ABBREVIATIONS

ADV. Acoustic Doppler Velocimeter

DEM. Digital Elevation Model

GPS. Global Positioning System.

RTK. Real-time Kinematic

SfM. Structure From Motion

CHAPTER 1   INTRODUCTION

1.1 Managing rivers: challenges and opportunities

Rivers are complex systems characterized by myriad interplays between hydraulics, geomorphology, sediment, and wood. Each of them influences and is influenced by the other through time and space and constantly changing. Rivers and riverine habitats are biodiversity hotspots (Allan et al.) that fulfill several essential ecological, economic, and social functions (Gostner et al. 2013) and create and maintain aquatic and riparian habitats.

Among these complex systems, the streams belonging to the alpine dominion represent the part that is still not fully understood or assessed. The harsh environment and terrain conditions to access the sites make their assessment a challenging subject. Our understanding of mechanics and spatial patterns in small watersheds is limited by our inability to obtain field measurements at relevant scales (Robinson et al. 2008).Understanding these streams' dynamics is crucial for the environment and safety. The dynamic component in hydrology, sedimentology, and, consequently, river morphology serves as a backbone for the entire river environment (Maddock 1999).

On a physical scale, fluvial disciplines are commonly gathered under the term hydromorphology, which captures the main contributory fields of hydrology and geomorphology, their interactions, and their arrangement and variability in space and time (Vaughan et al. 2009) and according to (Leopold et al. 1964) eight factors are forming the morphological traits of a river: channel width, depth, flow velocity, discharge, channel slope, the roughness of channel material, sediment load and sediment size.

Among all the investigations required to understand the alpine streams, there is a particular need to understand the variability of two primary eco-hydraulic descriptors, flow depth and velocity. Quantifying flow velocity is essential for engineering problems (determination of flood hydrograph, water levels, and sediment transport) and ecological assessment. (Comiti et al. 2007), and without reliable estimates of velocity and flow depth, the forces that mobilize sediments are difficult to obtain (Yager et al. 2007). Also, the understanding of their variability is the first step into the knowledge of aquatic habitat creation. Patterns of hydraulic variables, such as flow velocity or water depth, result from the interplay between hydrological and morphological conditions that create the physical habitat and, therefore, a direct response to the physical environment (Maddock 1999).

Although mountain channels provide crucial aquatic habitat (Nehlsen et al. 1991) (Frissell 1993) supply sediment to estuaries and oceans (Milliman and Syvitski 1992) and transmit land use disturbances from headwater areas down through drainage networks (Reid 1993), they have received relatively little study compared to lowland rivers (Montgomery and Buffington 1997). Only in the past decade, the number of studies focusing on hydraulics and morphology of the mountain streams has increased. Many such studies base their main approach on simplified laboratory flumes or modeling, which significantly simplifies the mountain channels' complexity and dynamicity.

Most of the European streams are highly exploited, engineering interventions have

altered their morphology, and water quality is also altered, primarily by wastewater disposal, and that is why this master thesis is a unique possibility that allows to work and collect data from two streams that are still untouched by large scale anthropogenic interventions.

Another essential aspect considered in pursuing this master project is the Flood Risk Directive (Directive 2007) of the European Union and the Water Framework Directive (Commission 2003). The first defines flood risk management plans to give rivers more space by considering the maintenance and restoration of flood plains. On the other hand, the Water Framework Directive urges member states to protect, enhance, and restore all surface water bodies to achieve good ecological status (European Commission, 2000). A proper understanding of these two directives implies that every engineering intervention should not only fulfill its first goal to protect but must also be designed with ecological improvement in mind (Gostner et al. 2013).

1.2 Research objective

In the context of what is stated above, the objective of this master project is the investigation of different geomorphic units from two alpine streams. This is done by measuring the flow depth and velocity in the field and analyzing their variability amongst the two streams. The approach used was to investigate both flow depth and velocity on the same unit for both streams (e.g., a riffle or a rapid on both the streams) and two units of the same type within one stream.

The geomorphic units were classified into one of the following types: cascade, rapid, riffle, step, glide, and pool. To define the units in the field, was used a combination of slope changes, sediment size and organization and flow characteristics visible on the water surface the as described in the units classification from (Rinaldi et al. 2016). The assigned type for each unit from the field survey is compared with photos taken in the field and the measured data of flow depth and velocity to assure the right assignment of type.

The two streams studied for this master's thesis project belong to the alpine environment, are pristine, and are in their reference state. One of the streams is Rio Carlino (Karlinbach), a tributary of the Adige River that flows entirely in the Alto Adige territory. The other stream is Ova dal Fuorn which flows within the Swiss National Park in Canton Grisons, Switzerland. They both flow at around 2000 m.a.s.l.

The other novelty of this master thesis is the possibility of collecting data from the Ova dal Fuorn, from the Swiss National Park. The Park is one if not the most protected and oldest of the Old Continent. It was established as a national park in 1914, and there has been no anthropogenic intervention on a small or large scale for more than 100 years. Therefore, the data collected from Ova dal Fuorn could constitute a unique database that can be enriched over time to understand the resilience of the geomorphic units in the face of climate change events. This is, though, a path that my thesis does not pursue.

1.3 Aim of the thesis

This master thesis aims to investigate the variability of the hydraulic components, namely flow depth and flow velocity within the same unit form both reach and from the same reach, and the influence of channel morphology and planform over said variability. It also tries to investigate and analyze the sediment nature and possible connections to the eco-hydraulics variability. The main research questions are the following:

x.   How do flow depth and velocity change from the same geomorphic unit on both streams?

xi.   Are flow depth and velocity variability influenced by channel morphology and geomorphic units' nature?

xii.   Does the size and nature of sediment also influence the variability of eco-hydraulic descriptors?

CHAPTER 2: MORPHOLOGY OF THE MOUNTAIN RIVERS: STATE OF THE ART

2.1 Characteristics of Mountain rivers

A mountain river, as the name implies and as described by (Wohl 2010) is a river that is located within a mountainous region. Mountain streams have also been defined using physical characteristics such as average gradient (Jarrett 1992) or some combination of slope, confinement, and substrate (Wohl and Merritt 2005).

These rivers are typically characterized by a steep longitudinal profile (Chin and Wohl 2005) (Comiti et al. 2009) and channel slopes larger than 3-5% (Comiti and Mao 2012)

Figure 1. Typical Mountain River morphology (Rio di Pinalto, looking upstream. April 2022)

The channel bed is composed of coarse mobile sediments (Figure 1), generally found in the pools or scouring holes downstream of steps, and by large, relatively immobile

boulders (Rickenmann 1991; Papanicolaou et al. 2004; Yager et al. 2007) can ar-range in steps spanning through the whole channel width (step-pool morphology) or in a more irregular manner (cascade morphology) (Montgomery and Buffington 1997).They exhibit great variability in the hydrologic regime, channel planform, channel gradient, grain size, and bedform (Wohl 2010).

Some other characteristics of mountain rivers from (Wohl 2010) include:

- High turbulent flow with numerous longitudinal transitions
- A limited supply of sediment of fine gravel and smaller size
- Bedload movement that is highly variable in space and time
- Substantial spatial variability in discharge
- Strongly seasonal discharge regime

The hydrologic regime of a mountain river predominantly reflects climate as ex-pressed directly through precipitation and indirectly through the influence of weath-ering, soils, and vegetation on runoff and infiltration. They are subdivided at the first level into those dominated by glacier melt, snowmelt runoff, or by rainfall runoff. Their hydraulics is also complex, and Wohl (Wohl 2010) best described them as stochastics. Much of the recent work done to quantify the hydraulics of mountain rivers goes in the direction of prediction of flow resistance coefficient concerning gradients, relative submergence, flow depth, and particle size distribution. In addi-tion, to quantify the contribution of the roughness components to the total flow resistance and characterize cross-stream and vertical velocity distributions and forces of lift and shear stress exerted on the channel boundaries.

2.1.1 Sediment transport in mountain rivers

Compared to their lowland counterparts, sediment transport in rivers and steep channels of the alpine dominion is more complex. It depends on many parameters and conditions, e.g., reduced sediment supply and transport capacity due to high losses in irregular channels (Rickenmann and McArdell 2007). Furthermore, sedi-ment supply is a function of the bed material (e.g., armouring, supply from upstream or lateral bank collapse.

The main form of transport is the bedload transport. It is a form of transportation in which the sediment load moves just above the bed with irregular collision rather than by the flow turbulence. It includes saltation (small jumps), rolling, and sliding on the bed. Bedload has the size of gravel up to cobbles and exerts an essential role

in shaping the morphology. Sediment can also move in the form of suspended loads and dissolved loads. The former belongs to the size of clay and silt, which is so light that it floats and may never touch the riverbed. The dissolved load is mainly ions that are dissolved in water. Even though bedload transport is a crucial process in the mountain river's evolution, it is still poorly understood and presents a large scale of unpredictability. For example, most bedload prediction equations overestimate bed-load rates to several orders of magnitude.

Four main approaches are widely used to estimate the bedload transport based on shear stress (Recking et al. 2008), stream discharge (Rickenmann 1991)(Schoklitsch 1962), stream power, and stochastic functions for sediment movement (Einstein 1950) .The ability to predict and quantify the bedload transport is crucial in hydraulic engineering (Chanson 2004) as one of the tools that enable us to protect lives and settlements and mitigate the threat of sediment movement.

2.2 Functional multiscale hierarchies

Rivers are complex systems where abiotic and biotic components interact at different spatial and temporal scales (Belletti et al. 2017). Rivers can thus be viewed as a set of hierarchically organized subsystems, where the more minor spatial and temporal levels nest within those at larger spatial and temporal scales see, e.g (Frissell et al. 1986; Amoros and Petts 1993; Rinaldi et al. 2013; Gurnell et al. 2016).

If we were to look from above and going down, where "above" constitute the whole river system and "down "all the subsystems that make it up to the most miniature temporal and spatial scale, the idea is that of a pyramid. The processes and forms at larger scales dominate those of more minor scales, and the dominion moves down to the smallest or the unbreakable pieces of the mosaic. These scales are often thought of as dimensionless and proportional to channel width (W), with common names such as catchment (10^3-10^4 W), reach (10^2-10^3 W), morphological (channel or geomorphic unit) (10^0-10^1 W) (Wyrick et al. 2014).

This is a concept that has been explained and looked upon in many different studies. Because river hydromorphology has been incorporated into the European Water Framework Directive 2000/60 (Commission 2003), river physical forms and pro-cesses have been increasingly highlighted as essential components in the analysis and management of river systems. Several methods, protocols, and procedures have been used to describe, characterize, and classify physical habitats in river channels

since the 80s (Belletti et al. 2017). Each of them has used a different approach and different taxonomy. Following the hierarchical concept presented above, several reaches can be contained in a river segment, and several segments make up a land-scape. If the concept is presented in a pyramidal organizational hierarchy, moving towards the top the larger become the scale representative units. At the very bottom stand the smallest pieces of the whole system.

This concept is essential because it gives a concrete understanding of where and when the field survey takes place. River habitat is structured at many scales (Frissell et al. 1986). Still, it is at the reach scale where the river reality is easier to grasp and where most of the ecological and hydraulic phenomena occur.

The approach described by (Belletti et al. 2017) on the multiscale hierarchy (Figure 2) fits perfectly with the purpose of my thesis. It represents both conceptually and visually the key steps that lead to the "where" of my study project.
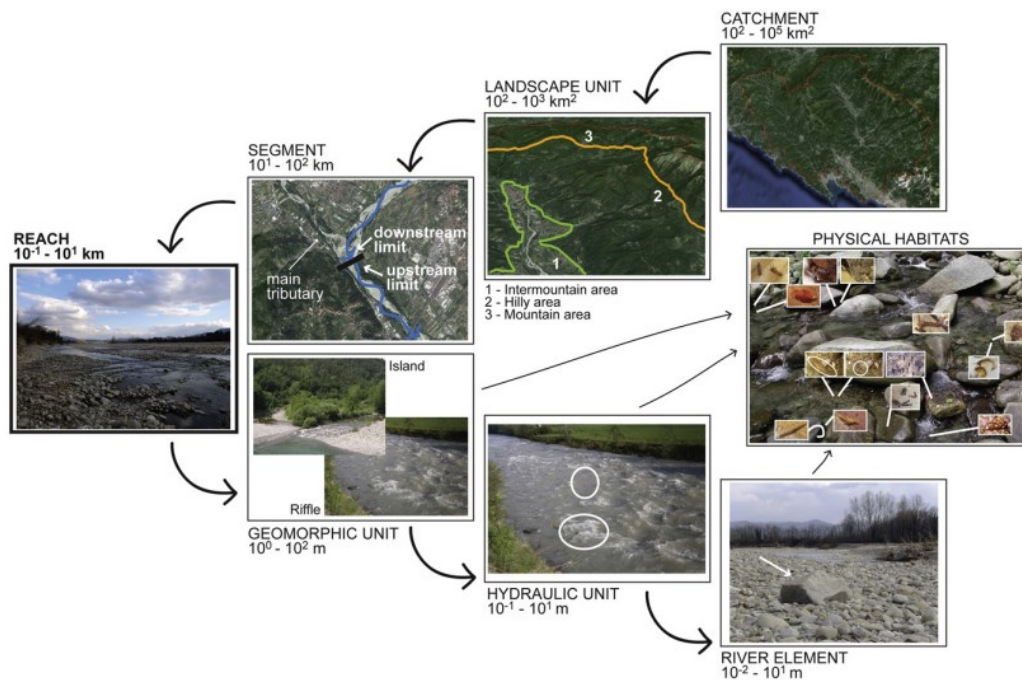
Figure 2. Spatial units and physical habitats within the nested hierarchical framework. From (Belleti et al., 2017)

2.3 Reach scale and geomorphic units

2.3.1 The reach scale

A reach in a channel can be defined and classified based on different aspects. The first is the channel morphology (channel pattern, e.g., sinuous, meandering, braided) and the confinement rate (confined, semi-confined, not confined). Regarding channel morphology a river can be classified based on their planform into single-thread (only one channel present) ,wandering (a transitional planform between single thread and multi-thread), multi-thread (presence of secondary channels (Rinaldi et al. 2012) (Figure 4) and regarding its lateral confinement (Figure 3) can be totally confined, semi-confined or unconfined (Fryirs and Brierley 2005). The second important aspect is the type of sediment that constitutes the channel bed. According to (Rinaldi et al. 2016), the following table (Table 1) explains better the spatial and temporal scale, the description and delineation criteria.
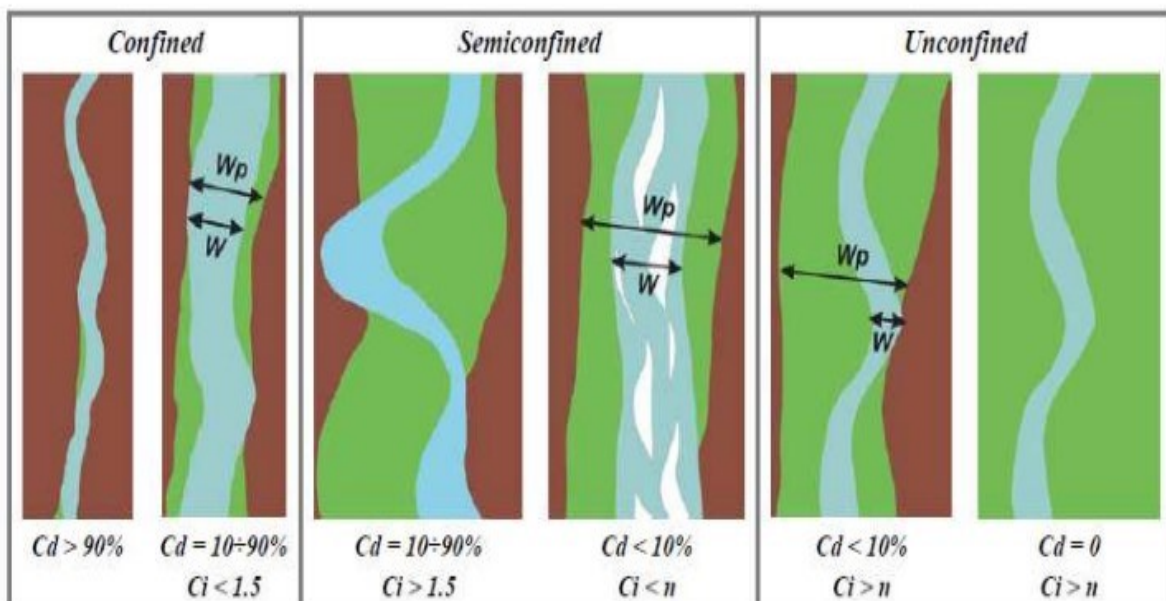
Figure 3. Confinement classes. In brown the hillslope and in green the alluvial plain. Cd the confinement degree and C**i**; the confinement index *Wp/W* where *Wp* alluvial plain width and *W* the channel width
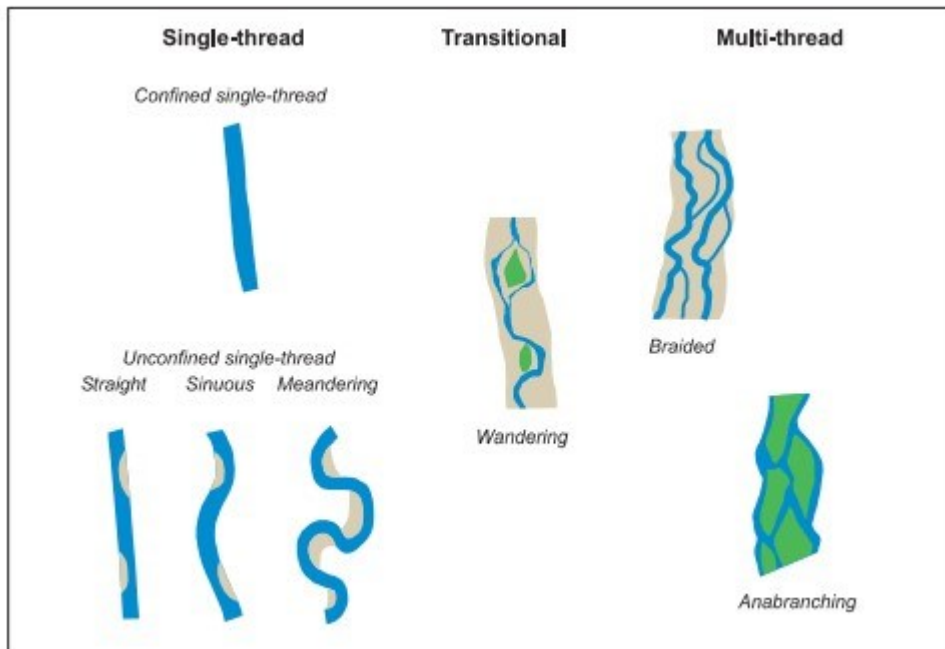
Figure 4 Typologies of river planform.

Table 1 Temporal and spatial scales of a reach from (Rinaldi et al.2016)

Unit	Spatial and temporal indicative scales	Description	Delineation criterions
Reach	10^{-1} - 10^1 (>20 times the channel width) 10^1 - 10^2 years	A portion of the channel that is characterized by guiding variables and uniform flow conditions	Channel morphology (planform and confinement) Other discontinuities such as discharge variations (tributaries), slope, clasts dimension, floodplain characteristics, artificial alterations of the longitudinal continuity

2.3.2 The geomorphic units

The geomorphic units are at the core of a river assessment and are the tiles upon which the whole system is built. A geomorphic unit is the most representative of river characteristics and is the key to understanding forms and processes. The analysis of geomorphic units provides a universal resource for undertaking systematic geomorphic research of river systems. (Brierley et al. 2021).

They have attracted river hydro-morphologists and managers because understanding them, their behavior, and the taxonomy is essential in understanding river complexity. As a result, several terms have been used to describe units of river morphology. They have been called habitat, morphological, and geomorphic units, among others. Since, for this master's thesis, my work was concentrated on the units with water presence and in-channel, the most inclusive terminology is the geomorphic unit.

Geomorphic units are the building blocks of river systems (Fryirs and Brierley 2012) (Wheaton et al. 2015)(Fryirs and Brierley 2005).

Morphological units are organized into different levels, which in turn are placed within a multiscale hierarchical methodological framework. These levels differ in terms of spatial scale (size) and degree of detail of characterization: larger spatial scales are associated with more general classes of analysis. In comparison, more minor spatial scales imply greater detail analysis levels (Rinaldi et al. 2016).

Table 2 temporal and spatial scales of a geomorphic unit (SUM)

Unit	Spatial and temporal indicative scales	Description	Delineation criterions
Geomorphic Unit	$10^0 - 10^2$ m (0.1-20 times the width of the channel)	Fluvial form created by erosion or sediment deposition, often in associa-	Morphological units in the riverbed and the floodplain are identifiable based on morphological, sedimentary, and

	$10^0 - 10^1$ years	tion with vegeta-tion	distinctive vegeta-tion.

Geomorphic units are the elementary spatial, physical features of the river mosaic at the reach scale that are nested within the overall hydro-morphological structure of a river and its catchment. (Belletti et al. 2017)

2.4 Classification of geomorphic units

A geomorphic unit is an area containing a landform created by erosion and deposition inside (in-channel or bankfull geomorphic unit) or outside (floodplain geomorphic unit) the river channel. Fluvial landforms are the building blocks of a river and are variously referred to as geomorphic units, morphological units, habitat units, and channel units. (Wheaton et al. 2015)

No single classification can satisfy all possible purposes or encompass all possible channel types; each channel classification in everyday use has advantages and dis-advantages for use in geological, engineering, and ecological applications (Montgomery and Buffington 1997).

The geomorphic units studied for this master thesis belong to the in-channel ones. These units are connected to the channel bed morphology closely. It influences their nature, sediment dimensions, and the type and is the base for the unit's nomencla-ture. They are specified as "channel units." The spatial scale of such geomorphic units is in the same order of magnitude as the channel width.

Following the units' characteristics, such as slope, sediment size, nature, morphology, and flow, distinctive features are described, and simple sketches and pictures are shown to give a clear idea of the physical trait of the unit and how it is found in natural conditions. For this part the ISPRA manual (Rinaldi et al. 2016) is referenced.

> Cascade

This type of unit consists mainly of boulders and large cobbles. The sediment is not organized, is chaotically spread (Figure 5), and remains out of the water surface even for the bankfull stage. As a result, the averaged slope is relatively high: S>7%, and the streams are confined. The flow is highly turbulent, and air and hydraulic jumps act as the primary energy dissipator.

(a)   (b)
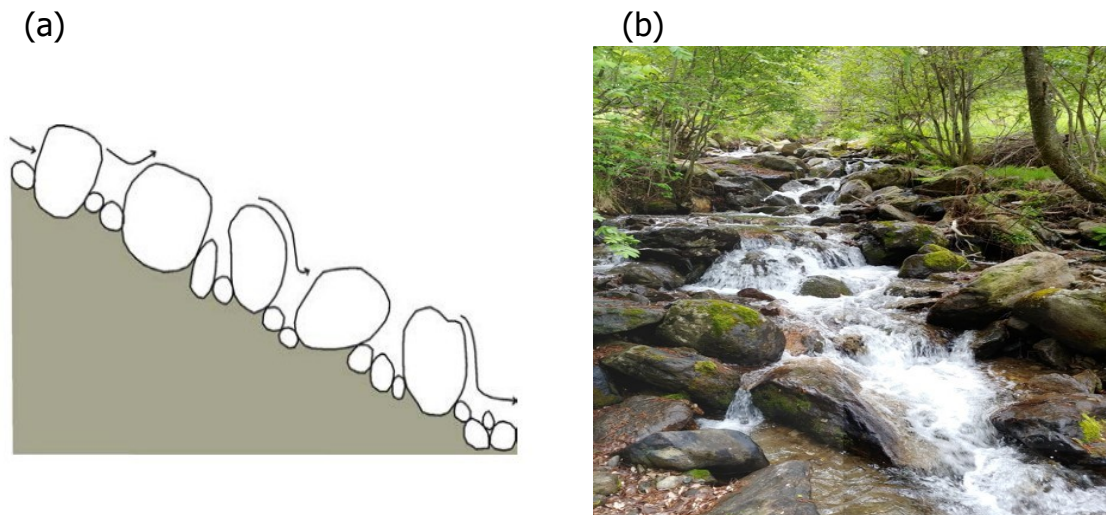
Figure 5. Channel unit: Cascade (a) modified sketch from Halwas and Church (2002) and (b) Photo from Rio di Pinalto, April 2022.

> Rapid

Units of alluvial channels are characterized chiefly by boulders and cobbles. Compared to the cascade, the sediment is more organized and sometimes will form lines that cover all the channel width, known as "transverse ribs" (Figure 6)
The flow is less turbulent than the cascade type, with occasional hydraulic jumps and broken standing waves.
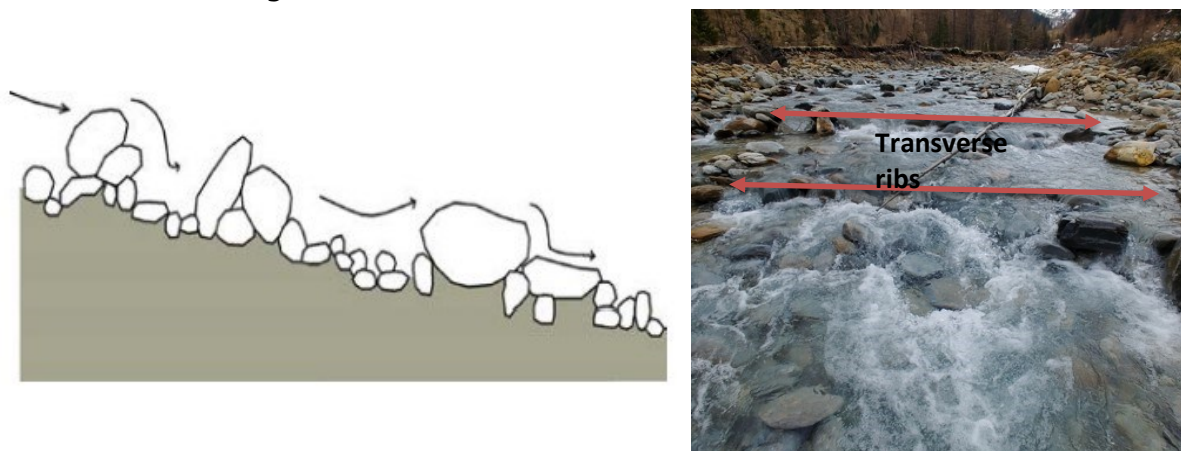
Figure 6. Channel unit: Rapid. First picture a modified sketch from Halwas and Church (2002) and second photo from Rio Carlino, May 2022.

➢ Riffle

Unit with a characteristic flow shallower and faster than the cascade and the rapid. Relatively small sediment is in the gravel range that rarely can be seen from the water surface. The flow is less turbulent and aired, when compared to the Cascade and Rapid. Unbroken standing waves and V-shaped (Figure 7) ripples pointing in the flow direction are present. Riffles are generally associated with the crest and back-slope of a transverse bar (Knighton 1999).

(a)   (b)
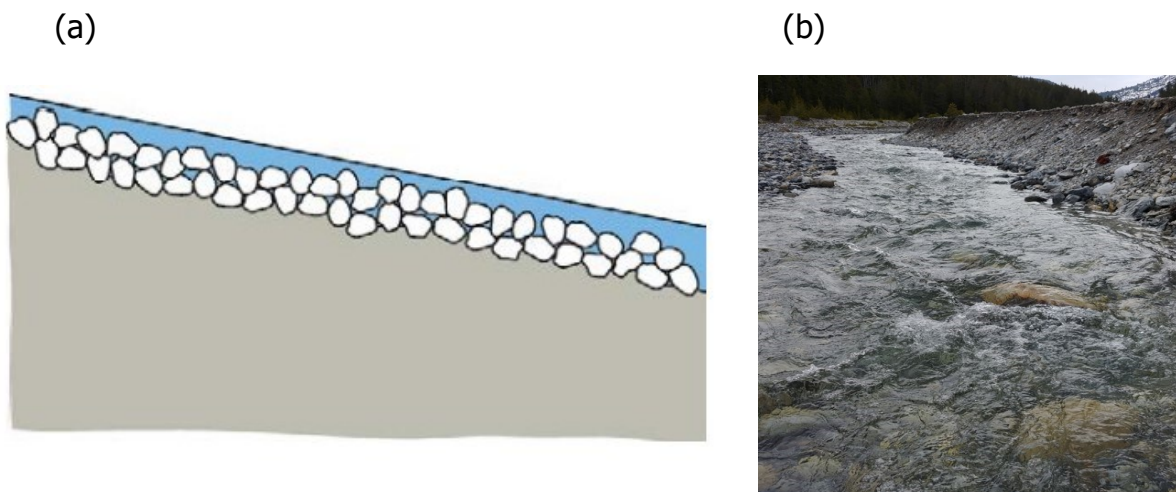
Figure 7. Channel unit: Riffle (a) modified sketch from Halwas and Church (2002) and Brierley and Fryirs (2005) and (b) Photo from Ova dal Fuorn, May 2022.

➢ Steps

These units are typical of streams with elevated slopes. Proper vertical steps (Figure 8) that occupy the whole channel width can be formed from a different material (rock, sediment, wood, or their combinations). Sometimes they are combined with pools (step-pool morphology), and the flow becomes an alternation of free jets and hydraulic jumps (the so-called *tumbling flow*), with flow resistance dominated by spill resistance. (Comiti and Mao 2012).

(a)   (b)
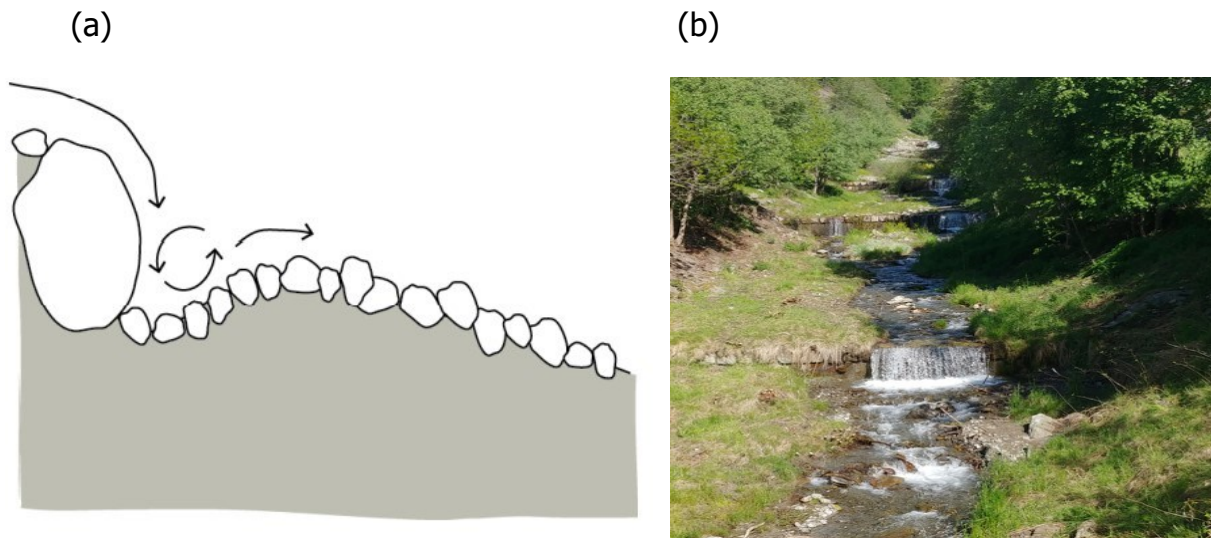
Figure 8. Channel unit: Step (a) modified sketch from Halwas and Church (2002) and Brierley and Fryirs (2005) and (b) Photo from Rio di Senales, April 2022

➢ Glide

It is a unit characterized by a channel bed and a free surface regular. The free surface is slightly rippled and almost parallel to the channel bed (Figure 9)
Visually, the flow presents very little turbulence, and there is almost no air presence. Glides are less inclined than rapids and riffles; their flow is more uniform, and there are no standing waves. Sometimes, they are named "runs" to address a glide of a limited length and between a step and a pool or a riffle and a pool.

(a)   (b)
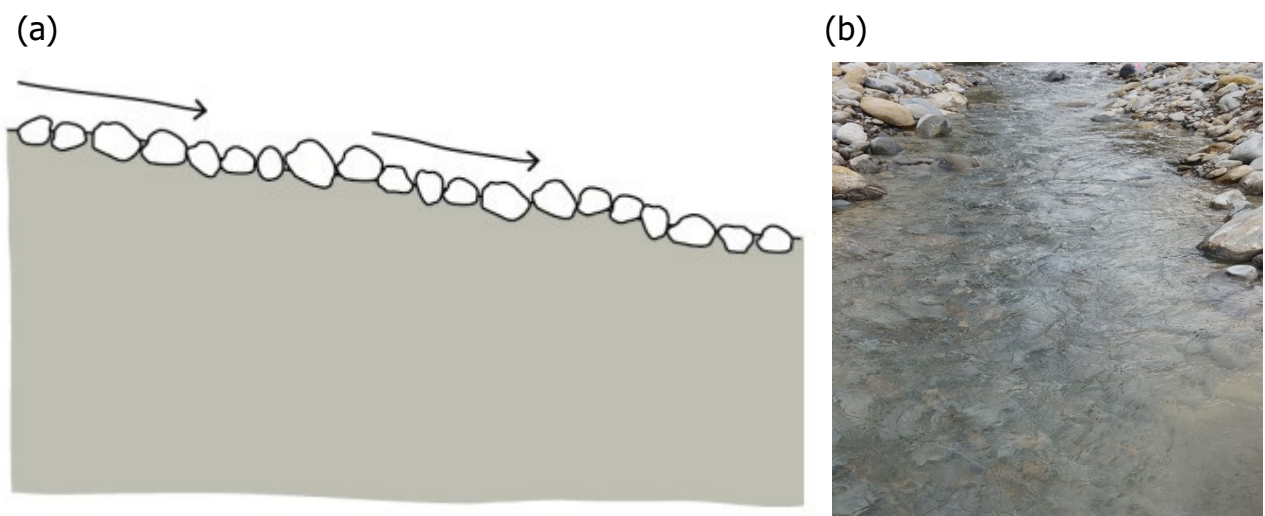
Figure 9. Channel unit: Glide (a) modified sketch from Halwas and Church (2002) and (b) Photo from Rio Carlino, May 2022.

➢ Pools

They are predominantly erosional units that occur as topographic depressions of the bottom of the riverbed with the reverse slope in the downstream portion and occupy the entire cross-section (Figure 10). Relatively high depths and low velocities characterize them. Their sediment appears to be finer when compared with other units. Pools often alternate with step or riffle in streams with a high gradient.

(a)
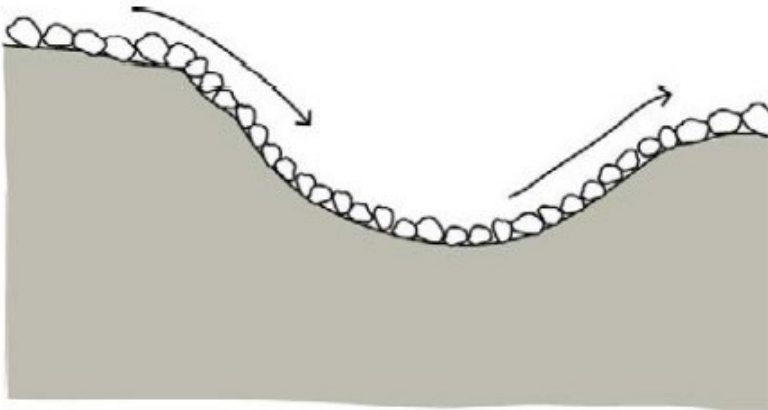
(b)

Figure 10. Channel Unit: Pool, (a) modified sketch from Knighton (1999) and (b) photo from Rio Bianco, June 2022, with the pool occupying the whole width of the channel (Patscheider&Partner Engineers)

CHAPTER 3 MATERIAL AND METHODS

3.1 STUDY SITES

3.1.1 Rio Carlino

The Rio Carlino (Karlinbach in German.) drains the Vallelunga (Langtaufers) with a total length of 17 km and a mean channel gradient of 6.2%. Its catchment covers 110 km^2 and lies between 3738 m (Palla Bianca) and 1498 m above sea level at the confluence with Lake Resia.

From a geological point of view, the catchment of the Rio Carlino consists mainly of mica schists and paragneiss. As can be deduced from the catchment high altitude, glaciers strongly influence Rio Carlino. On the valley floor, the grasslands are used for pastures.

Figure 11. Rio Carlino and the Vallelunga (Langtaufers) with the Palla Bianca in the back.   source: https://mapio.net/

Various tributaries of Rio Carlino are diverted for hydroelectric purposes, particularly Rio Rigolo. In addition, there are several villages along the Rio Carlino, Melago,

Caprone, Pedrossa, and Curon. The plant in Glorenza purifies its wastewater before being released into the river.

The climate has low rainfall and is typical of the inland Alps. However, the high mountain ranges in the upper Val Venosta (Vinschgau) retain a considerable part of the precipitation, which reaches an annual average of 600-670 mm. In Melago, the yearly is slightly higher, with an average of 750 mm. Most precipitation occurs in winter in the form of snow. The mean annual temperature is around 5° Celsius. The maximum during summer seldom goes beyond 30° Celsius; during winter, the minimum rarely goes lower than -20° Celsius (Source: *https://meteo.provincia.bz.it/*).

Rio Carlino has formed an alluvial plan of 10.7 hectares and after the interventions of the 80s of the last centuries, the upper part has undergone the realization of protection works on the external banks. In the lateral areas of the riverbed, rooms with low peat bogs have sometimes formed.

The vegetation is determined by the climatic characteristics of the inner Alps. Mountain spruce forests (*Picea abies*) cover the lower slopes and the central valley up to 1500-1600 m.a.s.l. After that, they are replaced by pure larch forests (*Larix decidua*), as in the Toloi forest near San Valentino. Finally, mixed forests of larch (*Larix decidua*) and stone pine (*Pinus cembra*) prevail on the shady Vallelunga. (*Source: Autonomous Province of Bozen/Bolzano, https://ambiente.provincia.bz.it/acqua/fiumi-torrenti-alto-adige*)

The study reach from Rio Carlino was selected based on two factors:
- To move as far as possible from the reaches that go through settlements but that were at the same time still accessible
- Ensure many geomorphic units were included within and along the reach.
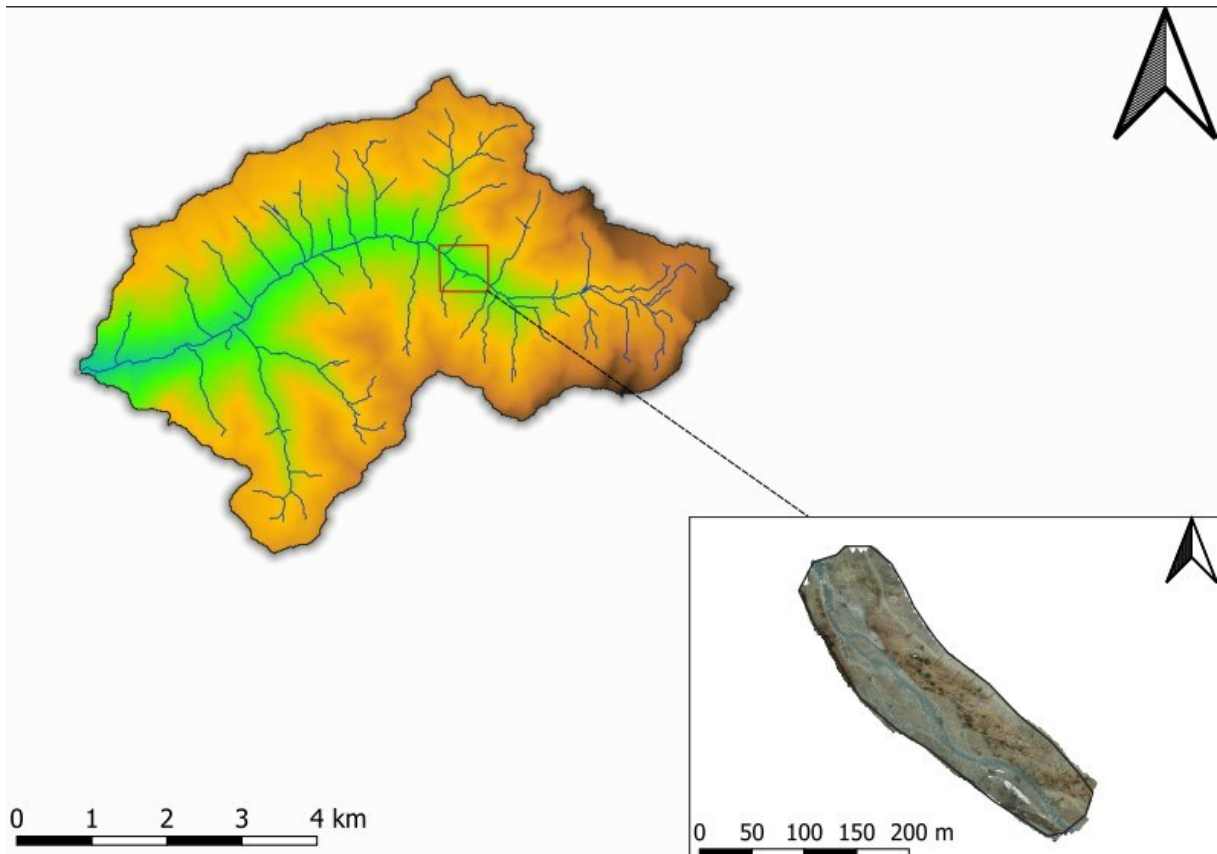
Figure 12. Map of of the study area from Rio Carlino (Karlinbach) with an overview of the reach of interest

3.1.2 Ova dal Fuorn

Ova dal Fuorn is a small almost natural stream with a total length of 14 km and a mean channel gradient of 3.4 %. Its catchment has an area of 55 km2 at the station of Zernez and is located in the south-eastern part of the canton of Grisons, close to the Italian border. This is a high-altitude mountainous catchment (from 1700 to 3200 m a.s.l.), with a regime strongly influenced by snow and also by intense convective events during summer (Paquet 2019).

The primary type of rock found within the catchment is dolomite (Haller et al. 2013), which provides the Ova dal Fuorn with much sediment because of its brittle structure (Rascher and Sass 2017).

The climate in the area – was measured at the nearest climate station Buffalora 5 km further upstream on 1968 m a.s.l. – is characterized by cold winters (mean tem-

perature in January -9.2°C) when most of the precipitation comes as snow and relatively wet summers (around 300 mm between June and August).

It is essential to mention that the Swiss National Park (SNP) is a Wilderness Area of category 1a according to IUCN, implying strict preservation of all natural processes. Therefore, landscape evolution has not been influenced by anthropogenic landscape design and protective geo-engineering structures.

Figure 13. Ova dal Fuorn looking downstream (Source: https://www.nationalpark.ch)

The vegetation is dominated by coniferous trees, mainly by mountain pine (*Pinus mugo*), the region's most common tree. Larch (*Larix decidua*) and Swiss stone pine (*Pinus cembra*) are often high up as the forest limit. On the shady slopes of the central Engadine valley can be found a mixed forest of larch and Norway spruce (*Picea abies*) but very rarely stands of spruce alone. (Source: https://www.national-park.ch/en/flora-and-fauna)

The same approach for the Rio Carlino was applied to pick the proper study reach from the Ova.The first critical issue was moving as far as possible from any anthropogenic engineering or landscape interventions, but the Swiss National Park had already thought about this. Combining an accessible location and presenting a certain degree of planform variability (meandering or braiding) became a critical task to overcome.The study reach is taken from a portion of the river that flows adjacent to the main road that leads to the nearest locality of Zernez. The reach is not far

from the SNP's dedicated parking location, making it easier to carry the instruments and 30 m down a mild slope, making it easy to reach the stream.
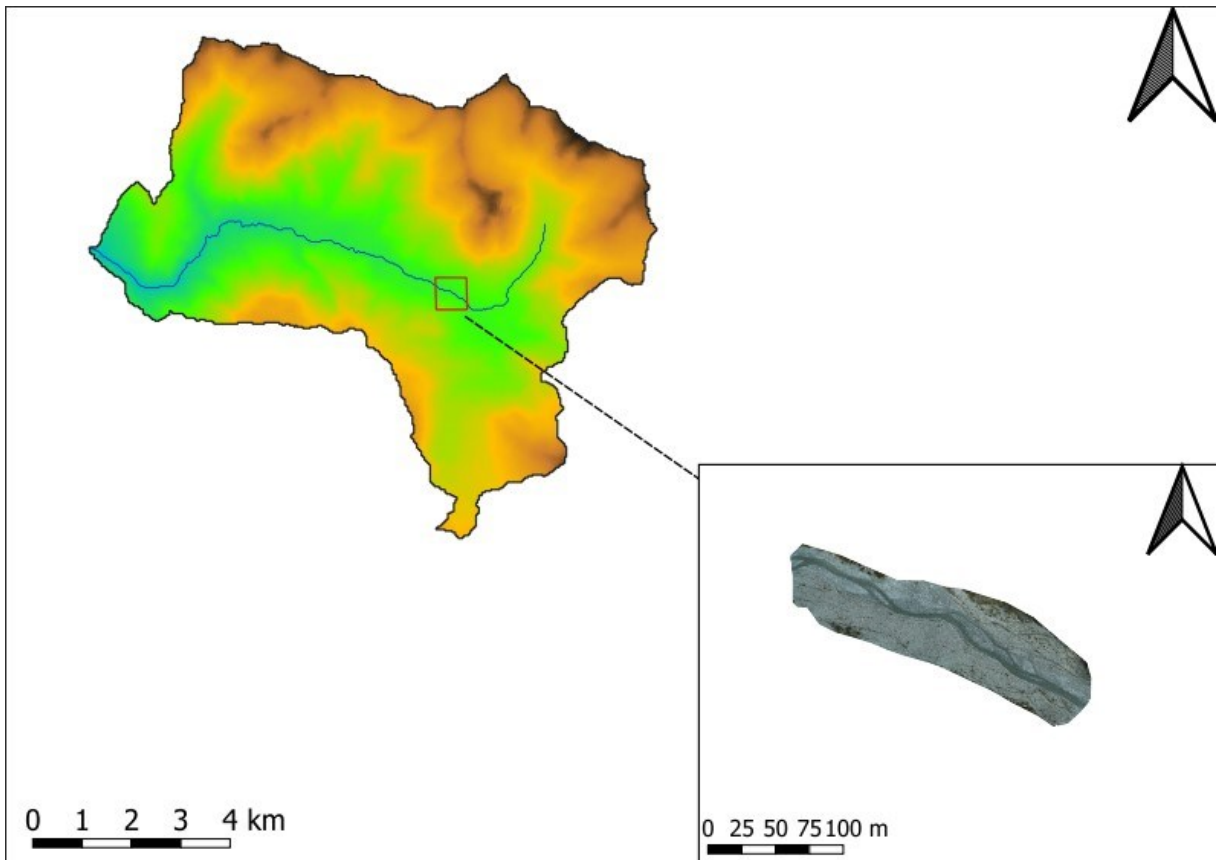
Figure 14. Map of the Ova dal Fuorn study area with an overview of the reach of interest

3.1.3 Reaches characterization

Reach 1 belongs to the Ova dal Fuorn river. Therefore, it has some different characteristics compared to the Rio Carlino reach. With an average slope of 3.4 %, it is less steep, and the channel is characterized by much finer sediment than Rio Carlino, mainly in the range of coarse gravel to small cobbles.
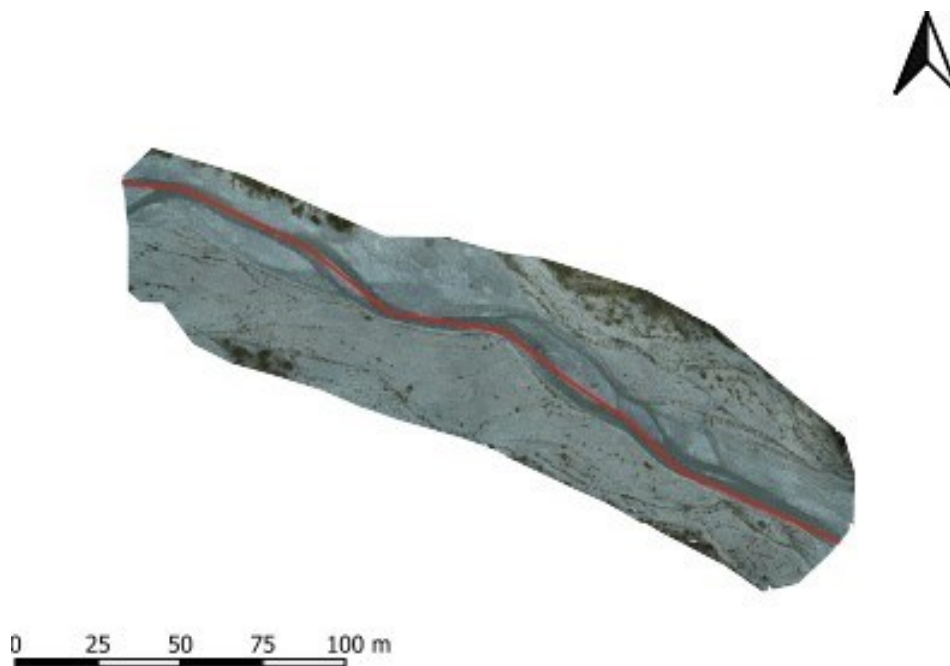
Figure 15. Longitudinal profile line in red from Ova dal Fuorn study reach

From Pos: 596586.721, 5167053.879   To Pos: 596371.004, 5167160.618
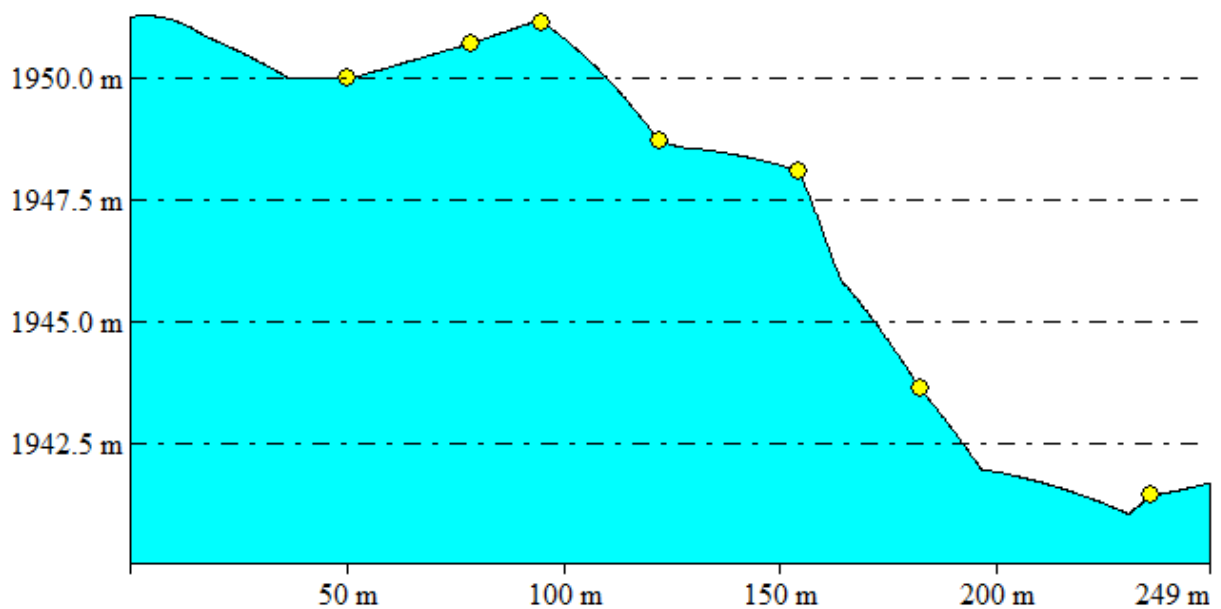
Figure 16 Longitudinal profile of the Ova dal Fuorn reach following the red line from figure 15. Extracted from Global mapper 13 software. DTM is created with the SfM algorithm from the aerial images

The dominating geomorphic unit is riffle with the presence of some glide units.

It has a wide floodplain and is confined on both orographic sides by hillslopes (Figure 17) that also provide much of the sediment found in the bed and banks. The left bank is much steeper than the right one, and the tree line reaches down to the bank. On the left side is also a temporary terrace that is probably inundated during bankfull stages.The morphology is braided with the presence of no more than one secondary channel.

Figure 17. Ova dal Fuorn floodplain and channel. Looking upstream, May 2022.

Reach 2 belongs to the Rio Carlino (Karlinbach) river (Figure 20). A 5.65 % average slope is steeper than Ova dal Fuorn, which is also reflected in the grain size of the bed material.

Figure 18.Longitudinal profile line in red from
the study reach of Rio Carlino

From Pos: 627413.250, 5187393.123   To Pos: 627173.391, 5187641.512
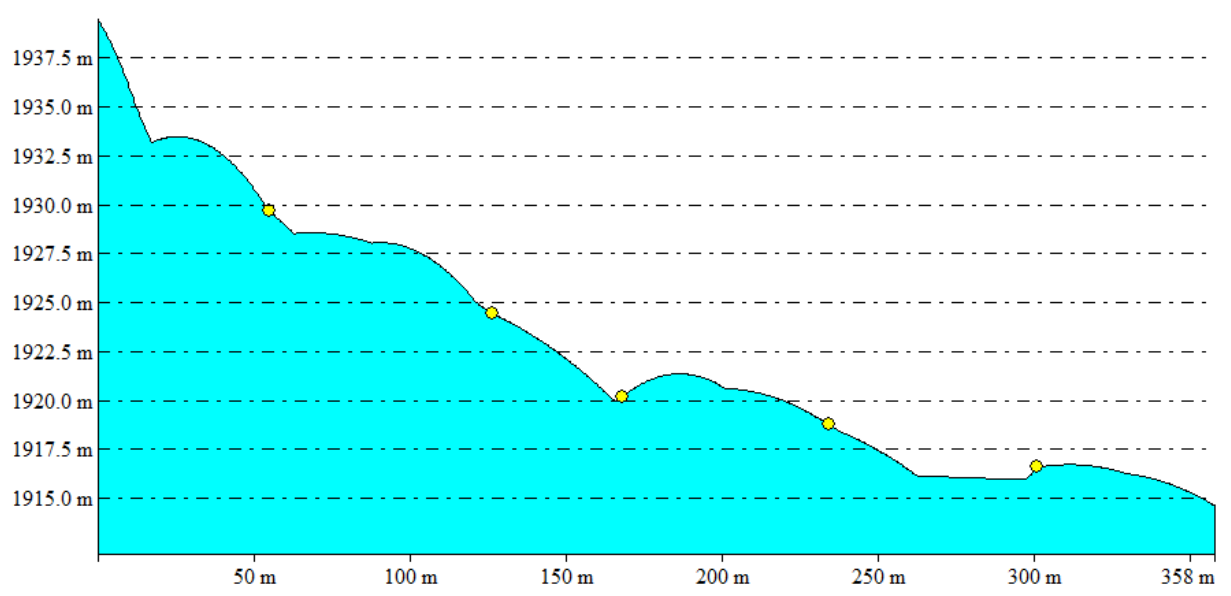
Figure 19. Longitudinal profile of the reach from Rio Carlino following the red line from Figure 18. Extracted from Global mapper 13 software. DTM is created with the SfM algorithm from the aerial images

The sediment size ranges from large cobbles to medium and sometimes medium to large boulders. The dominating geomorphic unit is rapid, with some presence of riffles and glides when moving downstream the reach.

The floodplain is also wide on both orographic sides and confined by steep hillslopes (Figure 20) with a heavy presence of larch (*Larix decidua*). The stream erosive capacity is more evident on the right bank, where a temporary terrace is formed along most of the reach length. The morphology is braided, with the presence of secondary channels.

Figure 20. Rio Carlino floodplain and channel. Looking Upstream, May 2022.

3.2 Field survey

The present research is based on field surveys and measurements of flow depth and velocity, as the core part of the study, carried out on two reaches 250-300 meters long.The measurements were carried out on the 5th and 6th of May. On the first day, the Ova dal Fuorn survey, and on the second day, the Rio Carlino. Besides, the measurements of flow depth and velocity were also performed on three drone flights at three different flight heights. Furthermore, line pebble counts (three for the Ova dal Fuorn and two for Rio Carlino) were conducted to cover the sediment analysis part. Samples of sediment were taken from the rivers' banks (3 for Ova dal Fuorn and 2 for Rio Carlino) to analyze in a laboratory for further volumetric analysis. The depth and velocity were measured along transects, on points spaced at 50 cm − 1 m between each other, depending on the width of the channel.

3.2.1 Flow Depth and Velocity

The flow depth and velocity measurements were taken using a Flow Tracker

Figure 21. ADV Flow Tracker main components (photo from the Flow Tracker manual)

Handheld ADV (Acoustic doppler velocimeter) commercialized by SonTek (Figure 21). The device is a handheld, portable, and precise measurement instrument. It uses the ADV technology and performs to high levels of accuracy, particularly in low flow. The data for the velocity was obtained in 2D, adjusting the wading rod to make

sure it was the value at the 60% of the depth of the total flow depth. The flow depth could be read on the wading rod, which is scaled. The handheld meter is attached to a wading rod, which measures the stream's depth and keeps the meter positioned correctly to the water current. The monitor faces the meter upstream while standing downstream of the meter and tagline.

All the components from Figure 21 are mounted on the wading rod (Figure 22), which makes using the Flow Tracker easier but also necessary for reading the value of the flow depth and making sure the value for the velocity is taken at 0.6 x Total
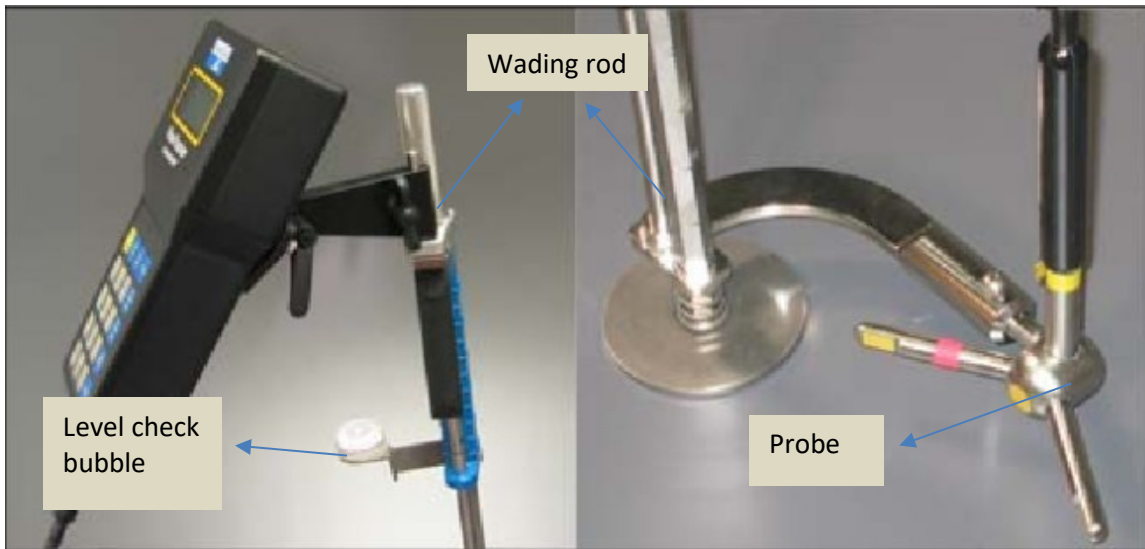
Figure 23. Flow Tracker mounted on the wading rod (Flow Tracker manual)
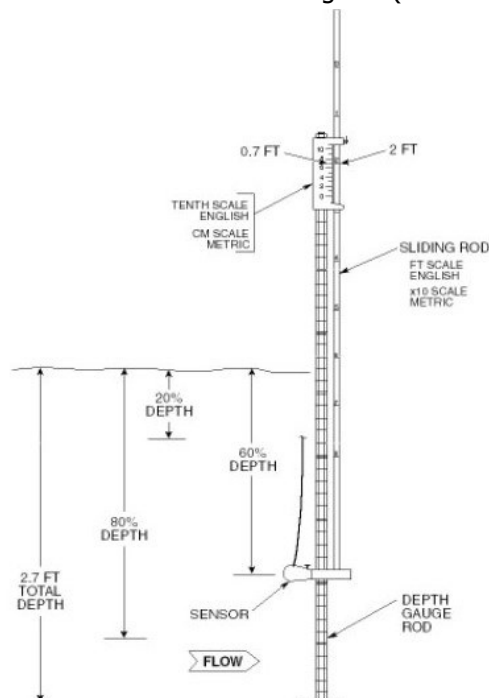
Figure 22. Different methods of velocity measuring linked to the total depth (Modified from Gravelle, 2015)

flow depth. The most commonly used techniques are: 1. the velocity distribution method; 2. the 0.6 depth method; 3. the two points method; and, 4. the three point method (Gravelle 2015).

Before starting, a quality control test must be performed before taking a flow measurement to ensure that the equipment is operating correctly. After establishing the cross-section, the ideal area would be laminar, smooth flow with minimal obstructions. Obstructions, including large rocks, can be moved out of the way of the cross-section, but only before flow measurements begin, never during the measurement. Ideal conditions for a stream flow measurement consist of uniform, straight stream reaches, stream bottoms made up of smaller substrate material with little or no aquatic vegetation or debris, little turbulence, no standing waves, and no eddies.

To measure with the Flow tracker, we entered in water in a team of two where one operated the Flow Tracker, and the second operator took note of the measured values of depth and velocity for each measurement. The operator taking notes was also responsible for georeferencing the point with the GPS and for taking several points around the unit itself, which will be used to create the unit's polygon over the Orthophoto. As a first step, the probe is pushed down until it touches the riverbed. Then, after the depth is read on the wading road, the probe is moved up at the same height by releasing the handle.The bubble is checked all the time, the probe is leveled as best as possible, and the colored markers on the probe are pointed perpendicular to the flow. The operator stands behind the device (downstream) to avoid noise and disturbance on the probe and cable. The Flow Tracker has different methods for measuring the velocity. The one used for this thesis measurement is Method 0.6. The measurement location at 0.6 * depth and the mean velocity equation is:

$$V_{mean} = V_{0.6} \qquad\qquad (1)$$

Figure 24. Measuring from Rio Carlino (Flow from right to left) operator stands downstream (facing upstream) of the Flow Tracker, May,2022. Underwater photo from the Flow Tracker manual (flow direction enters the screen)

The Total station used to locate the measuring points along the transects, around the perimeter of the geomorphic unit to facilitate the mapping and for geo referencing the GCP for the aerial photos was a Topcon HiPer VR and Topcon HiPer Probase and Rover, provided by Patscheider&Partner.

All the data were digitized and put into tables for each unit which are shown in Appendix 1 and is accompanied by a detailed description and a representative photo of the unit. (Note: the slope is measured with the Global mapper 13 software, and where

the Flow Tracker could not give a value in the corresponding field is written n.m. - non-measurable)

3.2.2 Aerial photography and orthophoto generation

To correctly map the units over the reach of the river, it became necessary to have a DEM and the most recent Orthomosaic (A mosaic of orthophotos) from the study reach, and the best way to obtain them was to use the algorithm known as SfM (Structure from Motion). What the algorithm does is: aims to simultaneously reconstruct the unknown 3D scene structure and camera positions and orientations from a set of feature correspondences (Snavely et al. 2008). In geosciences, SfM photogrammetry is a workflow that is virtually independent of spatial scale (Carrivick et al. 2016), and can provide point-cloud data comparable in density and accuracy to those generated by terrestrial and airborne laser scanning at a fraction of the cost (Westoby et al. 2012).

The algorithm can be executed using different software. Still, with the advice and insights from Dr.Giulia Marcheti, I decided that Agisoft Metashape Pro was the right one (they offered a month of a free trial, which was more than enough to finish the work). SfM algorithm (Structure from motion) allows the reconstruction of form, dimension, and geometry using as input the pictures taken form a camera that moves to different points.
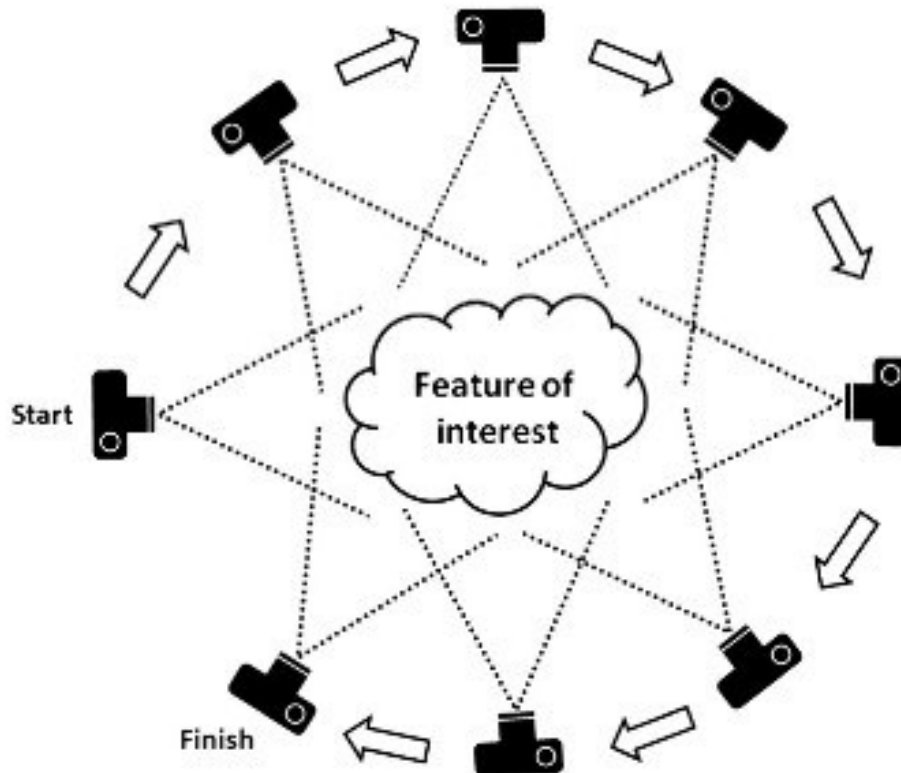
Figure 25. Structure from Motion algorithm visual description (Picture modified from Westoby et al. 2012). Instead of a single stereo pair, the SfM technique requires multiple, overlapping photographs.

For the correct input for the algorithm (aerial photos), the drone needed to have the RTK technology. The one we used was provided by Patscheider&Partner and is DJI Phantom 4 RTK (Figure 26). RTK (Real-time kinematic) is a technique that uses carrier-based ranging and provides ranges (and therefore positions) that are orders of magnitude more precise than the taken without. The aerial images were taken for three flight altitudes: 7-8 m altitude, 25 m, and 50 m of flight heights. In addition, GPS, and ground control points (GCP) were also taken along both reaches. For the 25 m and 50 m flight heights, the drone, after receiving the coordinates (limits of the area to cover), did all in an automated process, moving in a zig-zag pattern and taking a picture every 2 seconds in JPEG format.

The drone that was used for the aerial surveys was a Phantom 4 RTK with the following characteristics:

- Camera 1" CMOS sensor; Effective pixels: 20 M

- Optics Field of view (FOV) 84°; 8.8mm/24mm (35mm format equivalent) f/2.8 - f/11 autofocus 1 m - ∞
- ISO range
- Video:
  100 - 3200 (automatic)
  100 - 6400 (manual)
- Photo:
  100 - 3200 (automatic)
  100 - 12800 (manual)
- Mechanical shutter speed 8 - 1/2000 s
- Electronic shutter speed 8 - 1/8000 s
- Maximum image size 4864×3648 (4:3)
  5472×3648 (3:2)
- Video recording mode H.264, 4K: 3840×2160 30p
- JPEG photo format
- MOV video format
- Supported file systems FAT32 (≤ 32 GB);
- exFAT（> 32 GB）
- Supported microSD SD cards, maximum capacity: 128 GB class 10 or UHS-1 rated required
- Write speed ≥15 MB/
- Operating temperature range from 0 to 40 °C
  Source: (https://www.dji.com/it/phantom-4-rtk/info)

Figure 26. Dji Phantom 4 RTK drone

After acquiring all the photos, the elaboration was done with the aid of the Agisoft Metashape professional software. The workload was divided into several steps that lead to the final generation of the DEM and the Orthomosaic.

The first step was uploading the photos(Figure 27) into the software, and immediately after, Photoscan already had information about the location of the cameras from the field survey. This information is extracted from the EXIF metadata associated with the photos, initially saved by the GPS mounted on the drone (with accuracy on the order of tens of meters).
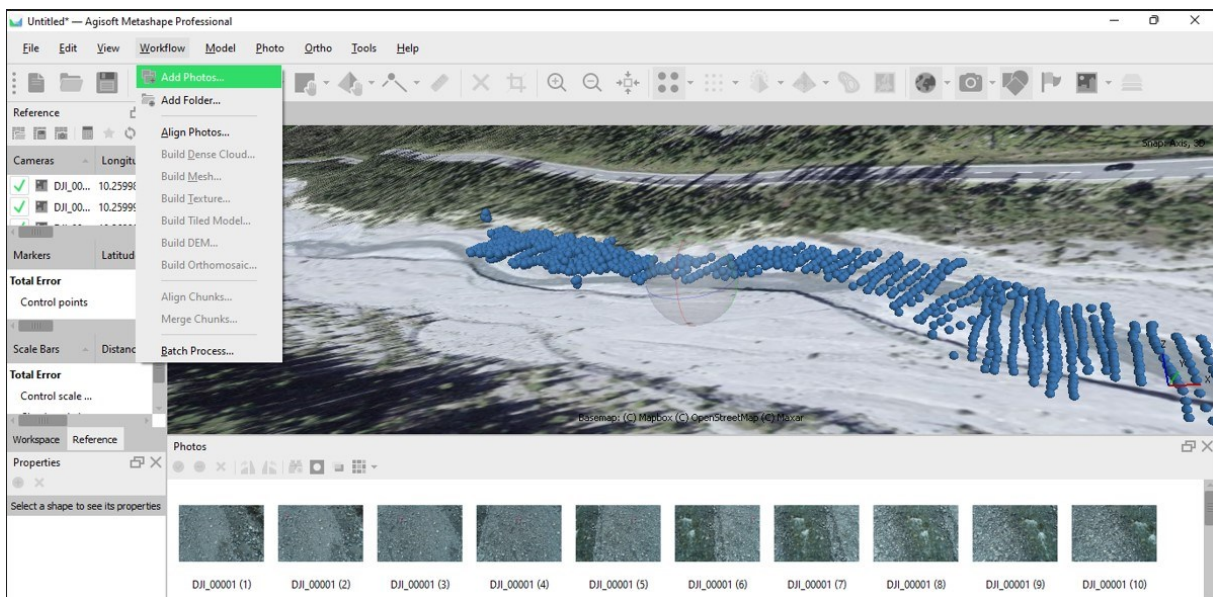
Figure 27 Interface of the Agisoft software. Photos added, and all the drone positions over Ova dal Fuorn are represented by blue dots. The dots show the exact position of the camera when the image was taken.

All the photos from the three flights were added, to guarantee the best quality for the DEM and the Orthomosaic. An essential part of the checkup was to be sure that the Reference System was set to the one used by the drone's GPS (WGS84) and all the unnecessary photos that might ruin the quality of the DEM and the Orthomosaic are removed (images where people are present, or photos took when the drone was changing the flight height).

The next step was the alignment of the photos. In this step, the software

Figure 28. GCP example from the Rio Carlino and clearly visible from the photos, May 2022.

reconstructed the position that the cameras had at the time of 'taking (then defines the angles of rotation and the coordinates of the grip center and the scale factor), starting from homologous points in consecutive photogrammetry's (collimation ofsome points of the stereoscopic model).

After the alignment, the GCP (ground control points) were included in the model to optimize the quality up to the range of centimeters. We had 6 GCP taken with GPS for each of the reaches, which were boulders marked (Figure 29) with an X sign visible from the photos. Therefore, optimizing the alignment after the inclusion of the GCP is good practice. In this step, the software used all the available info (GPS point coordinates and camera parameters) and minimizes the distance between the measured and projected points in the 3D model. In addition, it adjusts the camera parameters (focal length, lens distortion), thus correcting the distortion of the values caused by the camera lenses.

The following step was the construction of the dense cloud (Figure 30). The software projects new points, generating a dense cloud of points from the survey geometry and the position of the cameras that have been estimated with high accuracy. It then calculates different x, y, and z points, assigning color values.

This step utilizes the computer's processor in total and might last for several hours.
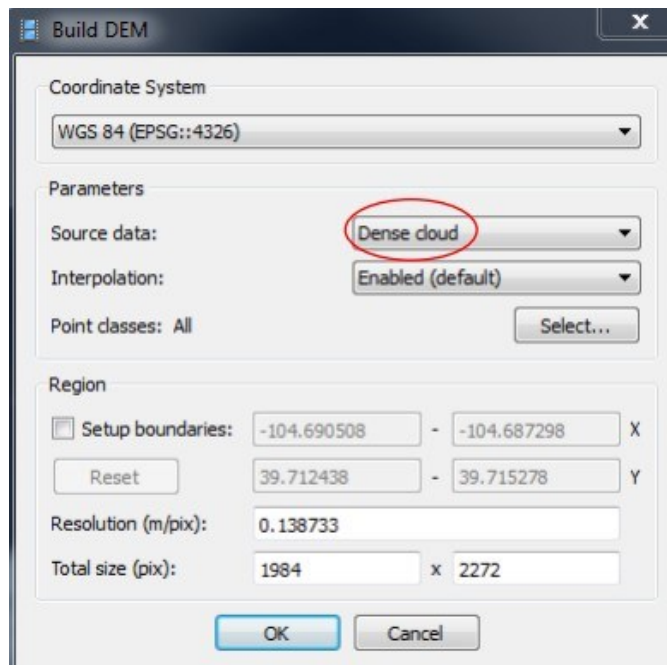
Figure 29. Interface of the command build DEM from Photoscan

After building the dense cloud, a digital elevation model can be generated from the model into a desired coordinate system and projection. To construct the DEM, the source data must always be the dense cloud.

After the DEM construction, the orthomosaic could be built, taking as a source the DEM. After completion, the DEM and the Orthomosaic (Figure 31 and 32) could be exported in the desired format.
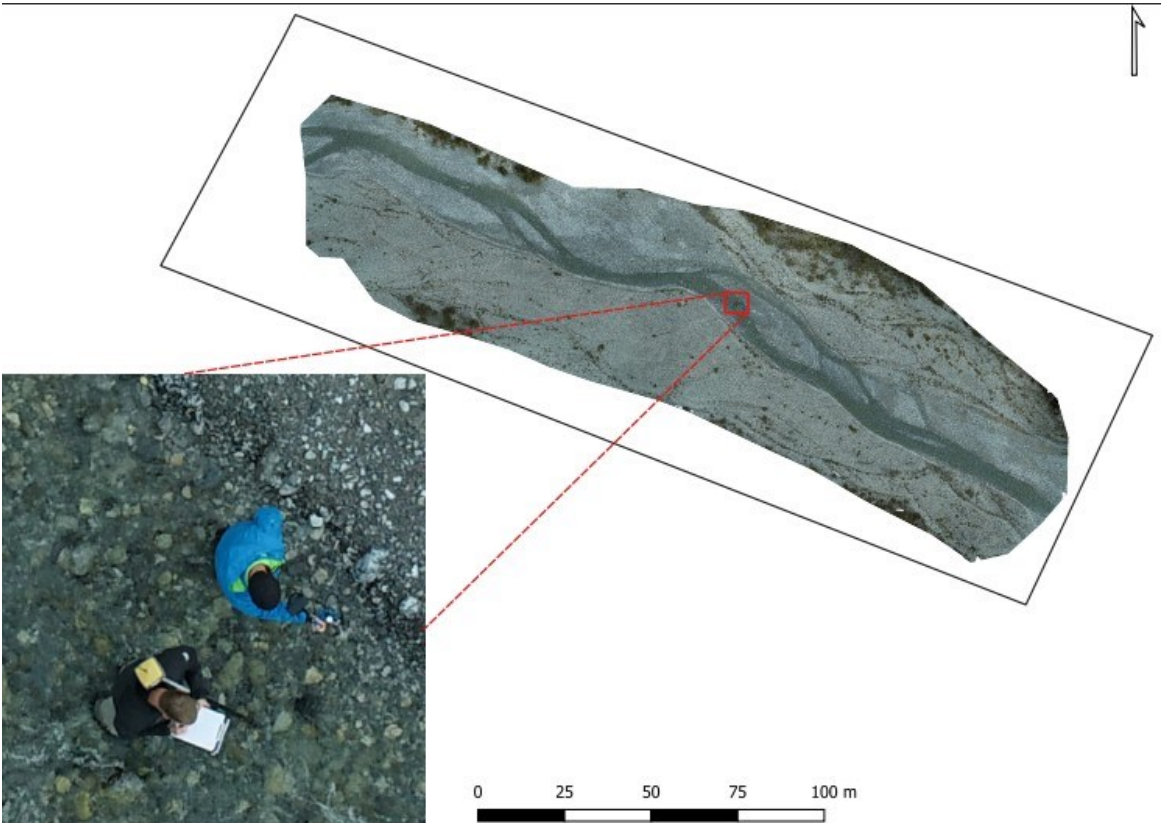
Figure 30. Orthomosaics generated with the Agisoft metashape from the aerial images for the Ova dal Fuorn
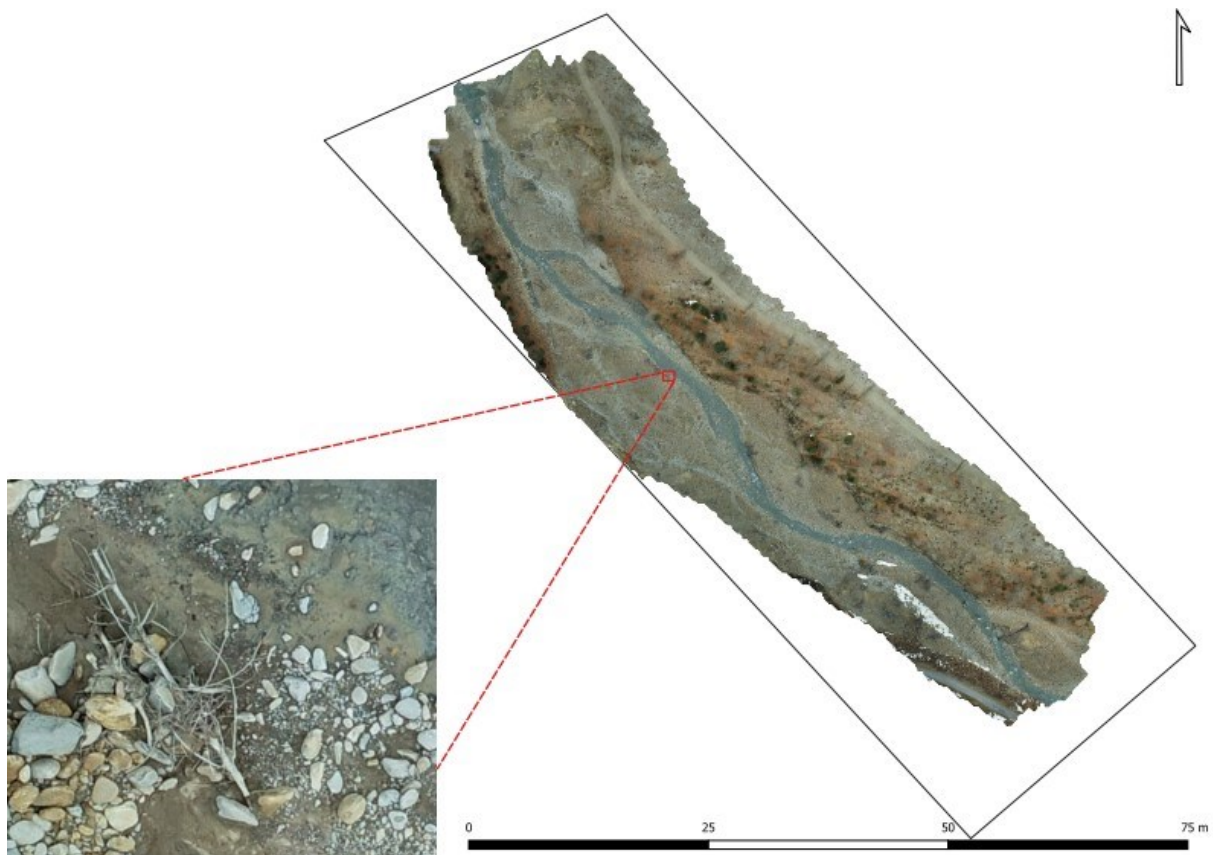
Figure 31 Orthomosaics generated with the Agisoft metashape from the aerial images for the Rio Carlino

3.2.2 Geomorphic units mapping and characterization

After the creation of the Orthophoto, the next step was the mapping the geomorphic units with the aid of GIS (QGIS). From a GIS perspective, the most typical data representation of a geomorphic unit would be in the form of a polygon (Wheaton et al. 2015). At first, all the GPS points downloaded from the device were layered above the Orthophoto. Since every measuring point along the transect was georeferenced, it allows the creation of a polygon that includes that specific geomorphic unit and the cross-sections for that unit.

The flow depth and velocity were measured on eleven geomorphic units for each reach.

For the Rio Carlino, the measuring points were taken along 40 cross-sections for a total of 771 measuring points (Figure 33). The number of the cross-sections and the number of points were decided based on the length and width of the part of the
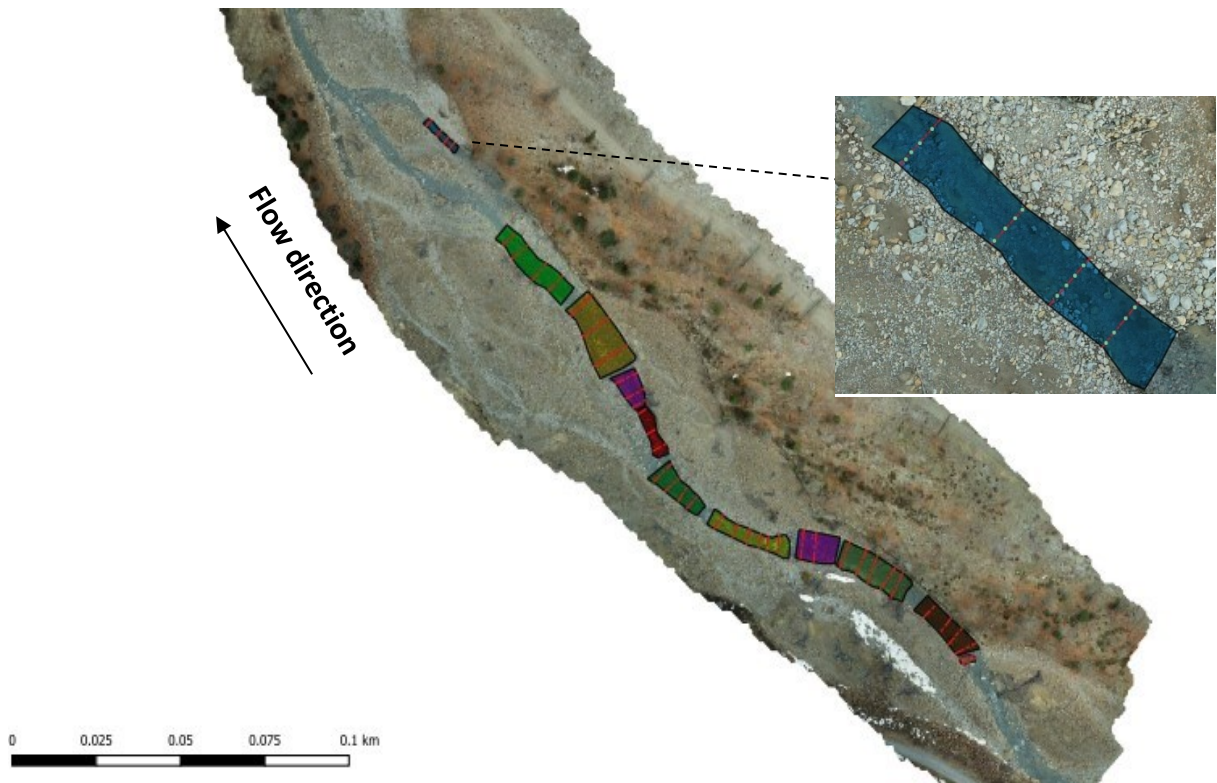
Figure 32. Overview of the units from Rio Carlino with the cross sections and the measuring points and a close from geomorphic unit nr.11

channel

included within the polygon of that geomorphic unit.

Geomorphic unit 11 is farthest downstream of the reach, before the stream enters under a bridge and suffers a constriction. It was classified as a glide because the surface is parallel with the bed and very plain. There is no presence of air nor any kind of waves and no presence of cobbles or boulders. The unit's depth is also low when compared to the other units from the stream, another distinctive characteristic of the glides.

Geomorphic unit 10, moving upstream from unit 11, shows a higher slope than unit 11, which is also reflected in the coarser sediment of the channel bed. The cobbles and boulders in the channel, peak out of the flow and form the "transverse ribs, " distinguishing characteristics of the rapids. The flow is more turbulent than from unit 11, and there is the presence of air and hydraulic jumps that act as the primary energy dissipator.

Geomorphic unit 9 was also classified as a rapid and presents the same characteristics.

Moving upstream, geomorphic unit 8 was classified as a glide but could also be named a Run. Primarily due to its short length and the position between two rapids. It has a slope of 4.2%, in the same range as unit 11.

Geomorphic unit 7 was classified as a rapid, and the distinguishing characteristics of the rapids are visible from the photos (Figure 35). Geomorphic unit 6 was classified as a riffle, although its slope remains high (Appendix 1) in the rapids condition. None of the characteristics of the rapids was present. The flow is not very turbulent, and there was almost no presence of air except sporadically. The ripples in the form of "V" in the flow direction were also visible on the water surface.

The geomorphic units 5, 4, 3, and 2 were all classified as rapids. This is because they fulfilled, morphologically and hydraulically, all the requirements of the rapids. From the photos that were taken on the site, the most distinctive characteristics of the rapids, such as "transverse ribs," cobblers and boulders out of the water, and the presence of air and waves, can all be seen.

Geomorphic unit 1 was classified as a pool but does not check all the pool boxes. Most important, it did not occupy the whole width of the channel. I decided to keep the unit because some of the characteristics of the pools are satisfied (high depth and low velocities, finer sediment). The pool was formed downstream of a big rock (see figure 31) that occupies the ¾ of the channel, and I decided to classify it as a constriction pool (or a forced pool).
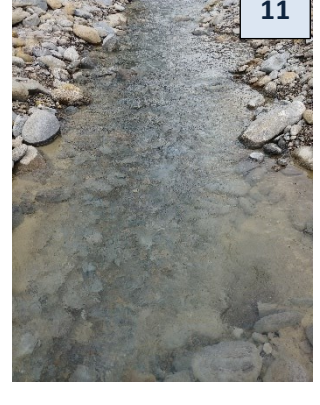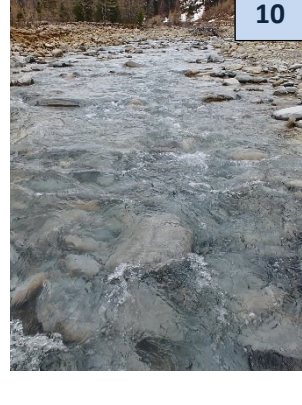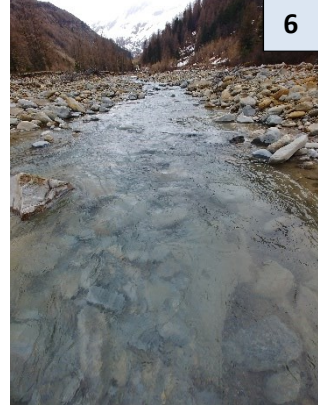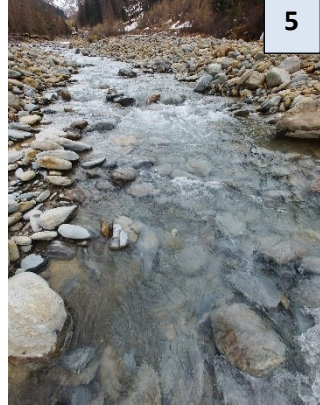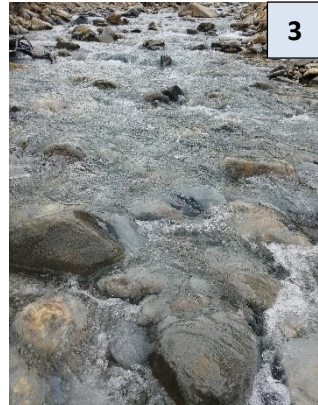
Figure 33. All the units from the Rio Carlino reach. Looking upstream (May 6th, 2022)

For the Ova dal Fuorn, we measured over the same number of units. For a total of 45 cross-sections and 696 measuring points (Figure 36). The measuring, as per Rio Carlino, started upstream and moved downstream.

The furthest unit downstream was the number 11. It was classified as a glide. The free surface of the flow showed very little turbulence, and the depth was low. There was no presence of air or waves.

Geomorphic unit 10 was classified as a riffle and presented all the characteristics of the riffles. The velocities registered were high, and the depths low, the V-shaped ripples pointing in the flow direction could be seen on the surface.

Geomorphic unit 9 was classified as a riffle too and presented the same morphological and hydraulic characteristics as unit 10.

Geomorphic unit 8 was classified as a Glide and belongs to the secondary channel. The depth is shallow, and the surface is parallel with the channel bed and undisturbed from any waves or peaking clasts.

The geomorphic unit 7 up to geomorphic unit 2 were all classified as riffles. They are interrupted by curves and visible changes of the channel slope, and geomorphic units 4 and 2 belong to the secondary channel.
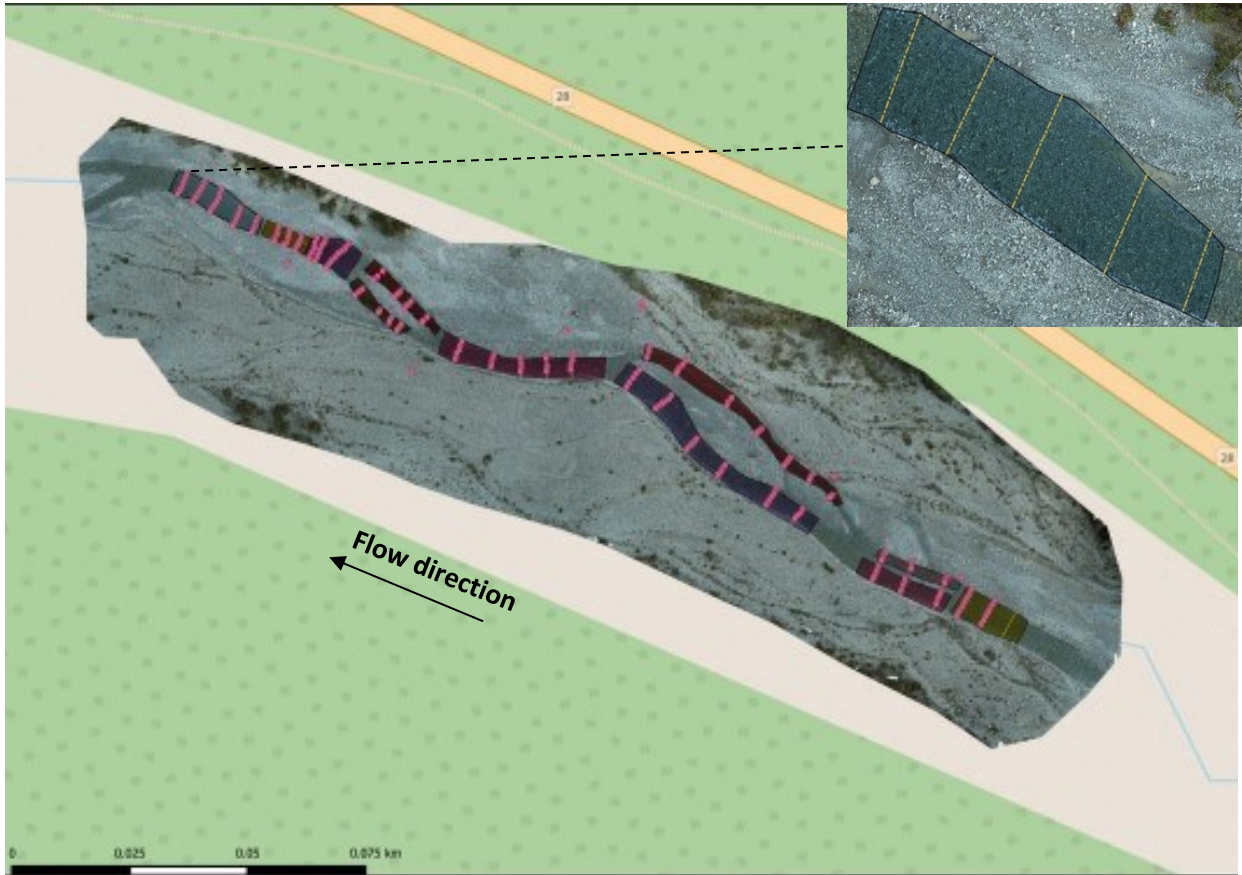
Figure 34 All the units form Ova dal Fuorn and a close up from unit 11. Lines show locations of the transects along which the velocity was measured

The last geomorphic unit is unit 1, classified as a glide: it manifests a low depth and similar flow characteristics as geomorphic unit 8.

Figure 35. All the units from Ova dal Fuorn study reach. Units 2 and 3 looking downstream and 8 flow from left to right. All the other photos are taken looking upstream (May 5th, 2022)

43

3.3 Grain size analysis

The line count method (Wolman 1954) is used to describe the grain size distribution of the surface and subsurface layers of mountain rivers. This method is beneficial for coarse material, where a laboratory sieve analysis is not feasible or not possible. Line count sampling enables a fast and easy determination of the grain size distribution with a manageable workload.

As stated, three line counts were conducted for the Ova dal Fuorn and two for Rio Carlino. There were also taken the same number of sediment samples were from the exact sites where the line counts were conducted and sent to the laboratory for volumetric analysis. The sampling sites were chosen close to the bank, for the Ova dal Fuorn 2 on the orographic right and one on the left, and Rio Carlino on the right orographic.

For the count of the pebbles, a tape was stretched along the flow direction, then the b-axis (second largest/most minor axis) of at least 100 grains was measured. Every grain with a diameter larger than 1 cm to 2 cm and directly lying under the tape was included in the sample.

For every class, there are three diameters related to as many axes:
- A: long axis
- B: intermediate axis
- C: short axis
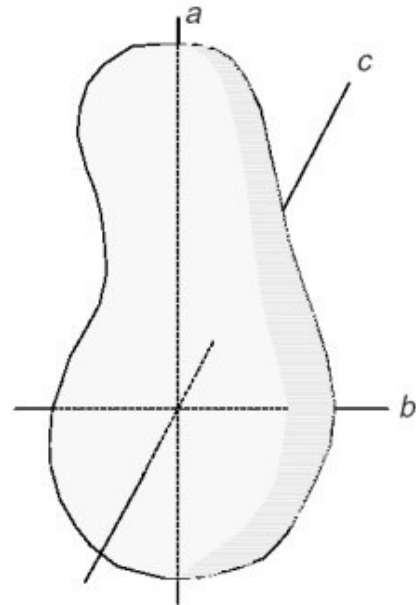
Figure 36. Clast shape and axis (a) measuring form Ova dal Fuorn and (b) Sketch from Bunte and Abt(2001)

In a sieve analysis is the B-axis that determines if the clast passes through the openings of the sieve. That is why for analogy, when a line count analysis is conducted, the B-axis diameter is measured and reported (Figure 39).

As only grains with a diameter bigger than 1 cm to 2 cm are included, the fine components of the material need to be estimated. The fine grain samples can be estimated by approximating the Fuller distribution. According to (FEHR 1987), it is a sufficiently accurate method and is not necessary to collect large samples of fine grain for further analysis in the laboratory.

$$p\,FU,i \quad = \sqrt{\frac{Di}{dmax}} \tag{2}$$

Where pF U, i is the cumulative frequency of the grain class i in the Fuller-curve [−] and $Dmax$ is the maximum diameter of the Fuller-curve [m].

Fehr developed a formula that calculated the volumetric weight analysis of the subsurface material by using the line count analysis of the surface material. The formula is:

$$\Delta p_i = \frac{\Delta q_i\, D_{mi}^{0.8}}{\sum_{i=1}^{k} \Delta q i D_{mi}^{0.8}} \tag{3}$$

Where Δpi is the weight of fraction I divided by the weight of the total sample (Volume-weight analysis of the subsurface layer) [−], *Δqi* is the number of grains of the grain class *I* divided by the number of grains of the total sample (line count analysis of the surface layer) [−], *Dmi* is the mean grain size of the grain class *i* [m], *k* is the number of fractions and 0.8 is the exponent for the conversion of the surface to the subsurface layer [−].Fehr (1987a) also describes the correction in favor of the fine grains that have been underestimated by the line count analysis with the following formula:

$$p_i c = 0.25 + 0.75 \sum_{i=1}^{k} \Delta p_i \quad (4)$$

Where pic is the corrected cumulative frequency of the grain class *i* [−] and *Δpi* is the weight of the grain class *i* divided by the weight of the total sample [−]. Sediments smaller than 1 cm to 2 cm make 25% of the complete material.

As a final step, the coarse and fine fractions of the Fuller distribution are merged. For the Rio Carlino, there were conducted two line counts (Figure 40). The first one at the coordinates N46.82881 and E10.66881.17 (UTM: 32N, WGS84, EPSG: 32632) on the orographic left of the geomorphic unit 8 and the second one at the site N46.82908 E10.66842, (UTM: 32N,
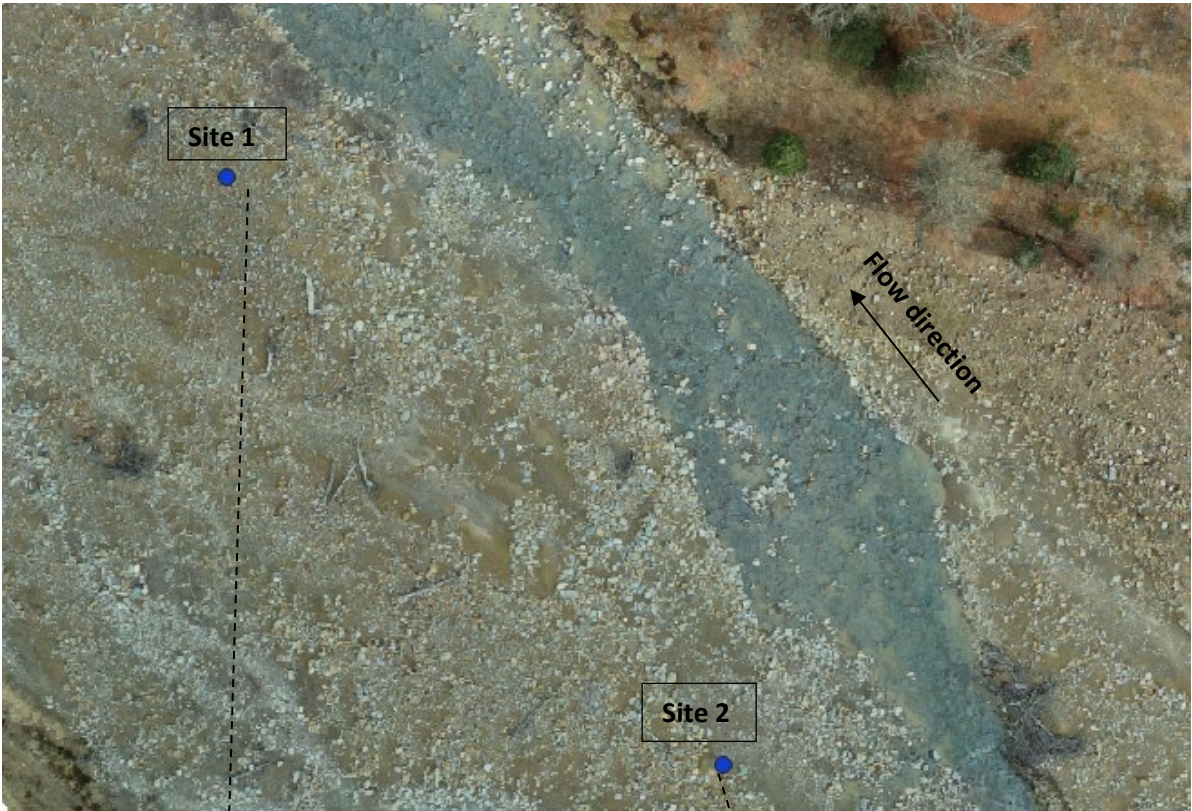
Figure 37. Sites from Rio Carlino where the line counts here conducted. Both the sites were chosen on the orographic right

WGS84, EPSG: 32632) on the orographic left of geomorphic unit 10.

The grain size analysis (Figure 41) results confirmed the field observations described in sub-chapter 3.3 on the reach characterization. At the exact sites where the line counts were conducted, the volumetric samples were extracted using a shovel trying also to remove the sublayer. Two buckets of 18-20 kilograms of material were taken and sent to the laboratory.
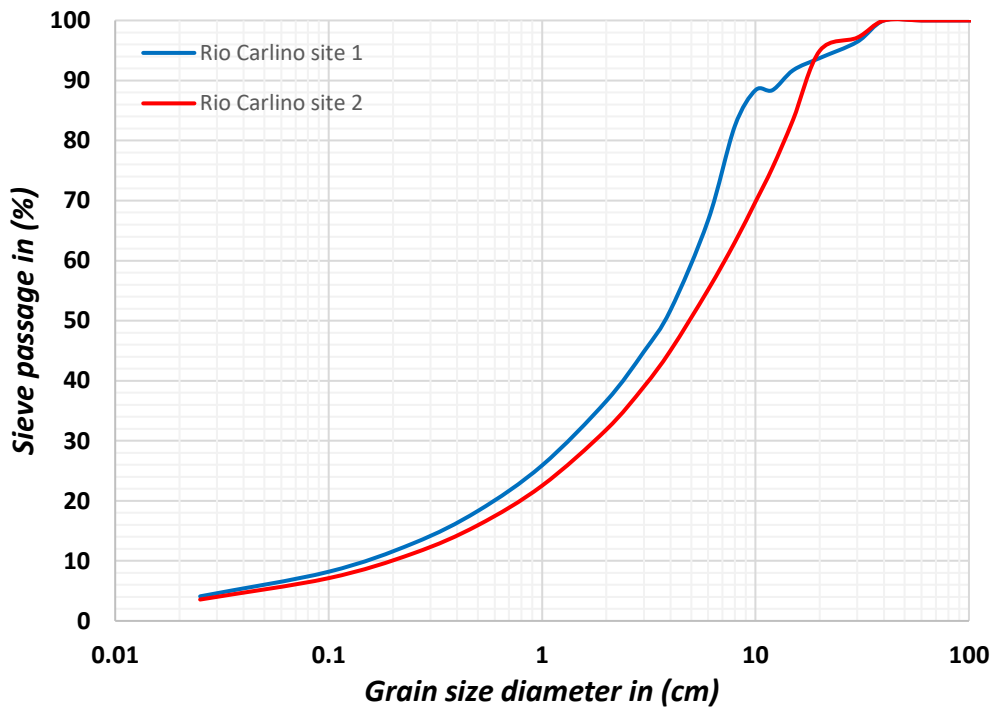
Figure 38 Averaged line count samples for Rio Carlino from both the sites

Table 3 Characteristic diameters from the line count for Rio Carlino

	Site 1	Site 2
D16(cm)	0.27	0.56
D30(cm)	1.44	1.84
D50(cm)	3.92	4.91
D84(cm)	8.56	15.31
D90(cm)	15.03	18.56
Dm (cm)	5.01	6.68

For the Ova dal Fuorn there were conducted three line counts (Figure 43). The first location is the orographic right of geomorphic unit 6 at the coordinates N46.65078, E10.26067, (UTM: 32N, WGS84, EPSG: 32632). The second location was again on the orographic right adjacent to the geomorphic unit 7 at coordinates N46.65086, E10.26044 (UTM: 32N, WGS84, EPSG: 32632). Finally, the third location was on the orographic left of geomorphic unit 10 at coordinates N46.65092, E10.25998, (UTM: 32N, WGS84, EPSG: 32632).

Figure 39. Sites from the ova dal Fuorn where the line counts were conducted
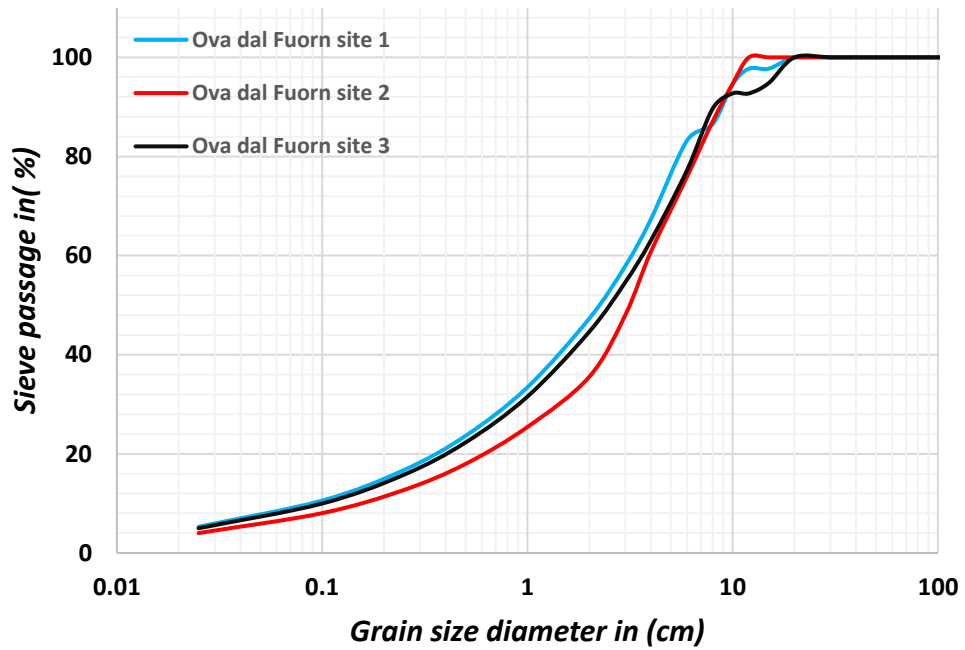
Figure 40. Averaged line count samples for all the studied site for Ova dal Fuorn

Table 4 Characteristic diameters form the line count for Ova dal Fuorn.

	Site 1	Site 2	Site 3
D16(cm)	0.21	0.31	0.24
D30(cm)	0.92	1.52	0.81
D50(cm)	2.23	3.11	2.33
D84(cm)	6.56	7.1	7.52
D90(cm)	9.08	9.34	8.11
Dm(cm)	3.16	3.702	3.36

CHAPTER 4 RESULTS AND DISCUSSION

4.1 Morphology and bed sediment

The field inspection and the spatial analysis of the geomorphic units revealed that the streams are quite different when looking at the morphology. The study reach from Rio Carlino is dominated by rapid morphology, where seven are rapids out of eleven studied geomorphic units. The relatively high number of rapid units indicates a higher channel gradient and a coarser bed material when compared to Ova dal Fuorn.

On the other hand, the study reach from Ova dal Fuorn is dominated by riffle type morphology; out of eleven units, nine belong to the riffle, and only two belong to the glide type. The domination by many of the riffle geomorphic units also represents the bed sediment's composition by gravel and cobbles and the lower channel gradient throughout the studied portion of the stream.

Table 5 Geomorphic units present in number and type for each study reach

	Ova dal Fuorn	Rio Carlino
Glide (Run)	2	2
Riffle	9	1
Rapid	-	7
Cascade	-	-
Step	-	-
Pool	-	1

The rest of the typologies, cascade, and step are absent. For both the missing morphologies, the main requirement is a slope of at least 7 % or higher, and none of the reaches have that kind of inclination. The cascade morphology sediment nature is on the range of large boulders that are partially emergent at low and intermediate flow (Halwas and Church 2002). Sediment of these large diameters is not present in any of the reaches. The only exception is the presence of a pool on the Rio Carlino reach, of the subtype of the forced pool, but that is also not a fully developed geomorphic unit.

When looking at the sediment size, Rio Carlino's is much coarser than the sediment from Ova dal Fuorn. Based on the results obtained from the line count analysis, the median diameters from Ova dal Fuorn vary from 3.1 to 3.7 cm. In comparison, the

median diameters from Rio Carlino range from 5 to 6.7 cm. The same trend also follows the representative diameters D16, D30, D50, D84, and D90. (Fig.44, Fig.45)
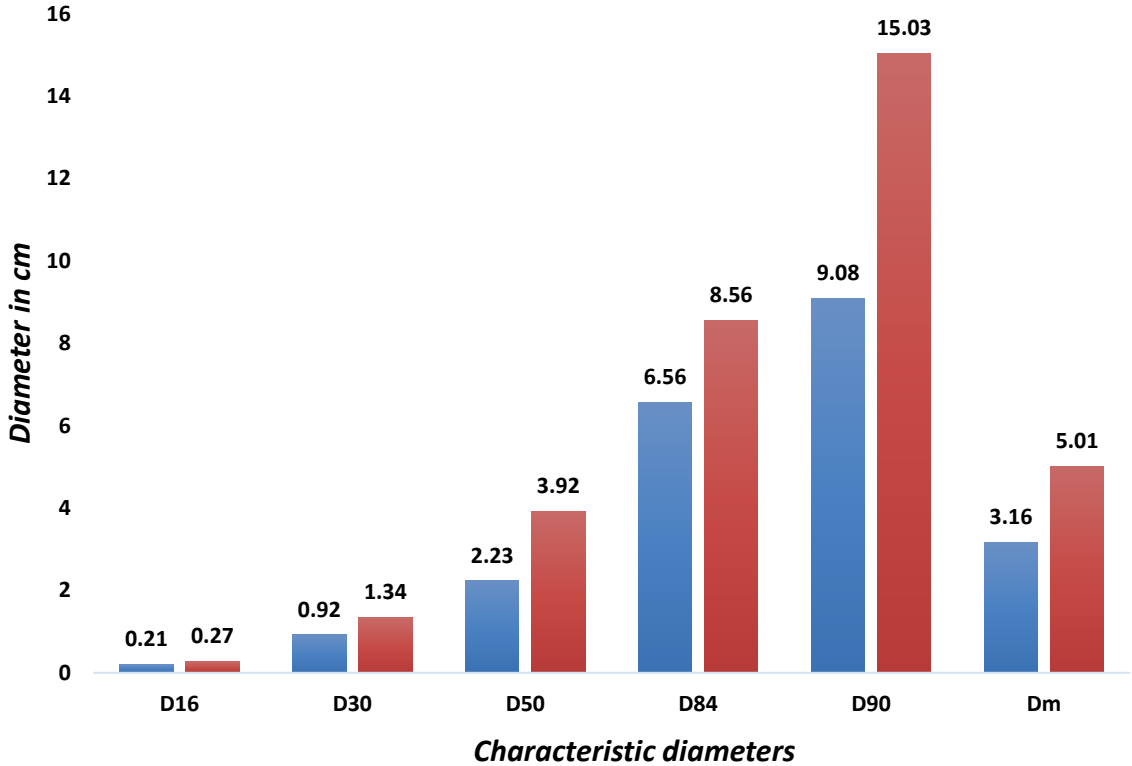
Figure 41. Characteristic diameters from both reaches from site 1 shown in cm. In blue the data from Ova dal Fuorn and in red the data from Rio Carlino
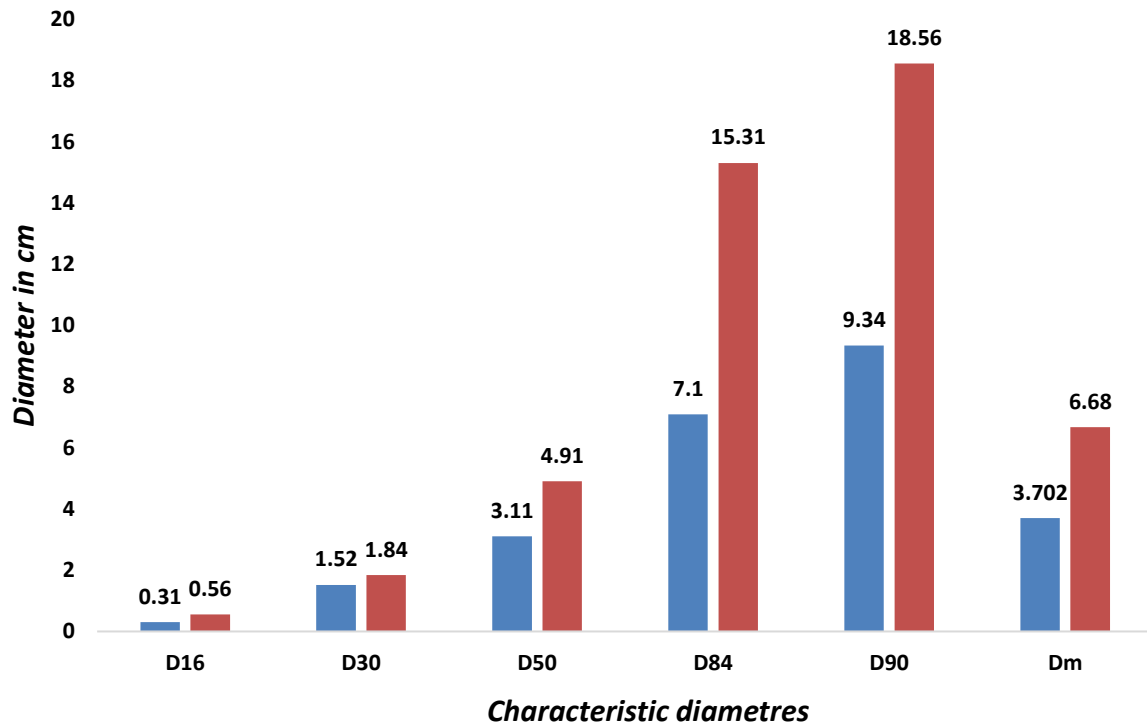
Figure 42. Characteristic diameters from both reaches from site 2 in cm. The red bars are the data from Rio Carlino and in blue the data from Ova dal Fuorn

Table 6 Grain size distribution analysis as reported form the laboratory for the samples exctracted from both the streams

Site	Ova dal Fuorn site 1	Ova dal Fuorn site 2	Ova dal Fuorn site 3	Rio Carlino site 1	Rio Carlino site 2
Initial dry weight	18561 gr	28371 gr	30300 gr	20332 gr	19586 gr
Cobbles	5.4 %	53 %	20.3 %	65.3 %	75.2 %
Gravel	81.5 %	45.9 %	69.8 %	31.6 %	24.1 %
Sand	10.7 %	0.7 %	8.6 %	2.8 %	0.6 5
Silt	2.4 %	0.3 %	1.3 %	0.2 %	0.1 %

The particle size distribution analysis from the laboratory classifies the material retrieved from the gravel bank for both the streams as a sub-rounded gravel and cobbles with the only difference that from Ova dal Fuorn the sand is grey color and from Rio Carlino is brown color.
It can be deducted (Table 6) that the material analyzed from Rio Carlino is much coarser as higher percentages of the samples are in the range of cobbles and for the Ova dal Fuorn the dominating is the gravel. This result reflects one more time what has been deducted from the line count analysis that the Rio Carlinos sediment differs from Ova dal Fuorn's in size and type.
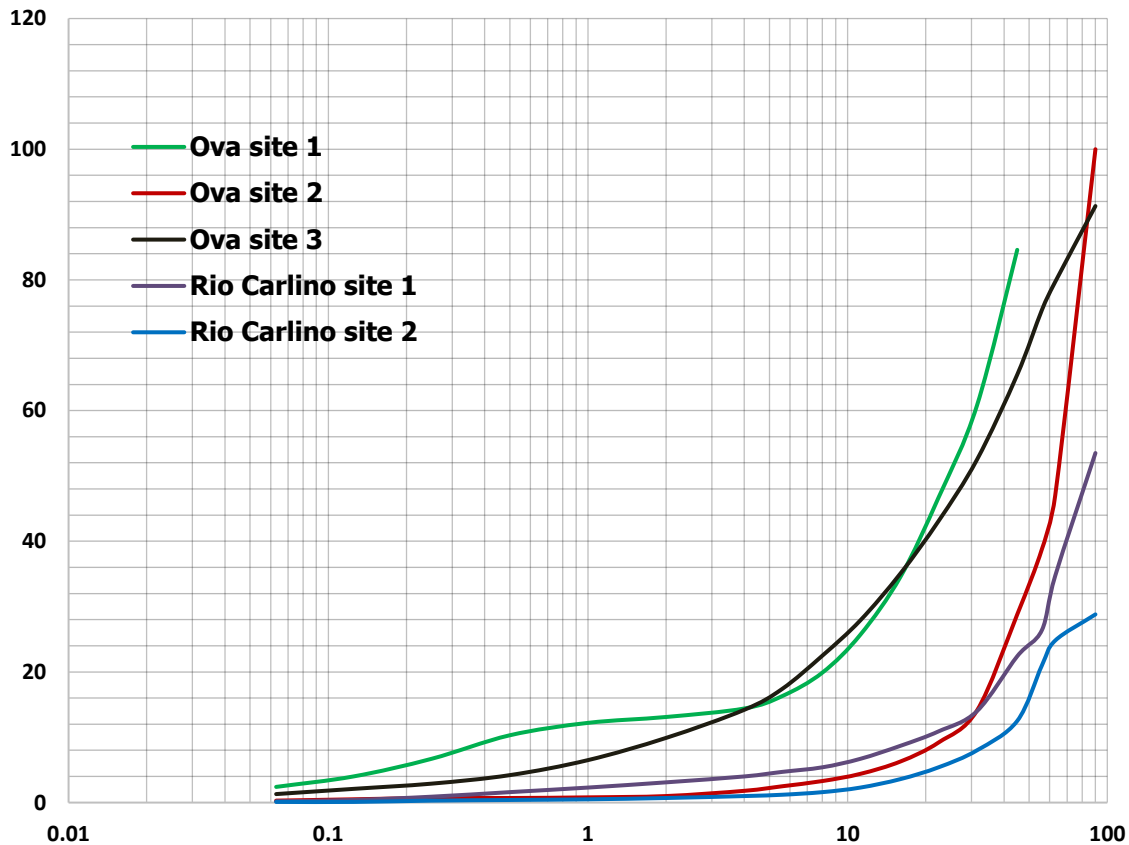
Figure 43. Curves of the grain size distributions of all the 5 sites from both the studied streams

4.2 Variability of flow depth and flow velocity in the study channels

When looking at the two important eco-hydraulic descriptors, flow depth and velocity, the results show a panorama different of what expected when the study sites where accessed. Even though Rio Carlino is steeper than Ova dal Fuorn and is dominated by a rapid morphology, the highest velocity values were registered in the riffle units from the latter (Appendix 1). This trend can be attributed to the presence of cobbles and boulders in the rapid units from Rio Carlino and to the hydraulic jumps that act as energy dissipators and contribute to lower velocities.

Overall, the velocity value is higher from Ova dal Fuorn, still the highest value was registered from Rio Carlino on the geomorphic unit 7 (Rapid), 3.329 m/s in the longitudinal (X) direction. The value can be attributed to two factors: the measuring point was on a "transverse rib" and the flow similar to jet the value is quite possible or to a possible human error during the measuring linked to the angle of the placing the instrument, due to the very coarse channel bed.

Looking at the depth, the deepest point, 44 cm, was registered along the Rio Carlino reach in geomorphic unit 7, which was classified as a riffle. Similarly, the deepest point for Ova dal Fuorn, 33 cm, was registered along a riffle and is close to the value recorded on Rio Carlino. Therefore, the overall depth of Rio Carlino is higher than the Ova

55

dal Fuorn and the median value for the depth from Rio Carlino is also higher.
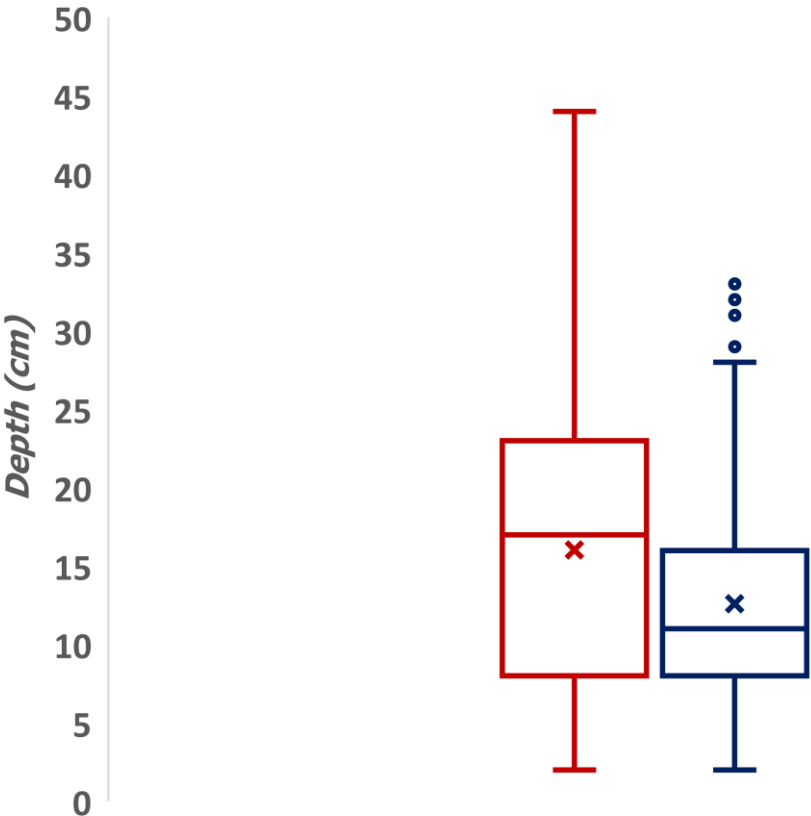
Figure 44. Flow depth from both the reaches, in red the data from Rio Carlino and in blue the data from Ova dal Fuorn.
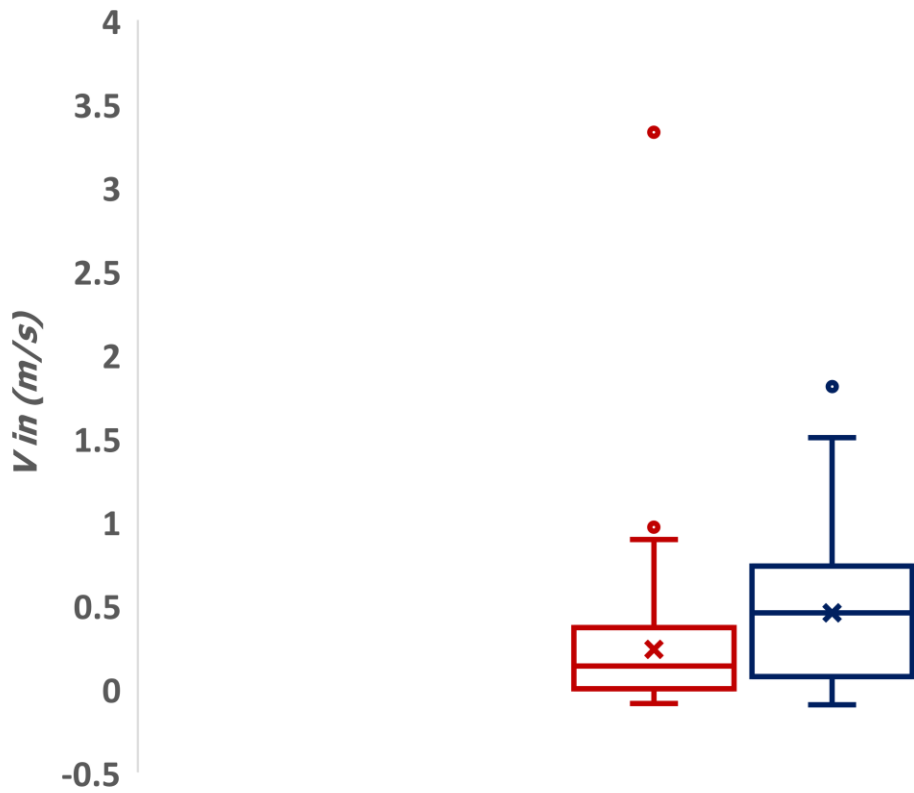
Figure 45 Velocities in the longitudinal direction for both the reaches. in red the data from Rio Carlino and in blue the data from Ova dal Fuorn
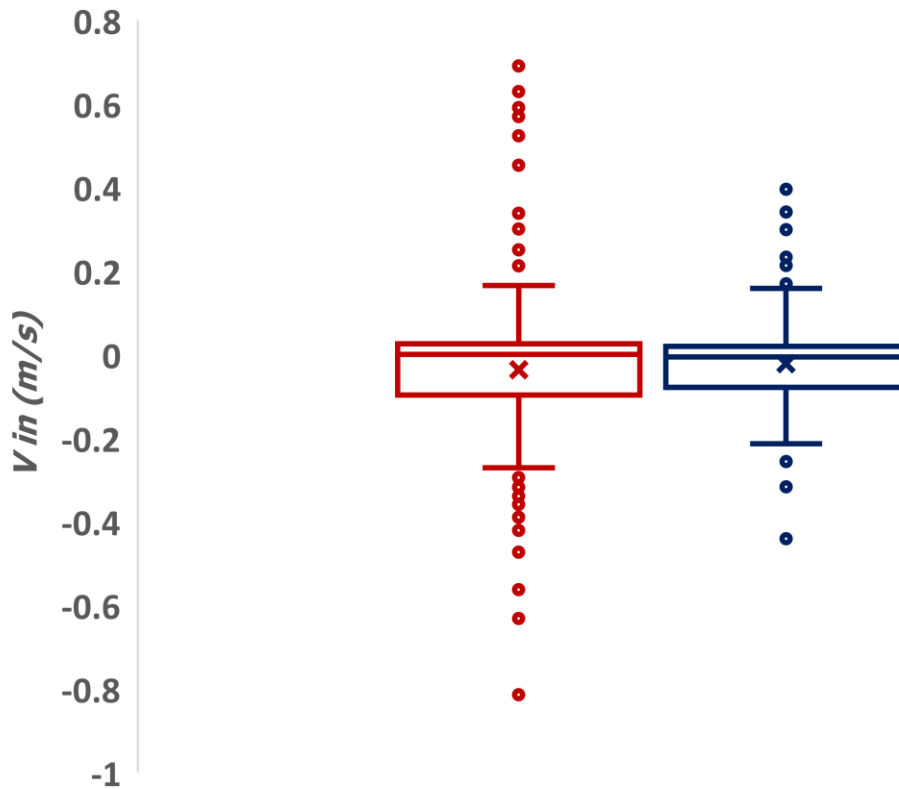
Figure 46. Velocities in transversal (Y) direction for both the channels. In red the data from Rio Carlino and in blue the data from Ova dal Fuorn

When looking at the velocities in the longitudinal direction (Figure 45), Ova dal Fuorn has higher values overall, and the median value of the velocity in the flow direction is higher for Ova dal Fuorn than Rio Carlino's. The reasonable explanation for this is the domination of the Ova dal Fuorn's reach from a riffle morphology. The outlier value for Rio Carlino jumps very high from the possible range of the velocities registered, and the outlier value for Ova dal Fuorn stays in the content of the maximum registered velocity.

The velocity along the transversal (Y) direction (Figure 46) shows more stability and similarity in values from both the reaches regarding the maximum, quartile ranges, and minimum values. Both the reaches present a series of outliers that fall in the expected range.

To better understand the influence of the geomorphology on the velocity and how the velocity varies, similar types of geomorphic units from both the streams are compared by looking at flow depth and velocity.

Geomorphic unit 6 is classified as a riffle for both the reaches that serve well as a comparative tool in terms of hydraulics and morphology. There are three geomorphic units classified as glides from Ova dal Fuorn and two from Rio Carlino that also serve well to the topic of variability between similar units from both reaches.
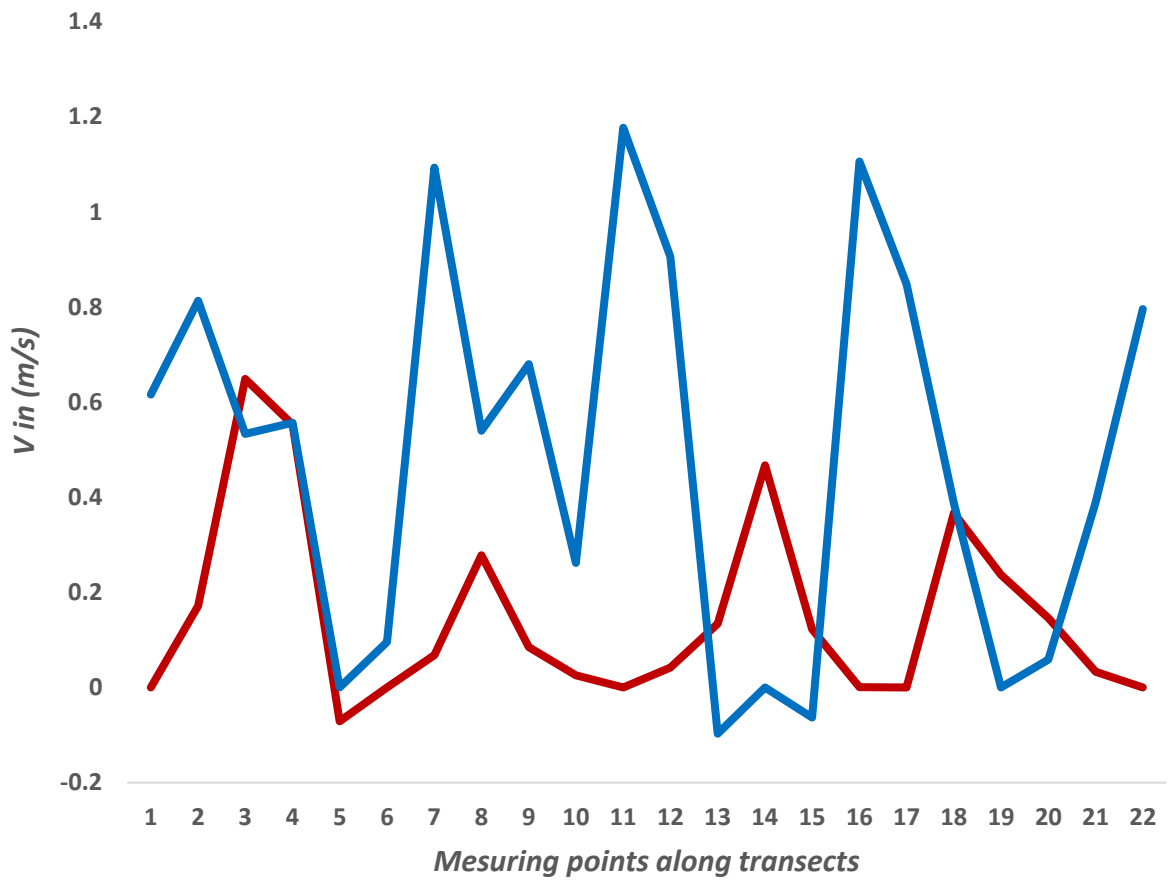
Figure 47. Velocities on the longitudinal (X) direction from a riffle unit from both the reaches. In red the graph representing the data from Rio Carlino and in blue the graph representing the data from Ova dal Fuorn
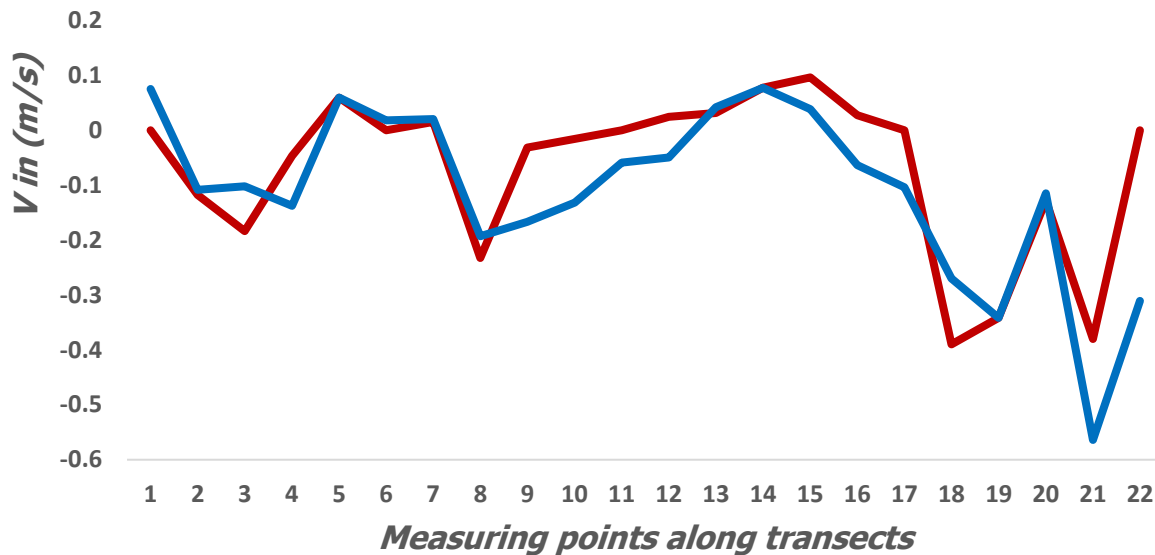
Figure 48. Velocities in the transversal (Y) direction for two riffle units form both the streams. In red the data from Rio Carlino and in blue the data from Ova dal Fuorn.

The graphs show that the velocities in the longitudinal (X) direction from Ova dal Fuorn are much higher than those registered from Rio Carlino (Figure.47), even though Rio Carlino is much steeper than Ova dal Fuorn. The slope from the riffles considered is at 6 % for the riffle from Rio Carlino and 2.3 (Apendinx 1) % for the riffle from Ova dal Fuorn. There is also a considerable difference in the maximum depth registered for both the riffles. The one from Rio Carlino riffle is 39 cm from Ova dal Fuorn is 29 cm. The main factor influencing the difference in velocity can be attributed to both the sediment size and the difference in depth, allowing the water to flow faster along the riffle from Ova dal Fuorn.The velocities in the transversal (Y) direction (Figure.48) are similar and do not differ much from each other.

The other standard geomorphic unit from both the reaches that can shed light upon the variability of the velocity is unit 11, classified as a Glide from both the streams. The registered maximum depth is 19 cm for the Ova dal Fuorn and 35 for Rio Carlino. The maximum velocities on the longitudinal direction are 0.807 m/s for the glide from Ova dal Fuorn and 0.445 m/s for the Rio Carlino one. Again, the values for the velocities in the transversal direction do not differ much as the maximal registered value from Ova dal Fuorn is 0.077 m/s and from Rio Carlino is 0.057 m/s.
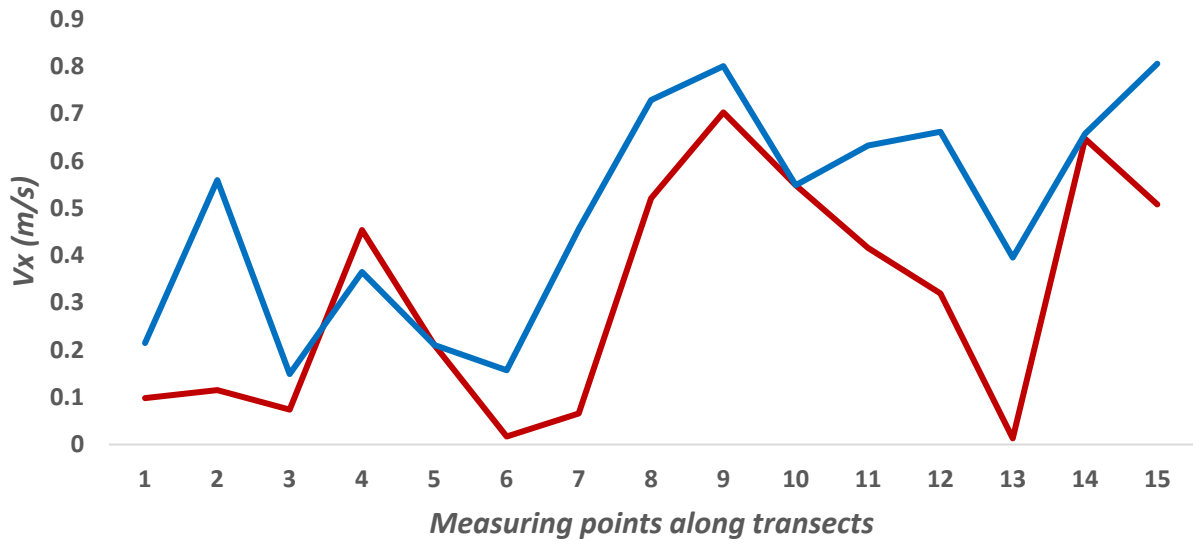
Figure 49. Velocities along a glide unit from both the reaches in the longitudinal (X) direction. In red graph represents the data from Rio Carlino and in blue on the data from Ova dal Fuorn
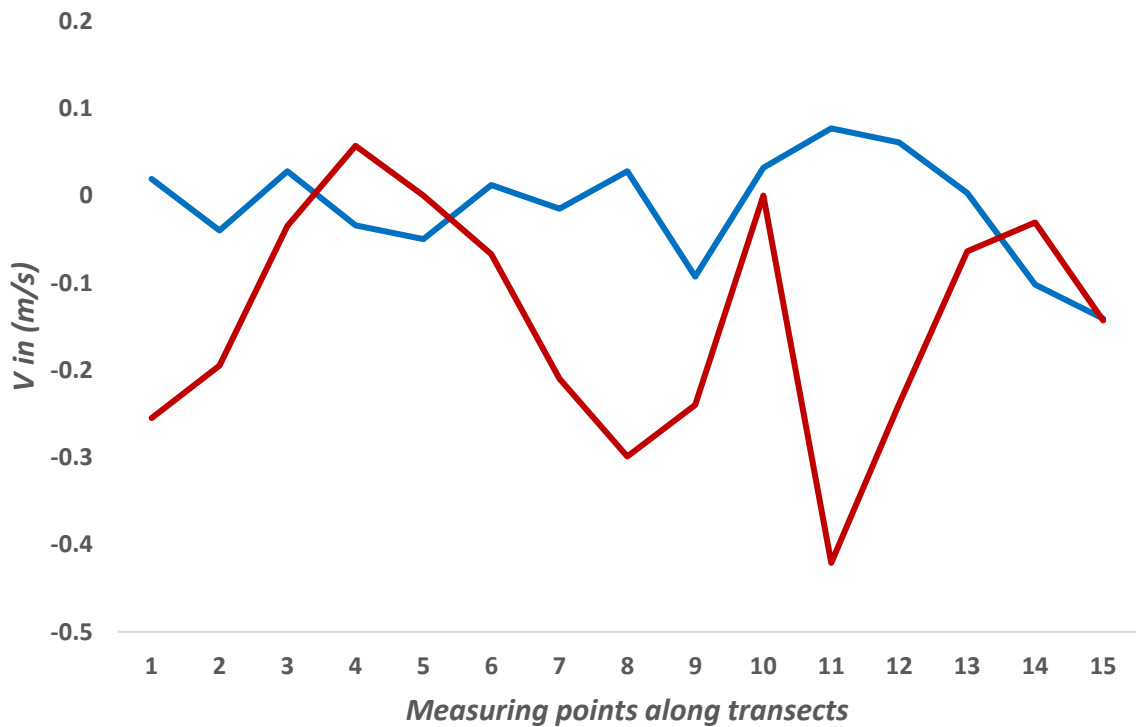
Figure 50. Velocities in the transversal (y) direction from a glide unit from both the streams. In red graph represents the data from Rio Carlino and in blue the data from Ova dal Fuorn

As can be deducted from the graphs (Figure.49, Figure.50), the differences, in this case, are less than when comparing the riffle unit. A low variability for the velocity on the longitudinal direction can be seen with higher values from Ova dal Fuorn when compared to the riffle unit, the increased difference that the velocities show along the transversal direction changes.

4.3 Inter-Units variability of flow depth and velocity

To look at the possible variability inside the same reach, the representative geomorphic units for each stream are compared. For the Ova dal Fuorn two consecutive riffles are considered, units 2 and 3, and for Rio Carlino, two straight rapids, precisely units number 2 and 3. The two rapids from Rio Carlino show almost the same maximum depth at 26 cm for the rapid nr.2 and 27 cm for the other. In terms of the slope, there is little difference, too, as rapid nr.2 has a slope of around 6 % the other has a slope of approximately 5.2 %.
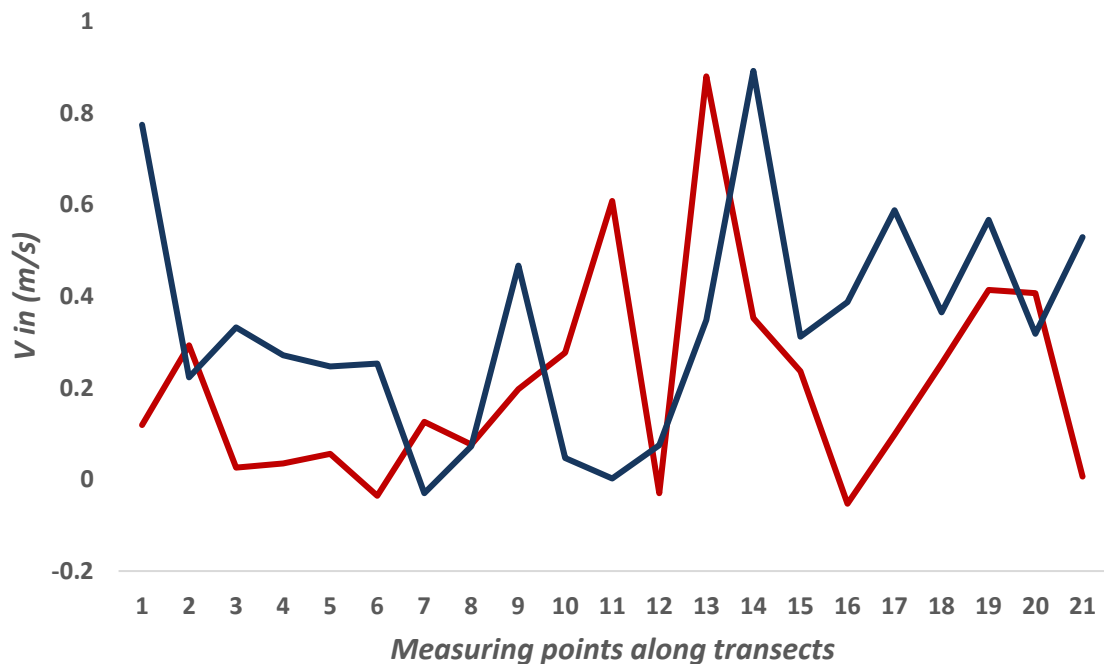
Figure 51. Velocities in the longitudinal (X) direction from two rapid units from Rio Carlino. The red graph represents the data from rapid nr.2 and the blue the data from rapid nr.3

Figure 52. Velocities in the transversal (Y) direction from two rapid units from Rio Carlino. The red graph represents the data from rapid nr.2 and the blue the data from rapid nr.3
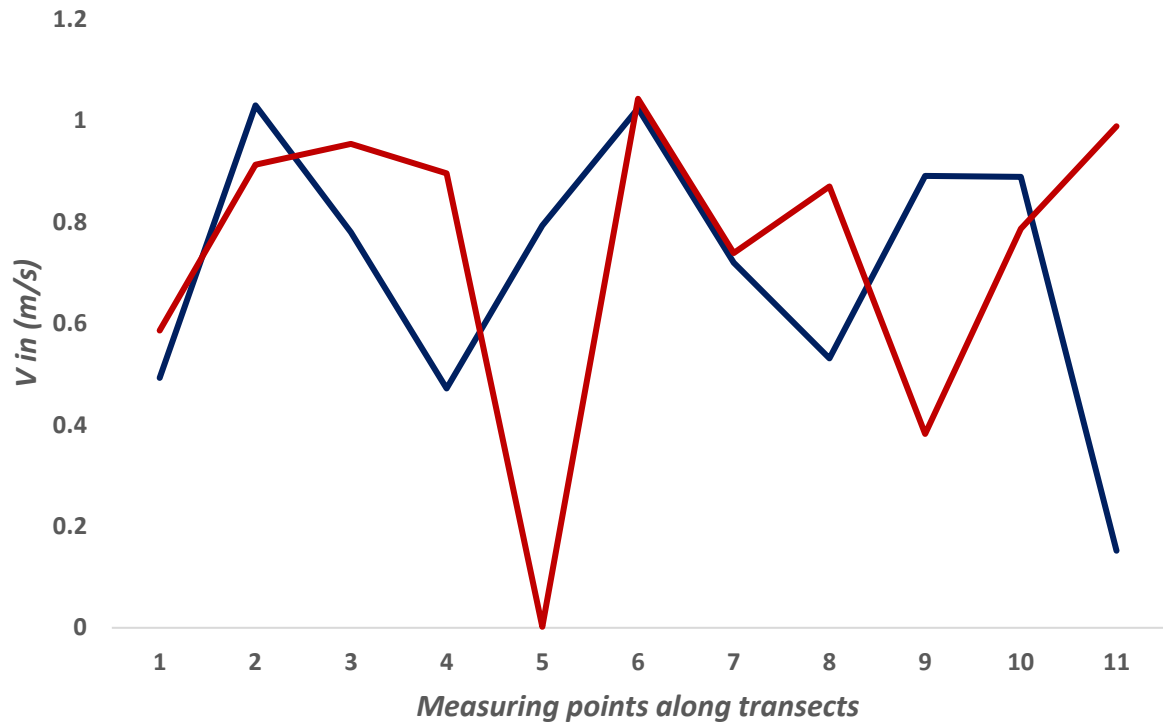
Figure 53. Velocities in the longitudinal (X) direction from two consecutive riffles from Ova dal Fuorn. The red graph represents the data from riffle nr.2 and the blue one the data from riffle nr.3
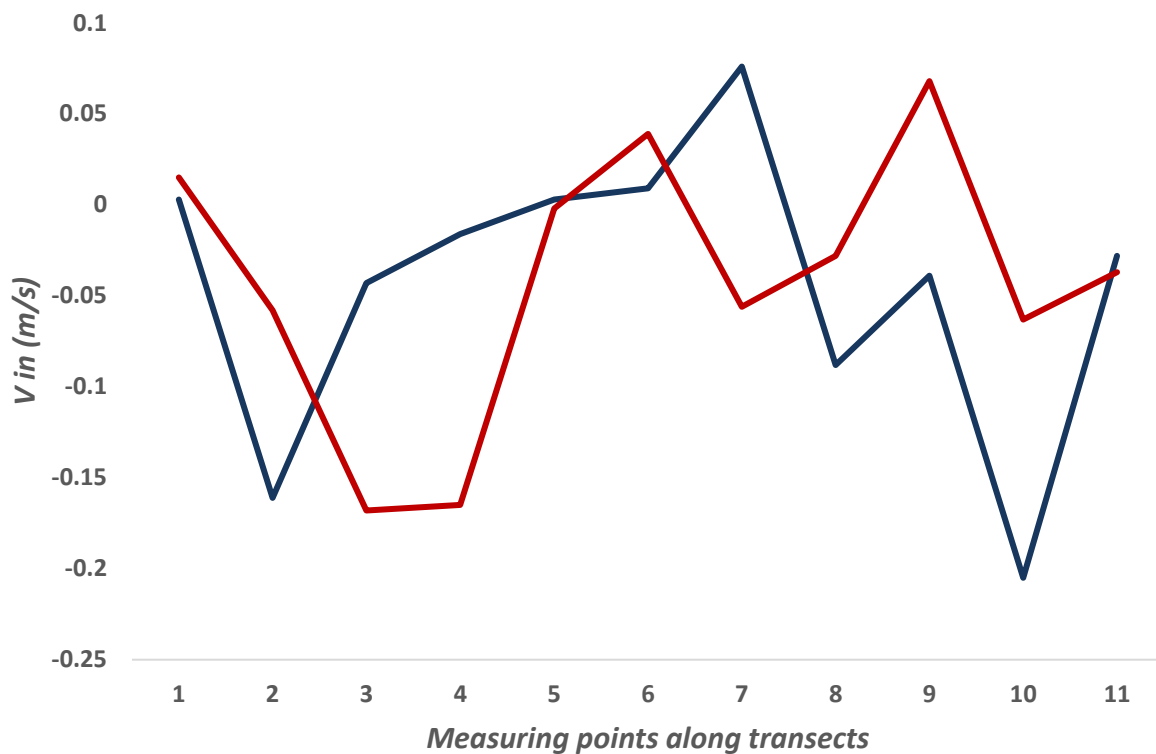
Figure 54. Velocities in the transversal (Y) direction from two consecutive riffle from Ova dal Fuorn. The red graph represents the data from riffle nr.2 and the blue one the data from riffle nr.3

The velocities from both rapids in the longitudinal (X) direction show minimal variability (Figure.51) and are similar in terms of values. For example, the maximum value from rapid 2 is 0.88 m/s, while the one measured on rapid 3 is 0.892 m/s, and the mean values are 0.2 for Rapid number 2 and 0.32 for rapid nr 3.

In this case, the higher deviations that the graphs of the velocities in the transversal (Figure.52) (Y) direction show, even though in single values, the units show quite a similarity. The maximum velocity measured for rapid nr 2 is 0.52 m/s, and for rapid nr 3, 0.35 m/s. The mean values are very similar as for rapid nr 2 is 0.019 m/s and for rapid nr 3 is 0.019 m/s.

The two riffles from Ova dal Fuorn are also very similar in terms of maximum and mean values. The exact value for the maximal depth was registered from both, 20 cm. The slope is also, very similar as riffle nr 2 has a slope of 1.15 %, and riffle nr 3 has a slope of 3 %. The maximum velocities on the longitudinal (X) direction are 1.03 m/s for riffle nr 2 and 1.04 m/s for riffle nr 3. The velocity in the transversal (Y) direction shows a similarity, and riffle nr 2 has a Vy= 0.076 m/s, and riffle nr 3 has a maximum value of the Vy = 0.068 m/s.

The graph for the velocities in the longitudinal (X) direction (Figure 53) show a low variability, except for measuring points 5 and 11, where the gap between the two measured values is quite large.

The situation is less variable when the values of velocities in the transversal (Y) direction (Figure 54) are plotted together. The graphs are very similar, except for two values from measuring points 3 and 4.
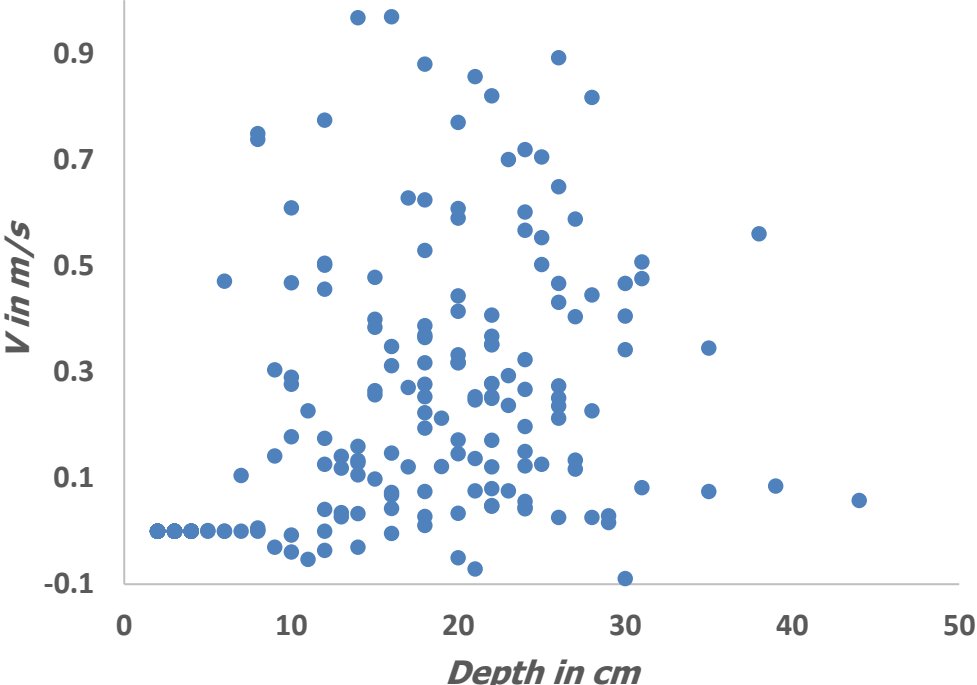
Figure 55. Depth-Velocity in the longitudinal (X) direction correlation for Rio Carlino
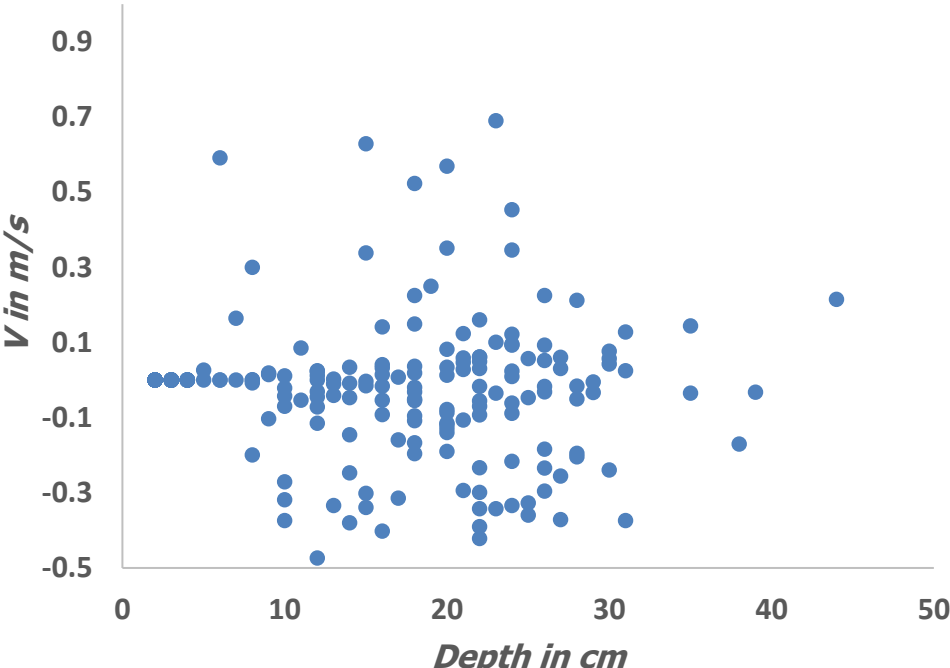
Figure 56. Depth-Velocity in the transversal (Y) direction correlation for Rio Carlino
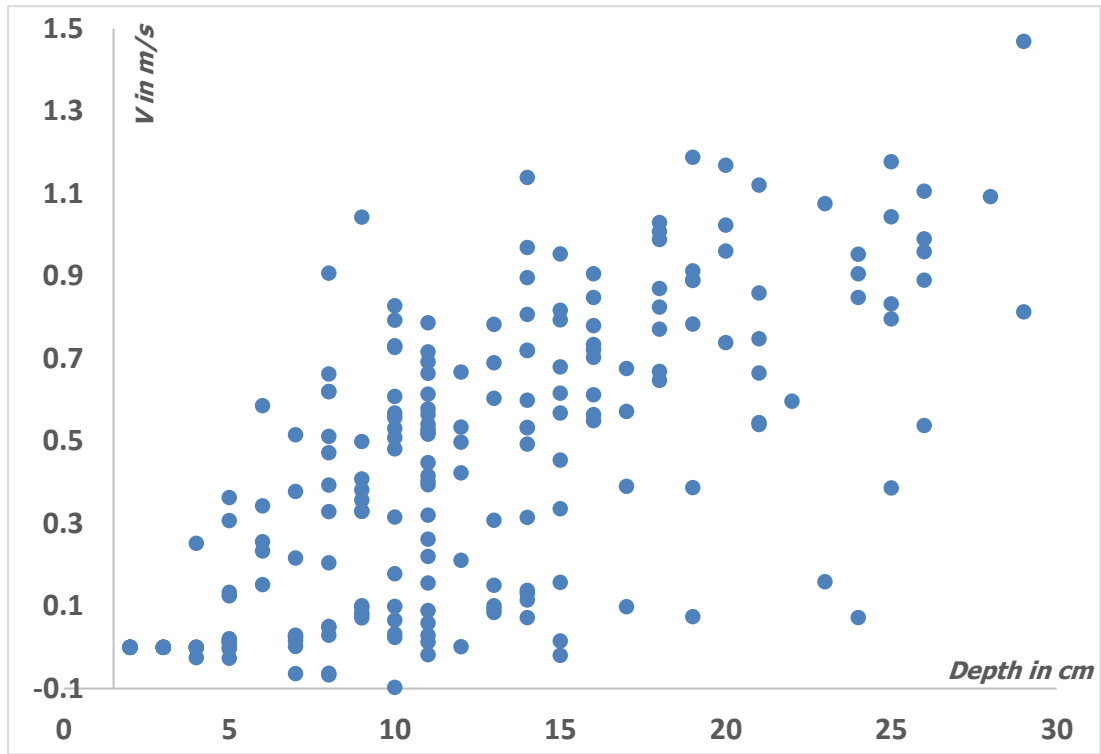
Figure 57. Depth-Velocity in the longitudinal (X) direction, correlation for Ova dal Fuorn
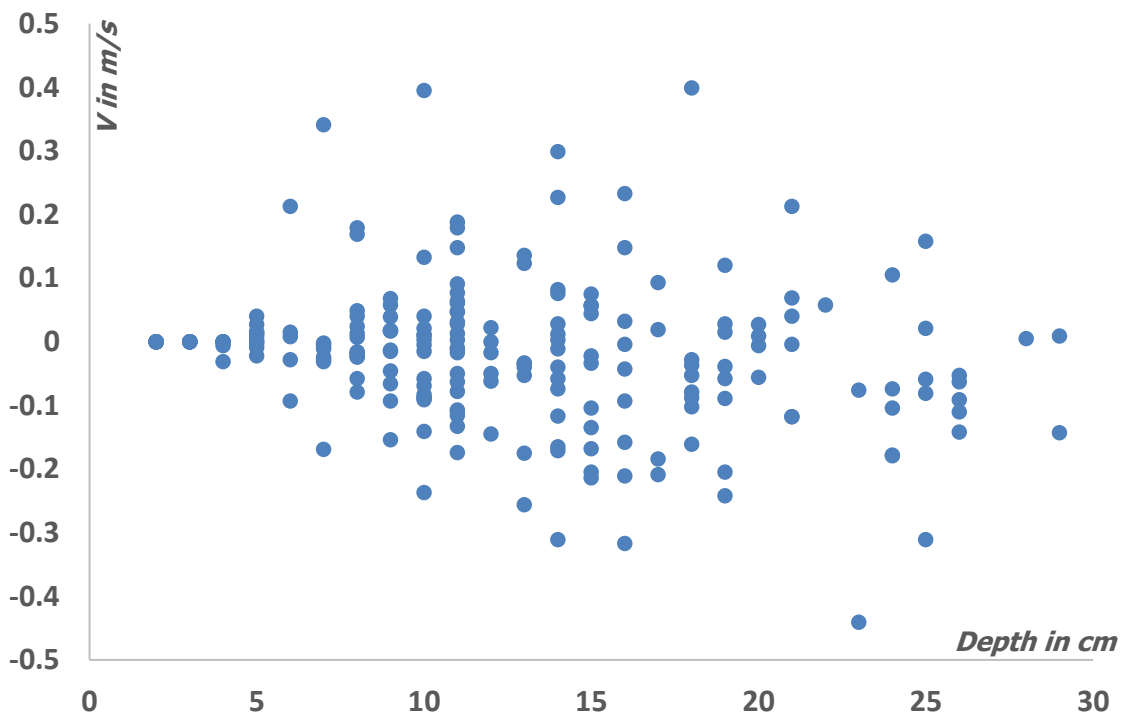
Figure 58.Depth-Velocity in the transversal direction (Y), correlation for Ova dal Fuorn
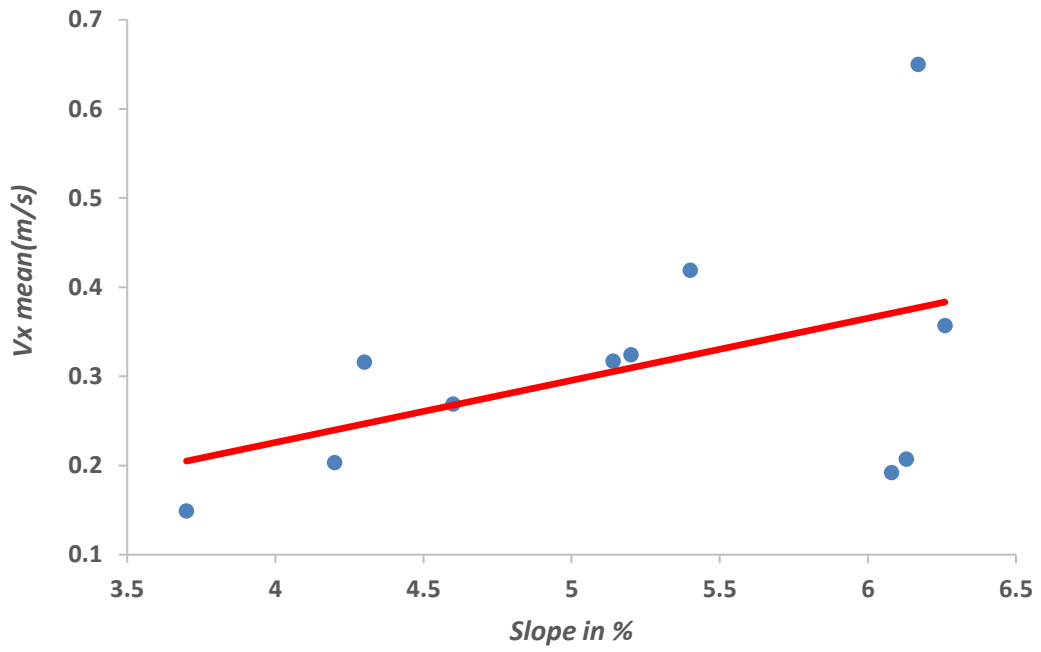
Figure 59. Slope-mean velocity in the longitudinal (X) direction correlation for Rio Carlino
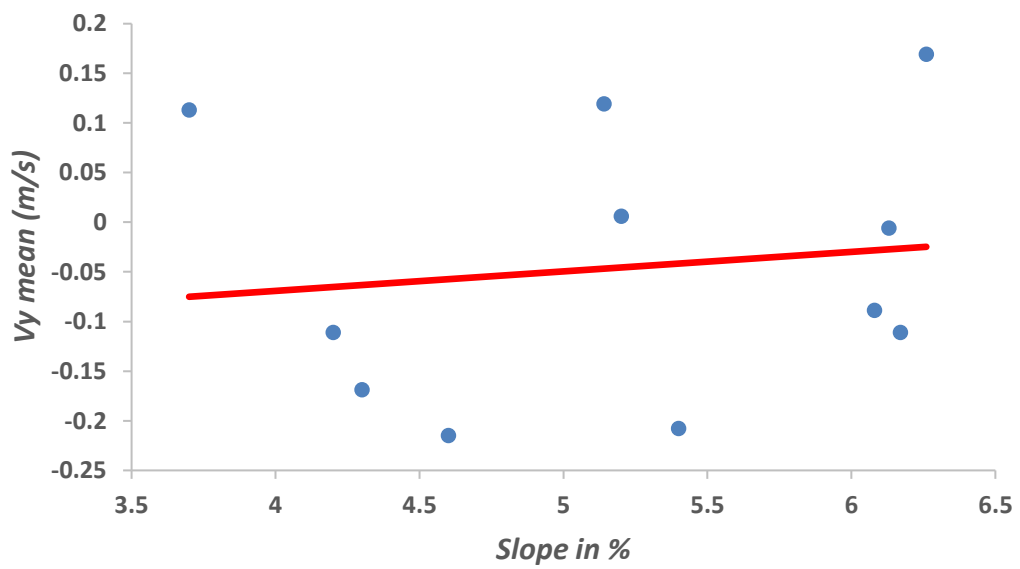
Figure 60.Slope-mean velocity in the transversal (Y) direction correlation for Rio Carlino
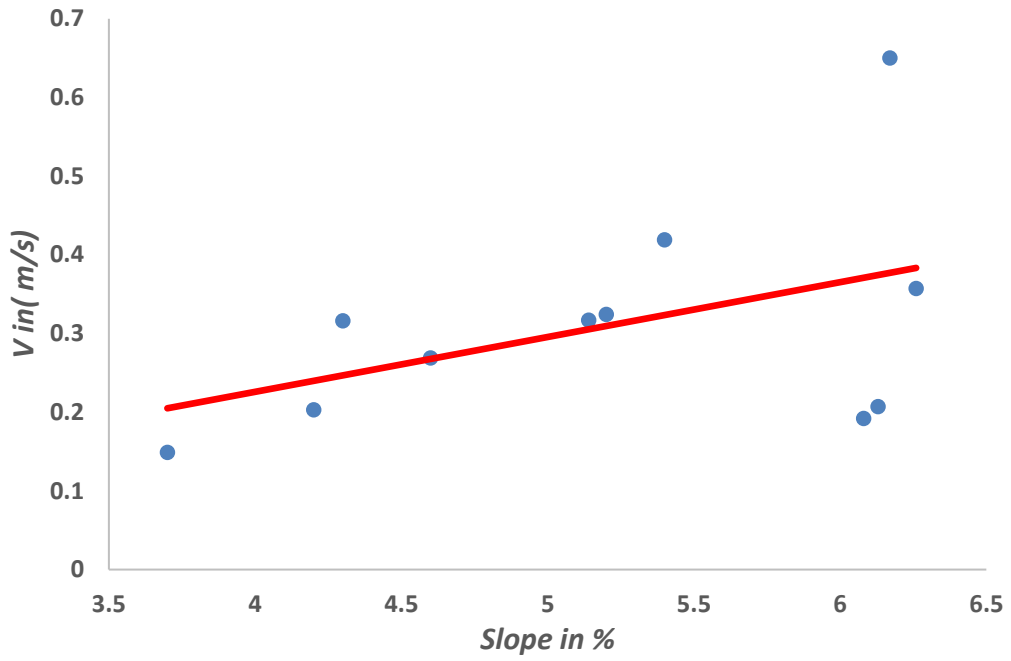
Figure 61.Slope- mean velocity in the longitudinal direction (X) correlation for Ova dal Fuorn
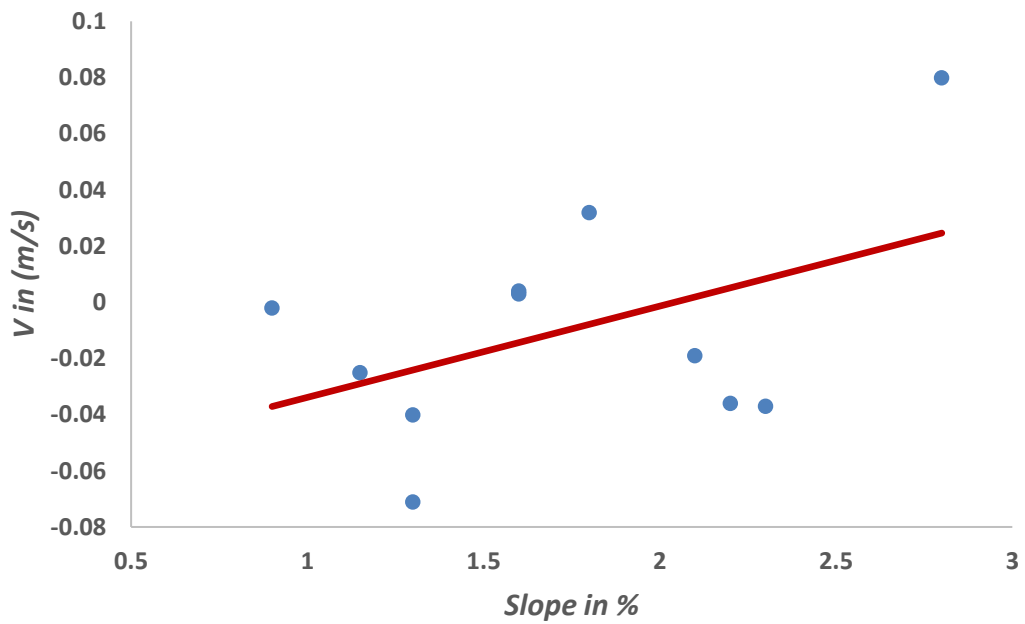
Figure 62. Slope-mean velocity in the transversal (Y) direction correlation for Ova dal Fuorn

There is a moderate positive relationship between the flow depth and velocity in the longitudinal (X) direction. This relationship is more evident and robust for Ova dal Fuorn (Figure 55 and Figure 56) than for Rio Carlino (Figure 57 and Figure 58). Between flow depth and velocity in the transversal direction (Y) there is a negative relationship. Again, the relationship is much more evident for the Ova dal Fuorn than for Rio Carlino.

To understand the influence of the slope on the velocity, the mean velocity is calculated for both directions and for every geomorphic unit from both streams. It is plotted against the slope of the unit in the regression analysis and from the graph it is not statistically significant. The P-value from the correlation between slope and velocity in the longitudinal direction (Figure.59) is 0.56. The graph from (Figure.60) where the velocity in the transversal (Y) regression is plotted against the slope shows no statistical significance but the P-value is quite low 0.15 indicating an influence of the slope on the velocity.

Graph from (Figure.61) shows the correlation of the slope-velocity in the longitudinal (X) direction for Ova dal Fuorn. Graphically there is no clear statistical significance, but the p-value calculated with a regression test is 0.16 indicating an influence of the slope on the velocity. In (Figure.62) the graph represents the correlation between slope and velocity in the transversal direction (Y) direction for Ova dal Fuorn and from the graph again there is no clear evidence of statistical significance and to support it the p-value is 0.7.

The results from the correlation of the slope and velocity in both directions might be influenced by the small number of samples (11). The other explanation is that the effect of the slope on the velocity is influenced by the sediment, In the case of Rio Carlino a higher slope translates into larger sediment which on their end act as energy dissipators (higher number of rapid units) and therefore into lower velocities. For Ova dal Fuorn the influence of a lower slope translates in higher velocities (high presence of riffles), which have lower sediment size of the channel and no presence of cobbles and boulders in it.

4.3 Discussion

This master thesis has demonstrated that morphology and sediment size and type are a good standard to classify the geomorphic units a criteria applied by (Halwas and Church 2002) even though the bed gradient for the geomorphic units in this study is less steep. Also (Montgomery and Buffington 1997) found that relative roughness (D/d) and the bed slope provide a good set of criteria to classify channel morphology at the reach scale.

The results of the analysis from this study suggest that both the flow depth and velocity are under the influence of morphology and a similar result is indicated by (Wilcox et al. 2011) where morphologic variations produced considerable variability in velocity

and turbulence. Here (Wilcox et al. 2011) illustrate through a relationship of morphology and hydraulics exclusively for step-pool structures. Another result made evident from this study is the high variability in the velocity, both in the longitudinal (X) direction and in the transversal (Y) direction, manifested between the same geomorphic unit from both the studied streams. The analysis proved that the main influencers in this case was the presence of coarser sediment in the range of cobbles and small boulders acting as the main energy dissipators. It is also highlighted that the combination of bed slope and characteristic channel sediment exerts a strong influence on the variability of flow velocity.

4.3.1 Uncertainties and challenges in measuring flow characteristics in alpine streams

Field measurements are always challenging, and this is truer than ever when alpine streams are the measuring target. The first challenge to overcome is always the possibility to be able to fully access the site and be able to measure. The obtained data can also be influenced by the technical skills of the operators that are measuring in the field.

Another aspect to keep in mind regarding measuring in alpine channels is the rapid change of water depth and morphology, which makes it challenging to select representative cross-sections for measurements.

The use of the measuring instruments itself such as the Flow Tracker can be highly influenced from the rough channel bed and presence of cobbles and boulders that make it difficult to level. The streams are not always clear and this also makes it difficult sometimes to read the flow depth and also orient the probe in the right direction.

CHAPTER 5 CONCLUSIONS

With all the possible uncertainties in mind, this master thesis research work revealed a relationship between the fluctuations of the values of the flow depth and velocity and the sediment, channel slope, and morphology, such as the type and extent of the geomorphic units.

Data analysis shows an intricate connection between channel slope and sediment and how this "duo" can play an imposing role in the flow velocity. The observations show that a lower slope does not necessarily mean lower velocity.

The influence of the slope can be noticed directly from the values of the velocity from the different geomorphic units. The highest values were registered in the riffles and those are the units with the lowest slope among all the units. While the influence of the sediment size be noticed in the rapids that the are the units with the highest slope amongst the studied ones. Their presence in the channel exerts a flow resistance that contributes to lower values of velocities. This conclusions rate of application can stand for the measured levels of slope and geomorphic units present in this master thesis. The statement of lower slope-higher velocity is uncertain for types of geomorphic units missing from the studied reaches such as cascades, with a higher slope than the rapids but with uncertainty on the comparison of their velocities. The other uncertainty arises from different flow conditions in terms of discharges as it is not possible to predict if the relationship geomorphic type-velocity and slope-velocity will still stand.

To answer the research question if the morphology influences flow depth and velocity from my research, the answer is yes, as from the same geomorphic units from both the reaches, there are registered different values of velocity, and the fluctuations from their graphs are considerable.

About the 3rd research question, if the size and nature of sediment influence the fluctuations of the velocity and depth, the answer is again yes. As seen from the field obtained values and from the 5th chapter, the geomorphic units from Rio Carlino, which have a coarser sediment bed, manifest lower velocities and higher depths in

the matter when compared to the geomorphic units from Ova dal Fuorn, which sediment size on the bed is finer. Even when looking at the same type of geomorphic unit, the sediment still exerts a strong influence.

5.1 Future work

Several answers were given concerning the flow depth and velocity variability under the influences of morphology and sediment. Nevertheless, further work is needed to fully understand the impact of the "duo" on the flow.

To explain the observed hydraulic behavior of the studied geomorphic units, further field investigations are needed, especially data of the two primary eco-hydraulic descriptors. To give generalizing power to the results from this master thesis, a 3rd stream in the same conditions as Ova and Rio Carlino must be added.

Also, to have a more extensive panorama of the variability and fluctuations of flow depth and velocity, at least another set of fields obtained data from a different condition of discharge is needed if not two.

The data gathered for this master thesis constitutes a good starting point for a database that can be enriched over time with flow depth and velocity measurements and a plain view of the rivers through orthophotos. Such a database can be a valuable tool in the recent light of rapid climate changes and their influence on the alpine streams and their habitats. The data can help river managers and hydraulic engineers form protection agencies for any possible structural engineering intervention.

Also, the whole dataset from Ova dal Fuorn, given the very close-to, if not entirely pristine and natural conditions, can serve as a benchmark for river restoration in the future.

BIBLIOGRAPHY

Allan JD, Castillo MM, Capps KA Stream Ecology Structure and Function of Running Waters Third Edition

Amoros C, Petts GE (1993) Hydrosystèmes fluviaux. Masson

Belletti B, Rinaldi M, Bussettini M, et al (2017) Characterising physical habitats and fluvial hydromorphology: A new system for the survey and classification of river geomorphic units. Geomorphology 283:143–157. https://doi.org/10.1016/j.geomorph.2017.01.032

Brierley G, Fryirs K, Reid H, Williams R (2021) The dark art of interpretation in geomorphology. Geomorphology 390:. https://doi.org/10.1016/j.geomorph.2021.107870

Carrivick JL, Smith MW, Quincey DJ (2016) Structure from Motion in the Geosciences. John Wiley & Sons

Chanson H (2004) Hydraulics of open channel flow. Elsevier

Chin A, Wohl E (2005) Toward a theory for step pools in stream channels. Prog. Phys. Geogr. 29:275–296

Comiti F, Cadol D, Wohl E (2009) Flow regimes, bed morphology, and flow resistance in self-formed step-pool channels. Water Resour Res 45:. https://doi.org/10.1029/2008WR007259

Comiti F, Mao L (2012) Recent Advances in the Dynamics of Steep Channels. In: Gravel-Bed Rivers: Processes, Tools, Environments

Comiti F, Mao L, Wilcox A, et al (2007) Field-derived relationships for flow velocity and resistance in high-gradient streams. J Hydrol 340:48–62. https://doi.org/10.1016/j.jhydrol.2007.03.021

Commission E (2003) Common implementation strategy for the water framework directive (2000/60/EC). Guid Doc N 8:

Directive EC (2007) 60/EC of the European Parliament and of the Council of 23 October 2007 on the assessment and management of flood risks. Brussels Eur Comm

Einstein HA (1950) The Bed-Load Function for Sediment Transportation in Open Channel Flows. Soil Conserv Serv 1–31

FEHR R (1987) Etude des galets des rivières de montagne: conversion et comparaison de différents méthodes d'analyse (fr). Eidgenössische Tech Hochschule Zürich, Zürich

Frissell CA (1993) Topology of Extinction and Endangerment of Native Fishes in the Pacific Northwest and California (U.S.A.). Conserv Biol 7:. https://doi.org/10.1046/j.1523-1739.1993.07020342.x

Frissell CA, Liss WJ, Warren CE, Hurley MD (1986) A hierarchical framework for stream habitat classification: Viewing streams in a watershed context. Environ Manage 10:199–214. https://doi.org/10.1007/BF01867358

Fryirs K, Brierley G (2005) Chapter Seven Stage Four : River Management

Applications and Implications in Bega Catchment. Pract Appl River Styles® Framew As a Tool Catchment-Wide River Manag a Case Study From Bega Catchment, New South Wales 18–41

Fryirs KA, Brierley GJ (2012) Geomorphic Analysis of River Systems

Gostner W, Parasiewicz P, Schleiss AJ (2013) A case study on spatial and temporal hydraulic variability in an alpine gravel-bed stream based on the hydromorphological index of diversity. Ecohydrology 6:652–667. https://doi.org/10.1002/eco.1349

Gravelle R (2015) Discharge Estimation: Techniques and Equipment. Geomorphol Tech 5:1–8

Gurnell AM, Rinaldi M, Belletti B, et al (2016) A multi-scale hierarchical framework for developing understanding of river behaviour to support river management. Aquat Sci 78:1–16. https://doi.org/10.1007/s00027-015-0424-5

Haller R, Hauenstein P, Anderwald P, et al (2013) Beyond the inventory - Change detection at the landscape level using aerial photographs in four protected areas of the Alps. 5:257–264

Halwas KL, Church M (2002) Channel units in small, high gradient streams on Vancouver Island, British Columbia. Geomorphology 43:243–256. https://doi.org/10.1016/S0169-555X(01)00136-2

Jarrett RD (1992) Hydraulics of mountain rivers. Channel flow Resist Centen Manning's formula 287–298

Knighton AD (1999) Downstream variation in stream power. Geomorphology 29:. https://doi.org/10.1016/S0169-555X(99)00015-X

Leopold LB, Wolman MG, Miller JP (1964) Fluvial processes in geomorphology WH Freeman and Co. San Fr 522pp

Maddock I (1999) The importance of physical habitat assessment for evaluating river health. Freshw Biol 41:. https://doi.org/10.1046/j.1365-2427.1999.00437.x

Milliman JD, Syvitski JPM (1992) Geomorphic/tectonic control of sediment discharge to the ocean: the importance of small mountainous rivers. J Geol 100:. https://doi.org/10.1086/629606

Montgomery DR, Buffington JM (1997) Channel-reach morphology in mountain drainage basins. Bull Geol Soc Am 109:. https://doi.org/10.1130/0016-7606(1997)109<0596:CRMIMD>2.3.CO;2

Nehlsen W, Williams JE, Lichatowich JA (1991) Pacific Salmon at the Crossroads: Stocks at Risk from California, Oregon, Idaho, and Washington. Fisheries 16:. https://doi.org/10.1577/1548-8446(1991)016<0004:psatcs>2.0.co;2

Papanicolaou AN, Bdour A, Wicklein E (2004) One-dimensional hydrodynamic/sediment transport model applicable to steep mountain streams. J Hydraul Res 42:357–375. https://doi.org/10.1080/00221686.2004.9641204

Paquet E (2019) Synthetic hydrograph generation by hydrological donors. Hydrol Sci J 64:570–586. https://doi.org/10.1080/02626667.2019.1593418

Rascher E, Sass O (2017) Evaluating sediment dynamics in tributary trenches in an alpine catchment (Johnsbachtal, Austria) using multioral terrestrial laser scanning. Zeitschrift fur Geomorphol 61:27–52. https://doi.org/10.1127/zfg_suppl/2016/0358

Recking A, Frey P, Paquier A, et al (2008) Feedback between bed load transport and

flow resistance in gravel and cobble bed rivers. Water Resour Res 44:. https://doi.org/10.1029/2007WR006219

Reid LM (1993) Research and Cumulative Watershed Effects

Rickenmann D (1991) Hyperconcentrated Flow and Sediment Transport at Steep Slopes. J Hydraul Eng 117:. https://doi.org/10.1061/(asce)0733-9429(1991)117:11(1419)

Rickenmann D, McArdell BW (2007) Continuous measurement of sediment transport in the Erlenbach stream using piezoelectric bedload impact sensors. Earth Surf Process Landforms 32:. https://doi.org/10.1002/esp.1478

Rinaldi M, Belletti B, Comiti F, et al (2016) Sistema di rilevamento e classificazione delle Unità Morfologiche dei corsi d'acqua (SUM). Versione aggiornata

Rinaldi M, Surian N, Comiti F, et al (2012) Guidebook for the evaluation of stream morphological conditions by the Morphological Quality Index (MQI). Version 1:85

Rinaldi M, Surian N, Comiti F, Bussettini M (2013) A method for the assessment and analysis of the hydromorphological condition of Italian streams: The Morphological Quality Index (MQI). Geomorphology 180–181:. https://doi.org/10.1016/j.geomorph.2012.09.009

Robinson DA, Campbell CS, Hopmans JW, et al (2008) Soil Moisture Measurement for Ecological and Hydrological Watershed-Scale Observatories: A Review. Vadose Zo J 7:. https://doi.org/10.2136/vzj2007.0143

Schoklitsch A (1962) Die Gründung der Wehre. In: Handbuch des Wasserbaues. Springer, pp 652–653

Snavely N, Seitz SM, Szeliski R (2008) Modeling the world from Internet photo collections. Int J Comput Vis 80:189–210. https://doi.org/10.1007/s11263-007-0107-3

Vaughan IP, Diamond M, Gurnell AM, et al (2009) Integrating ecology with hydromorphology: a priority for river science and management. Aquat Conserv Mar Freshw Ecosyst 19:113–125

Westoby MJ, Brasington J, Glasser NF, et al (2012) 'Structure-from-Motion'photogrammetry: A low-cost, effective tool for geoscience applications. Geomorphology 179:300–314

Wheaton JM, Fryirs KA, Brierley G, et al (2015) Geomorphic mapping and taxonomy of fluvial landforms. Geomorphology 248:273–295. https://doi.org/10.1016/j.geomorph.2015.07.010

Wilcox AC, Wohl EE, Comiti F, Mao L (2011) Hydraulics, morphology, and energy dissipation in an alpine step-pool channel. Water Resour Res 47:1–17. https://doi.org/10.1029/2010WR010192

Wohl E (2010) Mountain Rivers Revisited. American Geophysical Union

Wohl E, Merritt D (2005) Prediction of mountain stream morphology. Water Resour Res 41:. https://doi.org/10.1029/2004WR003779

Wolman MG (1954) A method of sampling coarse river-bed material. EOS, Trans Am Geophys Union 35:951–956

Wyrick JR, Senter AE, Pasternack GB (2014) Revealing the natural complexity of fluvial morphology through 2D hydrodynamic delineation of river landforms. Geomorphology 210:14–22. https://doi.org/10.1016/j.geomorph.2013.12.013

Yager EM, Kirchner JW, Dietrich WE (2007) Calculating bed load transport in steep

boulder bed channels. Water Resour Res 43:.
https://doi.org/10.1029/2006WR005432

MEASUREMENT DATA OF FLOW DEPTH AND VELOCITY

- Ova dal Fuorn

Point(GPS)	Depth [cm]	Vx [m/s]	Vy [m/s]	C-S	Unit
137	17	0.098	0.019	1	1 (Glide)
138	14	0.115	-0.04	1	1 (Glide)
139	19	0.0741	0.028	1	1 (Glide)
140	15	0.454	-0.034	1	1 (Glide)
141	12	0.211	-0.05	1	1 (Glide)
142	5	0.017	0.012	1	1 (Glide)
1012	10	0.066	-0.015	2	1 (Glide)
1013	11	0.521	0.028	2	1 (Glide)
1014	16	0.703	-0.093	2	1 (Glide)
1015	16	0.549	0.032	2	1 (Glide)
1016	11	0.416	0.077	2	1 (Glide)
1017	11	0.32	0.061	2	1 (Glide)
1018	11	0.013	0.003	2	1 (Glide)
1019	18	0.647	-0.102	3	1 (Glide)
1020	10	0.508	-0.141	3	1 (Glide)
1021	8	0.62	-0.079	3	1 (Glide)
1022	11	0.716	-0.011	3	1 (Glide)
1023	14	0.807	-0.074	3	1 (Glide)
1024	14	0.719	-0.011	3	1 (Glide)
1025	5	-0.027	-0.009	3	1 (Glide)

Slope (%)	0.9
Unit Area(m2)	93.7
Max Velocity In the X direction (m/s)	0.807
Max Velocity In the Y direction (m/s)	0.077
Max Depth(cm)	19
Mean velocity in the X direction(m/s)	0.377
Mean velocity in the Y direction(m/s)	-0.02

Figure 63. Data measurements for flow depth and velocities in the X (longitudinal) direction and Y (transversal) direction form geomorphic unit 1

Point	Depth [cm]	Vx [m/s]	Vy[m/s]	C-S	Unit
1026	14	0.493	0.003	4a	2 (Riffle)
1027	18	1.03	-0.161	4a	2 (Riffle)
1028	16	0.78	-0.043	4a	2 (Riffle)
1029	8	0.472	-0.016	4a	2 (Riffle)
1035	10	0.793	0.003	5a	2 (Riffle)
1036	20	1.024	0.009	5a	2 (Riffle)
1037	14	0.72	0.076	5a	2 (Riffle)
1038	3	n.m	n.m	5a	2 (Riffle)
1044	10	0.531	-0.088	6a	2 (Riffle)
1045	19	0.891	-0.039	6a	2 (Riffle)
1046	19	0.889	-0.205	6a	2 (Riffle)
1047	6	0.152	-0.028	6a	2 (Riffle)

Slope (%)	1.3
Unit Area(m2)	39.8
Max Velocity In the X direction (m/s)	1.03
Max Velocity In the Y direction (m/s)	0.076
Max Depth(cm)	20
Mean velocity in the X direction(m/s)	0.71
Mean velocity in the Y direction(m/s)	-0.04

Figure 64. Data measurements for flow depth and velocities in the longitudinal and transversal direction form geomorphic unit 1

Point	Depth [cm]	Vx [m/s]	Vy[m/s]	C-S	Unit
1030	6	0.586	0.015	4b	3 (Riffle)
1031	19	0.913	-0.058	4b	3 (Riffle)
1032	15	0.954	-0.168	4b	3 (Riffle)
1033	14	0.896	-0.165	4b	3 (Riffle)
1034	7	0.002	-0.002	4b	3 (Riffle)
1039	9	1.043	0.039	5b	3 (Riffle)
1040	20	0.739	-0.056	5b	3 (Riffle)
1041	18	0.87	-0.028	5b	3 (Riffle)
1042	9	0.382	0.068	5b	3 (Riffle)
1043	4	n.m	n.m	5b	3 (Riffle)
1048	11	0.787	-0.063	6b	3 (Riffle)
1049	18	0.989	-0.037	6b	3 (Riffle)
1050	15	0.015	0.057	6b	3 (Riffle)
1051	11	0.614	-0.017	6b	3 (Riffle)
1052	7	-0.064	-0.024	6b	3 (Riffle)

Slope (%)	1.15
Unit Area(m2)	76
Max Velocity In the X direction (m/s)	1.043
Max Velocity In the Y direction (m/s)	0.068
Max Depth(cm)	20
Mean velocity in the X direction(m/s)	0.623
Mean velocity in the Y direction(m/s)	-0.025

Figure 65. Data measurements for flow depth and velocities in the longitudinal and transversal direction form geomorphic unit 1

Point	Depth [cm]	Vx [m/s]	Vy[m/s]	C-S	Unit
1086	8	-0.067	-0.02	13	4 (Riffle) 2nd channel.
1087	16	0.612	-0.211	13	4 (Riffle) 2nd channel.
1088	10	0.099	-0.058	13	4 (Riffle) 2nd channel.
1089	11	0.089	0.047	14	4 (Riffle) 2nd channel.
1090	11	0.517	0.179	14	4 (Riffle) 2nd channel.
1091	5	0.013	0.008	14	4 (Riffle) 2nd channel.
1092	3	n.m	n.m	15	4 (Riffle) 2nd channel.
1093	10	0.568	0.021	15	4 (Riffle) 2nd channel.
1094	8	0.329	0.049	15	4 (Riffle) 2nd channel.
1095	2	n.m	n.m	16	4 (Riffle) 2nd channel.
1096	9	0.499	-0.066	16	4 (Riffle) 2nd channel.
1097	7	0.026	-0.027	16	4 (Riffle) 2nd channel.
1098	9	0.101	-0.013	17	4 (Riffle) 2nd channel.
1099	9	0.357	-0.154	17	4 (Riffle) 2nd channel.
1100	8	0.205	0.04	17	4 (Riffle) 2nd channel.
1101	2	n.m	n.m	18	4 (Riffle) 2nd channel.
1102	4	n.m	n.m	18	4 (Riffle) 2nd channel.
1103	10	0.727	0.04	18	4 (Riffle) 2nd channel.
1105	11	0.578	-0.133	18	4 (Riffle) 2nd channel.
1104	2	n.m	n.m	18	4 (Riffle) 2nd channel.
1106	7	0.029	-0.008	19	4 (Riffle) 2nd channel.
1107	5	0.125	0.002	19	4 (Riffle) 2nd channel.
1108	8	0.663	0.169	19	4 (Riffle) 2nd channel.
1109	8	0.029	0.007	19	4 (Riffle) 2nd channel.

Slope (%)	1.6
Unit Area(m2)	139
Max Velocity In the X direction (m/s)	0.727
Max Velocity In the Y direction (m/s)	0.179
Max Depth(cm)	16
Mean velocity in the X direction(m/s)	0.311
Mean velocity in the Y direction(m/s)	0.003

Figure 66. Data measurements for flow depth and velocities in the longitudinal and transversal direction form geomorphic unit 4

Point	Depth [cm]	Vx [m/s]	Vy[m/s]	C-S	Unit
1055	10	0.178	-0.237	7	5 (Riffle)
1056	26	0.89	-0.142	7	5 (Riffle)
1057	20	1.169	-0.006	7	5 (Riffle)
1058	11	-0.018	-0.01	7	5 (Riffle)
1059	7	0.515	0.341	8	5 (Riffle)
1060	19	1.501	-0.242	8	5 (Riffle)
1061	25	1.044	-0.081	8	5 (Riffle)
1062	11	0.448	0.148	8	5 (Riffle)
1063	2	n.m	n.m	8	5 (Riffle)
1064	8	0.511	0.024	8	5 (Riffle)
1065	5	n.m	n.m	8	5 (Riffle)
1066	11	0.403	-0.107	9	5 (Riffle)
1067	21	0.859	-0.118	9	5 (Riffle)
1068	26	0.99	-0.11	9	5 (Riffle)
1069	13	0.084	-0.035	9	5 (Riffle)
1070	10	0.032	-0.005	10	5 (Riffle)
1071	32	1.256	-0.307	10	5 (Riffle)
1072	23	1.076	-0.441	10	5 (Riffle)
1073	14	0.315	-0.311	10	5 (Riffle)
1074	4	0.252	-0.031	10	5 (Riffle)
1075	8	0.62	-0.024	11	5 (Riffle)
1076	15	0.817	0.057	11	5 (Riffle)
1077	18	1.008	-0.053	11	5 (Riffle)
1078	16	0.734	0.148	11	5 (Riffle)
1079	5	0.011	0.014	11	5 (Riffle)
1080	3	n.m	n.m	11	5 (Riffle)
1081	12	0.001	0	12	5 (Riffle)
1082	12	0.667	-0.145	12	5 (Riffle)
1083	16	0.906	0.233	12	5 (Riffle)
1084	11	0.664	0.047	12	5 (Riffle)
1085	6	0.256	0.008	12	5 (Riffle)

Slope (%)	2.2
Unit Area(m2)	238
Max Velocity In the X direction (m/s)	1.501
Max Velocity In the Y direction (m/s)	0.341
Max Depth(cm)	32
Mean velocity in the X direction(m/s)	0.644
Mean velocity in the Y direction(m/s)	-0.036

Figure 67. Data measurements for flow depth and velocities in the longitudinal and transversal direction form geomorphic unit 5

Point (GPS)	Depth [cm]	Vx [m/s]	Vy[m/s]	C-S	Unit
1110	15	0.616	0.075	20	6 (Riffle)
1111	29	0.813	0.0092	20	6 (Riffle)
1112	14	0.533	0.082	20	6 (Riffle)
1113	10	0.557	-0.091	20	6 (Riffle)
1114	2	n.m	n.m	20	6 (Riffle)
1115	9	0.096	0.018	21	6 (Riffle)
1116	28	1.093	0.005	21	6 (Riffle)
1117	21	0.54	0.04	21	6 (Riffle)
1118	15	0.68	-0.135	21	6 (Riffle)
1119	11	0.262	-0.116	22	6 (Riffle)
1120	25	1.177	-0.059	22	6 (Riffle)
1121	24	0.906	-0.074	22	6 (Riffle)
1122	10	-0.097	0.011	22	6 (Riffle)
1123	3	n.m	n.m	22	6 (Riffle)
1124	8	-0.063	-0.058	23	6 (Riffle)
1125	26	1.106	-0.091	23	6 (Riffle)
1126	24	0.848	-0.104	23	6 (Riffle)
1127	19	0.387	0.12	23	6 (Riffle)
1128	3	n.m	n.m	23	6 (Riffle)
1129	11	0.059	0.013	24	6 (Riffle)
1130	17	0.39	-0.184	24	6 (Riffle)
1131	25	0.796	-0.311	24	6 (Riffle)
1132	18	0.669	-0.088	24	6 (Riffle)
1133	8	0.05	0.013	24	6 (Riffle)

Slope (%)	2.3
Unit Area(m2)	150
Max Velocity In the X direction (m/s)	1.177
Max Velocity In the Y direction (m/s)	0.12
Max Depth(cm)	29
Mean velocity in the X direction(m/s)	0.573
Mean velocity in the Y direction(m/s)	-0.037

Figure 68. Data measurements for flow depth and velocities in the longitudinal and transversal direction form geomorphic unit

Point(GPS)	Depth [cm]	Vx [m/s]	Vy[m/s]	C-S	Unit
1134	16	0.848	-0.317	25	7 (Riffle)
1135	24	1.807	-0.179	25	7 (Riffle)
1137	24	0.953	0.105	25	7 (Riffle)
1136	11	0.029	-0.078	25	7 (Riffle)
1138	15	-0.02	-0.022	26	7 (Riffle)
1139	26	0.538	-0.053	26	7 (Riffle)
1140	24	0.072	-0.178	26	7 (Riflle)
1141	4	-0.025	-0.006	26	7 (Riffle)
1142	11	0.565	0.188	27	7 (Riffle)
1143	25	0.386	0.158	27	7 (Riffle)
1144	31	1.037	-0.19	27	7 (Riffle)
1145	11	0.528	0.091	27	7 (Riffle)
1146	5	0.133	0.04	28	7 (Riffle)
1147	10	0.731	0.01	28	7 (Riffle)
1148	33	1.016	-0.034	28	7 (Riffle)
1149	11	0.156	-0.05	28	7 (Riffle)

Slope (%)	2.1
Unit Area(m2)	49.3
Max Velocity In the X direction (m/s)	1.807
Max Velocity In the Y direction (m/s)	0.188
Max Depth(cm)	33
Mean velocity in the X direction(m/s)	0.621
Mean velocity in the Y direction(m/s)	-0.019

Figure 69. Data measurements for flow depth and velocities in the longitudinal and transversal direction form geomorphic unit

Point(GPS)	Depth [cm]	Vx [m/s]	Vy[m/s]	C-S	Unit
1150	4	n.m	n.m	29	8 (Glide/Run)2nd Channel
1151	14	0.13	0.012	29	8 (Glide/Run)2nd Channel
1152	13	0.093	0.123	29	8 (Glide/Run)2nd Channel
1153	2	n.m	n.m	30	8 (Glide/Run)2nd Channel
1155	8	0.393	-0.023	30	8 (Glide/Run)2nd Channel
1154	9	0.33	0.017	30	8 (Glide/Run)2nd Channel
1156	9	0.408	-0.093	31	8 (Glide/Run)2nd Channel
1158	11	0.541	-0.174	31	8 (Glide/Run)2nd Channel
1157	4	n.m	n.m	31	8 (Glide/Run)2nd Channel
1159	3	n.m	n.m	32	8 (Glide/Run)2nd Channel
1160	7	0.025	-0.011	32	8 (Glide/Run)2nd Channel
1161	8	0.907	0.179	32	8 (Glide/Run)2nd Channel

Slope (%)	1.6
Unit Area(m2)	37.7
Max Velocity In the X direction (m/s)	0.907
Max Velocity In the Y direction (m/s)	0.179
Max Depth(cm)	14
Mean velocity in the X direction(m/s)	0.353
Mean velocity in the Y direction(m/s)	0.004

Figure 70. Data measurements for flow depth and velocities in the longitudinal and transversal direction form geomorphic unit 8

Point	Depth [cm]	Vx [m/s]	Vy [m/s]	C-S	Unit
1162	9	0.071	0.017	33	9 (Riffle)
1163	12	0.423	-0.062	33	9 (Riffle)
1164	17	0.572	0.093	33	9 (Riffle)
1165	14	0.969	0.227	33	9 (Riffle)
1166	12	0.534	0.022	33	9 (Riffle)
1167	6	0.343	0.213	33	9 (Riffle)
1168	9	0.33	-0.015	33	9 (Riffle)
1169	7	0.216	-0.031	33	9 (Riffle)
1170	5	0.363	0.027	34	9 (Riffle)
1171	10	0.316	0.133	34	9 (Riffle)
1172	18	0.825	0.399	34	9 (Riffle)
1173	14	1.139	0.299	34	9 (Riffle)
1174	15	0.794	-0.205	34	9 (Riffle)
1175	14	0.138	0.028	34	9 (Riffle)
1176	5	0.307	0.016	34	9 (Riffle)
1177	2	n.m	n.m	35	9 (Riffle)
1178	13	0.604	0.136	35	9 (Riffle)
1179	22	0.597	0.058	35	9 (Riffle)
1180	11	0.22	0.064	35	9 (Riffle)
1181	5	0.021	-0.022	35	9 (Riffle)

Slope (%)	2.8
Unit Area(m2)	63
Max Velocity In the X direction (m/s)	1.139
Max Velocity In the Y direction (m/s)	0.399
Max Depth(cm)	22
Mean velocity in the X direction(m/s)	0.5
Mean velocity in the Y direction(m/s)	0.08

Figure 71. Data measurements for flow depth and velocities in the longitudinal and transversal direction form geomorphic unit 9

Point	Depth [cm]	Vx [m/s]	Vy[m/s]	C-S	Unit
1182	10	0.828	0.395	36	10 (Riffle)
1183	26	0.959	-0.063	36	10 (Riffle)
1184	29	1.469	-0.143	36	10 (Riffle)
1185	15	0.157	0.044	36	10 (Riffle)
1186	2	n.m	n.m	36	10 (Riffle)
1187	2	n.m	n.m	37	10 (Riffle)
1188	15	0.336	-0.104	37	10 (Riffle)
1189	25	0.833	0.021	37	10 (Riffle)
1190	21	0.545	0.213	37	10 (Riffle)
1191	13	0.101	-0.033	37	10 (Riffle)
1192	6	0.233	-0.093	38	10 (Riffle)
1193	19	1.188	0.015	38	10 (Riffle)
1194	21	1.121	-0.118	38	10 (Riffle)
1195	23	0.159	-0.076	38	10 (Riffle)
1196	5	-0.003	-0.003	38	10 (Riffle)

Slope (%)	1.8
Unit Area(m2)	34.4
Max Velocity In the X direction (m/s)	1.469
Max Velocity In the Y direction (m/s)	0.395
Max Depth(cm)	29
Mean velocity in the X direction(m/s)	0.671
Mean velocity in the Y direction(m/s)	0.032

Figure 72. Data measurements for flow depth and velocities in the longitudinal and transversal direction form geomorphic unit 10

Point	Depth [cm]	Vx [m/s]	Vy[m/s]	C-S	Unit
1197	9	0.083	0.058	39	11 (Riffle)
1198	21	0.748	-0.004	39	11 (Riffle)
1199	21	0.665	0.069	39	11 (Glide)
1200	20	0.961	0.027	39	11 (Glide)
1201	8	0.049	-0.016	39	11 (Glide)
1202	7	0.378	-0.169	40	11 (Glide)
1203	17	0.676	-0.209	40	11 (Glide)
1204	19	0.784	-0.089	40	11 (Glide)
1205	18	0.771	-0.079	40	11 (Glide)
1206	11	0.394	0.031	40	11 (Glide)
1207	3	n.m	n.m	40	11 (Glide)
1208	2	n.m	n.m	41	11 (Glide)
1209	10	0.608	-0.088	41	11 (Glide)
1210	11	0.692	-0.109	41	11 (Glide)
1211	13	0.15	-0.053	41	11 (Glide)
1212	14	0.599	-0.117	41	11 (Glide)
1213	15	0.568	-0.214	41	11 (Glide)
1214	14	0.072	-0.058	41	11 (Glide)
1215	3	n.m	n.m	42	11 (Glide)
1216	12	0.497	-0.017	42	11 (Glide)
1217	16	0.721	-0.158	42	11 (Glide)
1218	14	0.532	-0.171	42	11 (Glide)
1219	13	0.69	-0.256	42	11 (Glide)
1220	10	0.024	-0.069	42	11 (Glide)
1221	7	0.017	-0.004	43	11 (Glide)
1222	10	0.481	-0.083	43	11 (Glide)
1223	16	0.564	-0.004	43	11 (Glide)
1224	13	0.783	-0.175	43	11 (Glide)
1225	13	0.308	-0.04	43	11 (Glide)
1226	9	0.08	-0.046	43	11 (Glide)
		0.961	0.069		
		0.495	-0.071		

Slope (%)	1.3
Unit Area(m2)	102
Max Velocity In the X direction (m/s)	0.961
Max Velocity In the Y direction (m/s)	0.069
Max Depth(cm)	21
Mean velocity in the X direction(m/s)	0.495
Mean velocity in the Y direction(m/s)	-0.071

Figure 73. Data measurements for flow depth and velocities in the longitudinal and transversal direction form geomorphic unit unit 11

87

- Rio Carlino

Point (GPS)	Depth [cm]	Vx [m/s]	Vy [m/s]	C-S	Geomorphic Unit
1017	13	0.027	0.003	1	1(Pool)
1018	44	0.058	0.215	1	1(Pool)
1019	31	0.082	0.0251	1	1(Pool)
1020	16	-0.004	-0.016	1	1(Pool)
1021	29	0.016	-0.005	2	1(Pool)
1022	35	0.345	0.144	2	1(Pool)
1023	18	0.194	-0.054	2	1(Pool)
1024	6	0.471	0.591	2	1(Pool)

Slope (%)	3.7
Unit Area(m2)	8
Max Velocity In the Y direction (m/s)	0.471
Max Velocity In the X direction (m/s)	0.591
Max Depth(cm)	44
Mean velocity in the X direction(m/s)	0.149
Mean velocity in the Y direction(m/s)	0.113

Figure 74 Data measurements for flow depth and velocities in the longitudinal and transversal direction form geomorphic unit 1

Point(GPS)	Depth [cm]	Vx [m/s]	Vy [m/s]	C-S	Geomorphic Unit
1025	13	0.119	-0.041	3	2(Rapid)
1026	23	0.293	-0.035	3	2(Rapid)
1027	26	0.026	-0.017	3	2(Rapid)
1028	13	0.035	-0.01	3	2(Rapid)
1029	24	0.056	0.01	3	2(Rapid)
1030	6	n.m	n.m	3	2(Rapid)
1031	12	-0.036	-0.03	4	2(Rapid)
1032	25	0.126	-0.327	4	2(Rapid)
1033	23	0.076	0.101	4	2(Rapid)
1034	24	0.197	-0.216	4	2(Rapid)
1035	10	0.277	-0.07	4	2(Rapid)
1036	20	0.608	-0.115	4	2(Rapid)
1037	9	-0.03	0.015	5	2(Rapid)
1038	18	0.88	0.019	5	2(Rapid)
1039	22	0.352	0.031	5	2(Rapid)
1040	26	0.236	-0.031	5	2(Rapid)
1041	11	-0.053	-0.053	5	2(Rapid)
1042	15	0.098	-0.003	6	2(Rapid)
1043	18	0.253	0.523	6	2(Rapid)
1044	20	0.414	0.082	6	2(Rapid)
1045	22	0.407	0.05	6	2(Rapid)
1046	8	0.006	-0.007	6	2(Rapid)

Slope (%)	6.13
Unit Area(m2)	108
Max Velocity In the X direction (m/s)	0.88
Max Velocity In the X direction (m/s)	0.523
Max Depth(cm)	26
Mean velocity in the X direction(m/s)	0.207
Mean velocity in the Y direction(m/s)	-0.006

Figure 75. Data measurements for flow depth and velocities in the longitudinal and transversal direction form geomorphic unit 2

Point	Depth [cm]	Vx [m/s]	Vy [m/s]	C-S	Geomorphic Unit
1047	2	n.m	n.m	7	3 (Rapid)
1048	12	0.774	0.025	7	3 (Rapid)
1049	18	0.223	0.149	7	3 (Rapid)
1050	20	0.332	0.351	7	3 (Rapid)
1051	17	0.271	0.008	7	3 (Rapid)
1052	21	0.247	0.028	7	3 (Rapid)
1053	22	0.253	-0.07	7	3 (Rapid)
1054	2	n.m	n.m	7	3 (Rapid)
1056	14	-0.03	-0.008	8	3 (Rapid)
1057	16	0.073	0.041	8	3 (Rapid)
1058	26	0.467	0.225	8	3 (Rapid)
1059	22	0.047	0.062	8	3 (Rapid)
1060	8	0.002	0.001	8	3 (Rapid)
1061	6	n.m	n.m	8	3 (Rapid)
1062	2	n.m	n.m	9	3 (Rapid)
1063	18	0.075	0.037	9	3 (Rapid)
1064	16	0.348	0.033	9	3 (Rapid)
1065	26	0.892	-0.563	9	3 (Rapid)
1066	16	0.312	0.142	9	3 (Rapid)
1067	8	n.m	n.m	9	3 (Rapid)
1068	2	n.m	n.m	10	3 (Rapid)
1069	18	0.387	-0.051	10	3 (Rapid)
1070	27	0.588	-0.371	10	3 (Rapid)
1071	18	0.365	-0.108	10	3 (Rapid)
1072	24	0.567	-0.088	10	3 (Rapid)
1073	2	n.m	n.m	10	3 (Rapid)
1074	3	n.m	n.m	11	3 (Rapid)
1075	20	0.318	-0.078	11	3 (Rapid)
1076	18	0.529	0.225	11	3 (Rapid)
1077	20	0.317	0.034	11	3 (Rapid)
1078	24	0.267	0.093	11	3 (Rapid)
1079	9	0.142	0.019	11	3 (Rapid)
1080	4	n.m	n.m	11	3 (Rapid)
1081	2	n.m	n.m	11	3 (Rapid)

Slope (%)	5.2
Unit Area(m2)	160
Max Velocity In the X direction (m/s)	0.892
Max Velocity In the Y direction (m/s)	0.351
Max Depth(cm)	27
Mean velocity in the X direction(m/s)	0.324
Mean velocity in the Y direction(m/s)	0.006

Figure 76. Data measurements for flow depth and velocities in the longitudinal and transversal direction form geomorphic unit 3

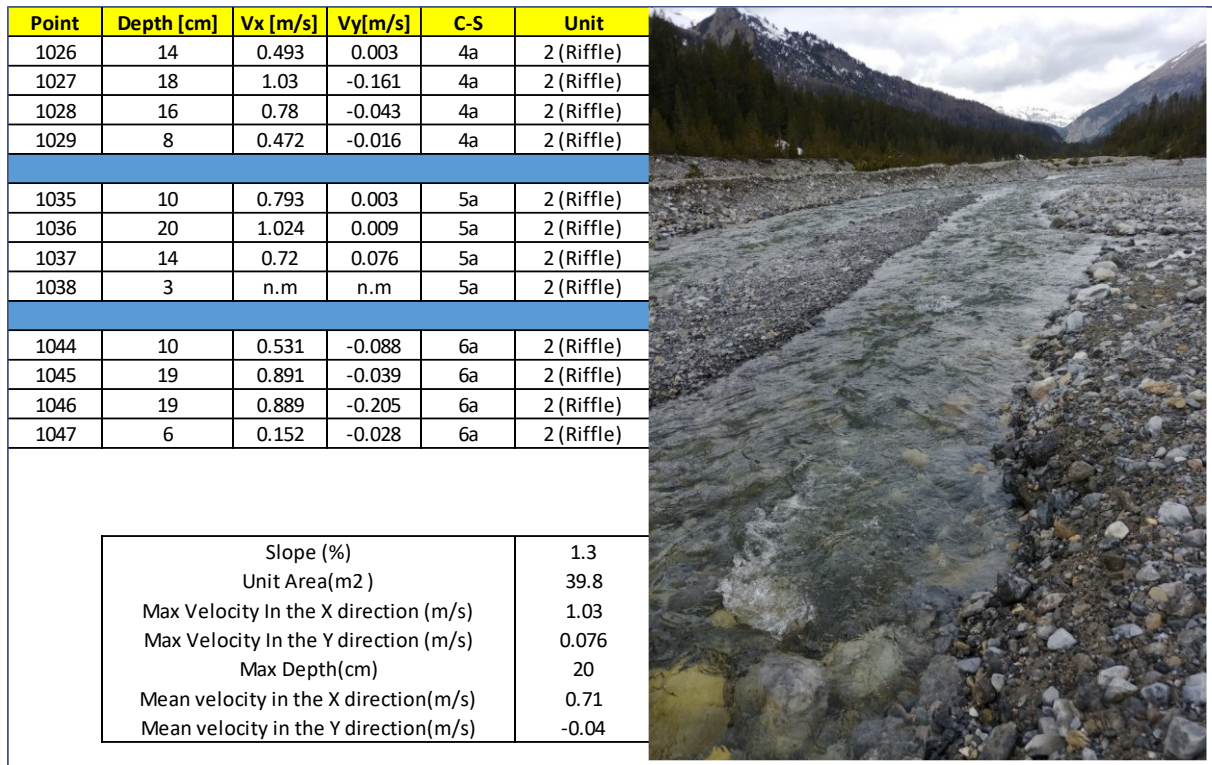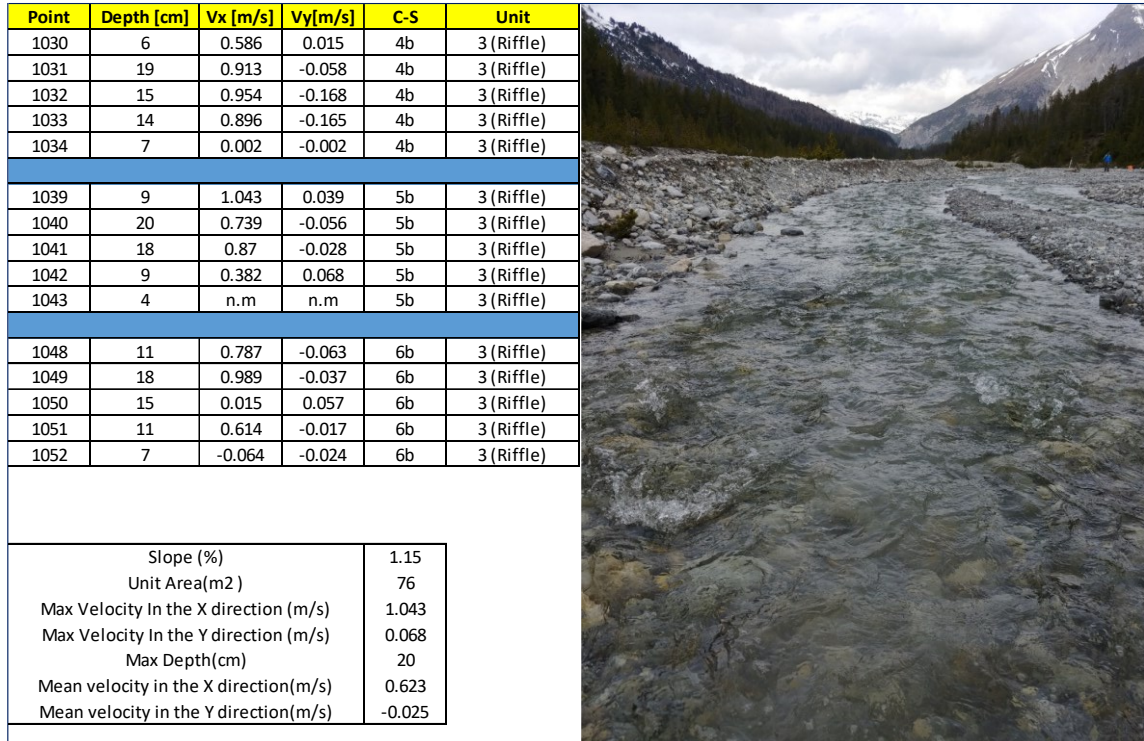| Point	Depth [cm]	Vx [m/s]	Vy [m/s]	C-S	Geomorphic Unit
1082	2	n.m	n.m	12	4(Rapid)
1083	12	0.505	0.012	12	4(Rapid)
1084	18	0.317	-0.095	12	4(Rapid)
1085	24	0.719	0.122	12	4(Rapid)
1086	22	0.25	0.062	12	4(Rapid)
1087	15	0.384	0.629	12	4(Rapid)
1088	21	0.137	0.124	12	4(Rapid)
1089	3	n.m	n.m	12	4(Rapid)
1090	10	-0.007	0.011	13	4(Rapid)
1091	19	0.213	0.25	13	4(Rapid)
1092	17	0.628	-0.159	13	4(Rapid)
1093	15	0.265	0.338	13	4(Rapid)
1094	20	0.77	0.569	13	4(Rapid)
1095	7	0.105	0.165	13	4(Rapid)
1096	3	n.m	n.m	13	4(Rapid)

Slope (%)	6.26
Unit Area(m2)	92
Max Velocity In the X direction (m/s)	0.77
Max Velocity In the Y direction (m/s)	0.629
Max Depth(cm)	24
Mean velocity in the X direction(m/s)	0.357
Mean velocity in the Y direction(m/s)	0.169
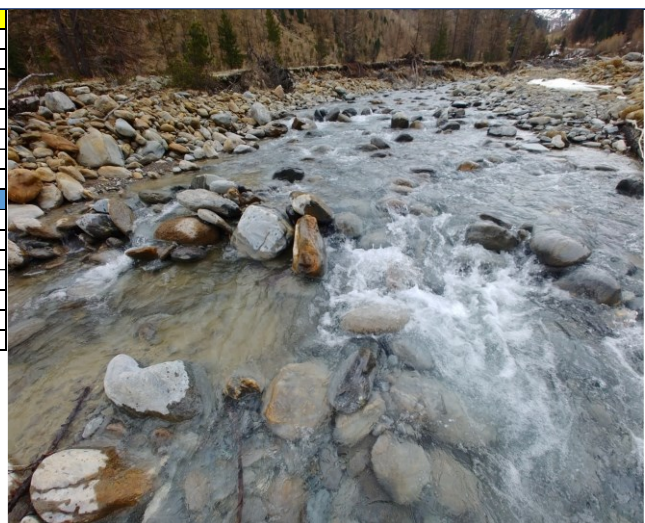
Figure 77. Data measurements for flow depth and velocities in the longitudinal and transversal direction form geomorphic unit 4

Point	Depth [cm]	Vx [m/s]	Vy[m/s]	C-S	Geomorphic Unit
1097	2	n.m	n.m	14	5(Rapid)
1098	22	0.351	-0.093	14	5(Rapid)
1099	25	0.705	-0.359	14	5(Rapid)
1100	15	0.257	-0.301	14	5(Rapid)
1101	22	0.278	-0.299	14	5(Rapid)
1102	11	0.227	0.085	14	5(Rapid)
1103	3	n.m	n.m	14	5(Rapid)
1104	12	0.175	0.023	15	5(Rapid)
1105	26	0.213	0.052	15	5(Rapid)
1106	16	0.969	-0.092	15	5(Rapid)
1107	22	0.82	-0.421	15	5(Rapid)
1108	14	0.133	0.034	15	5(Rapid)
1109	3	n.m	n.m	15	5(Rapid)
1110	2	n.m	n.m	16	5(Rapid)
1111	21	0.076	0.047	16	5(Rapid)
1112	31	0.476	0.128	16	5(Rapid)
1113	24	0.323	0.346	16	5(Rapid)
1114	29	0.029	-0.033	16	5(Rapid)
1115	4	n.m	n.m	16	5(Rapid)
1116	3	n.m	n.m	17	5(Rapid)
1117	27	0.404	0.061	17	5(Rapid)
1118	25	0.502	0.057	17	5(Rapid)
1119	26	0.251	0.093	17	5(Rapid)
1120	20	-0.05	-0.087	17	5(Rapid)
1121	4	n.m	n.m	17	5(Rapid)
1122	3	n.m	n.m	18	5(Rapid)
1123	24	0.045	-0.061	18	5(Rapid)
1124	30	0.405	0.043	18	5(Rapid)
1125	24	0.601	0.453	18	5(Rapid)
1126	12	0.041	-0.115	18	5(Rapid)
1127	2	n.m	n.m	18	5(Rapid)
1128	3	n.m	n.m	19	5(Rapid)
1129	23	0.7	0.69	19	5(Rapid)
1130	38	0.56	-0.17	19	5(Rapid)
1131	22	0.08	0.16	19	5(Rapid)
1132	14	0.106	-0.047	19	5(Rapid)
1133	4	n.m	n.m	19	5(Rapid)

Slope (%)	5
Unit Area(m2)	108
Max Velocity In the X direction (m/s)	0.969
Max Velocity In the Y direction (m/s)	0.629
Max Depth(cm)	38
Mean velocity in the X direction(m/s)	0.317
Mean velocity in the Y direction(m/s)	0.119

Figure 78. Data measurements for flow depth and velocities in the longitudinal and transversal direction form geomorphic unit 5
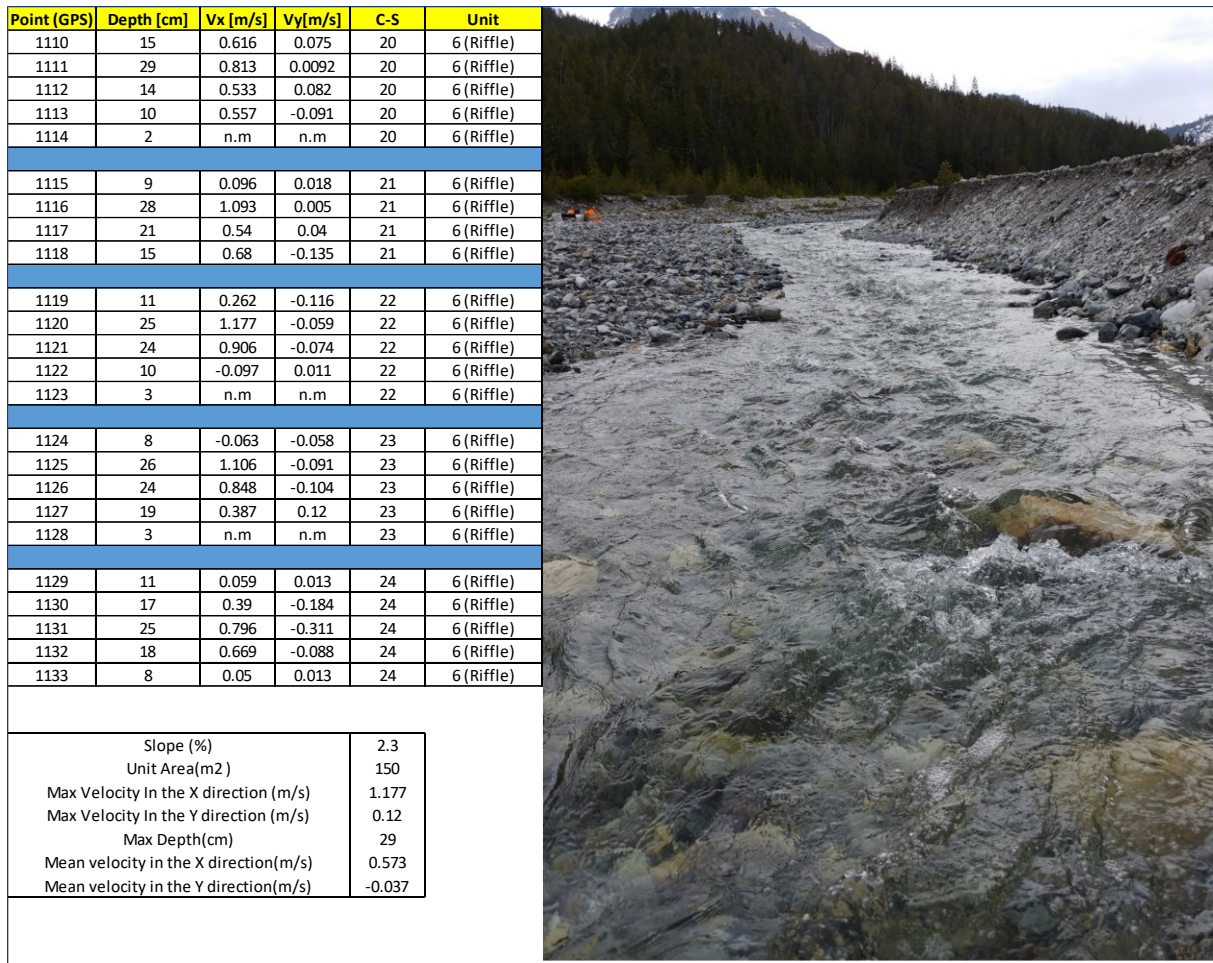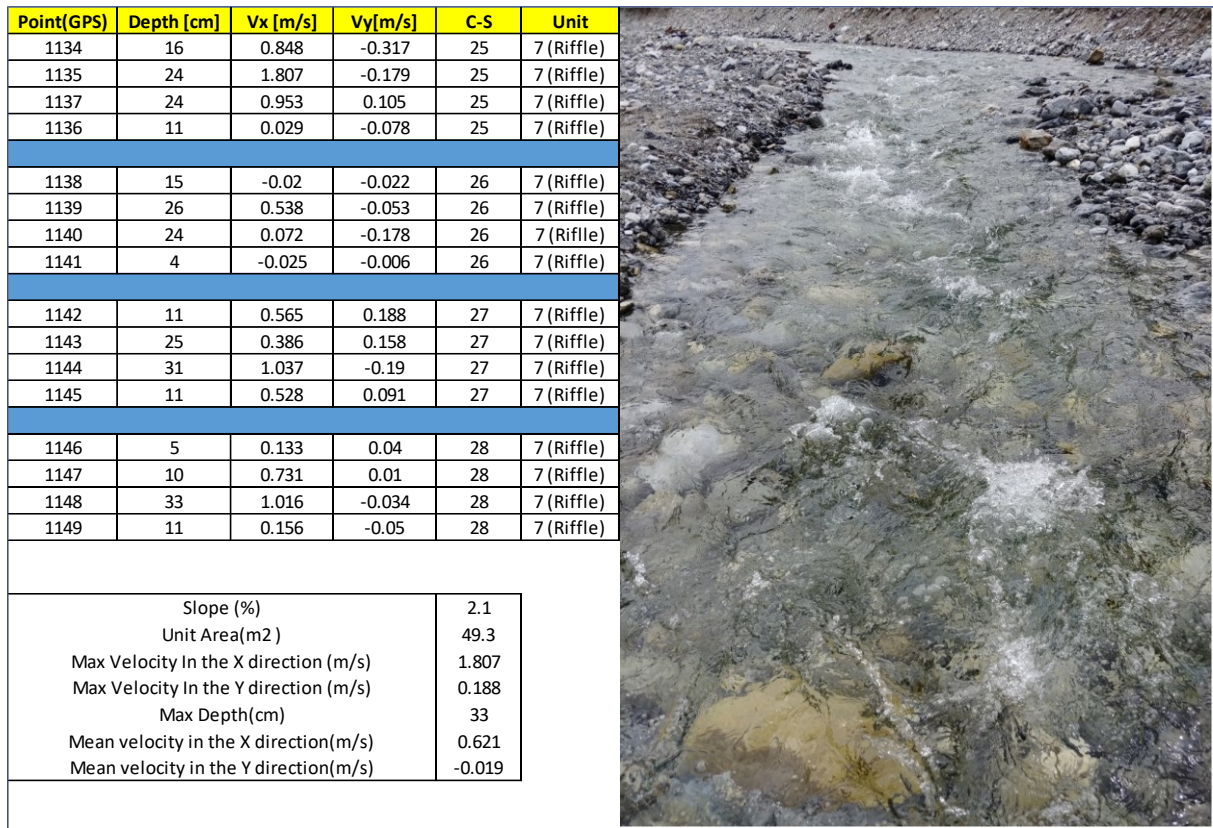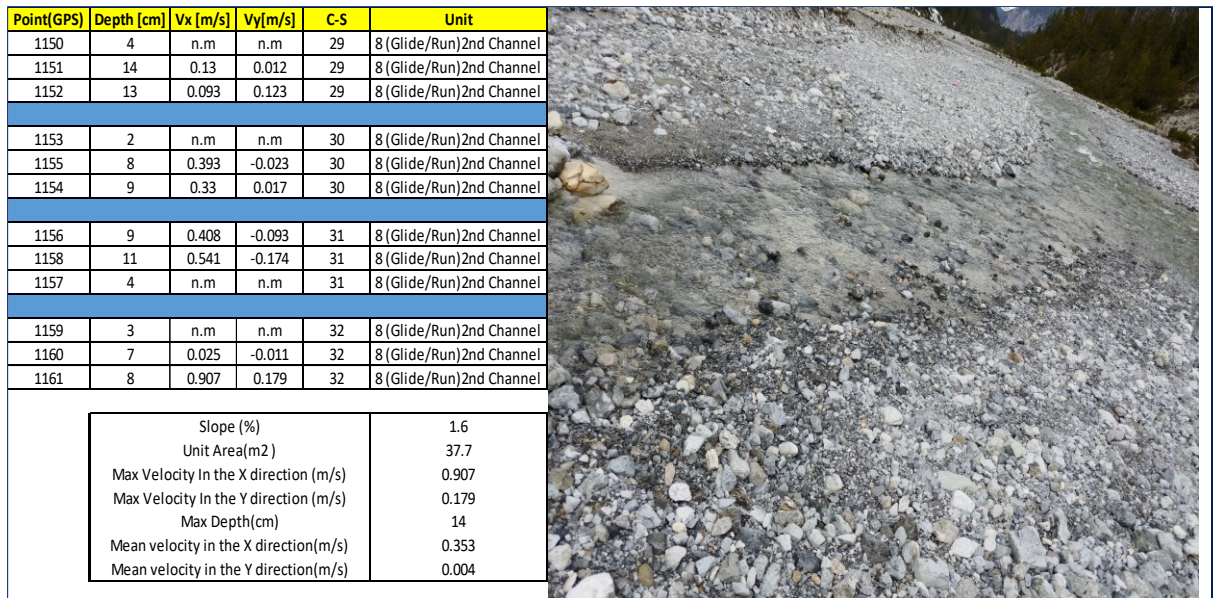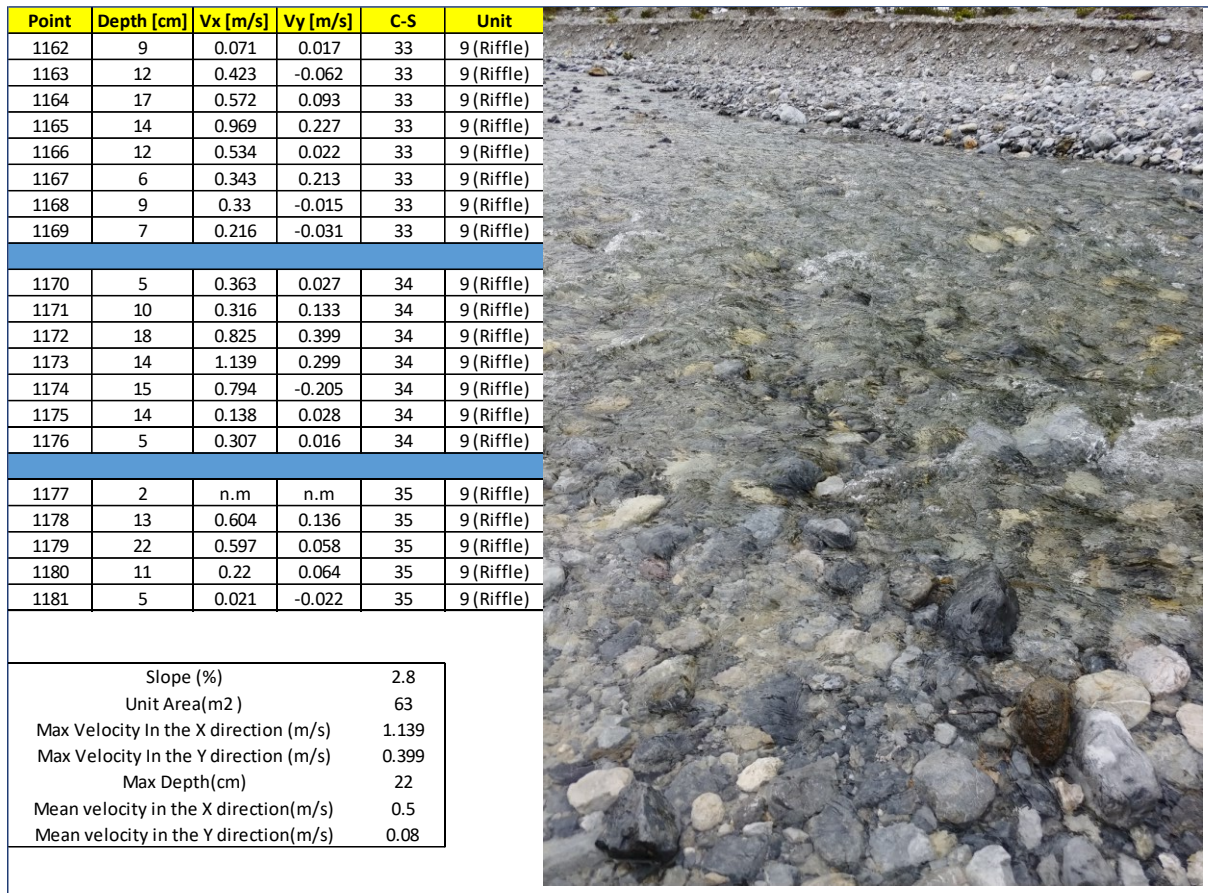
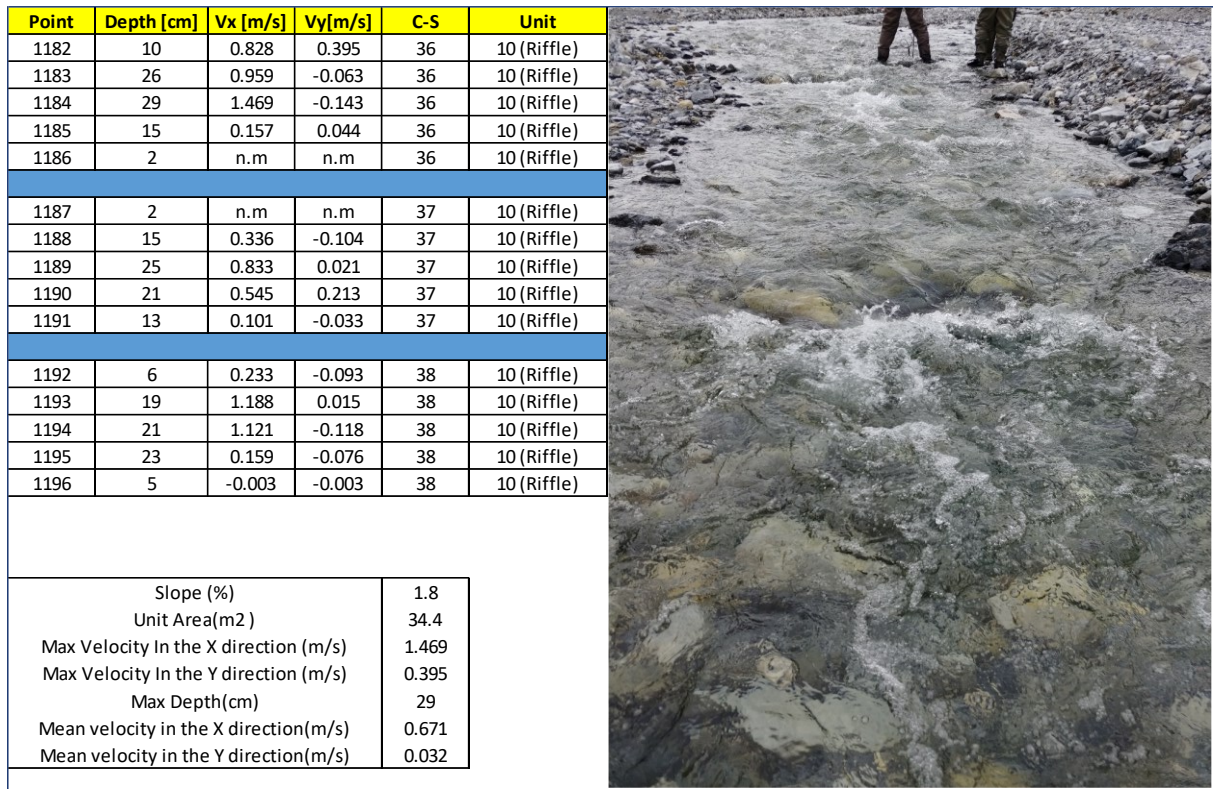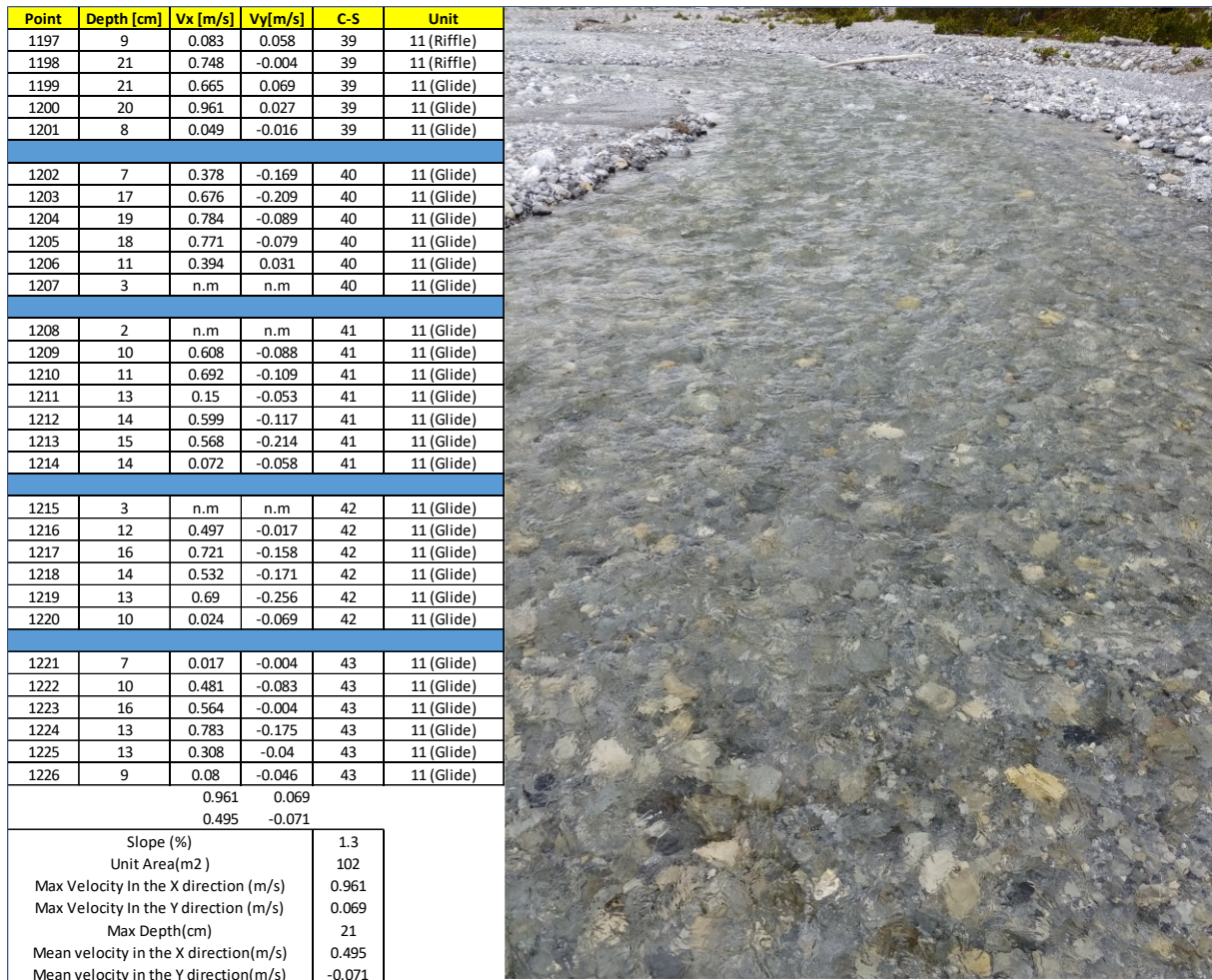| Point	Depth [cm]	Vx [m/s]	Vy[m/s]	C-S	Unit
1134	3	n.m	n.m	20	6(Riffle)
1135	20	0.172	-0.118	20	6(Riffle)
1136	26	0.649	-0.184	20	6(Riffle)
1137	25	0.553	-0.047	20	6(Riffle)
1139	21	-0.071	0.059	20	6(Riffle)
1040	4	n.m	n.m	21	6(Riffle)
1041	16	0.068	0.015	21	6(Riffle)
1042	22	0.278	-0.233	21	6(Riffle)
1043	39	0.085	-0.032	21	6(Riffle)
1044	28	0.026	-0.016	21	6(Riffle)
1045	12			21	6(Riffle)
1146	3	n.m	n.m	22	6(Riffle)
1147	24	0.042	0.024	22	6(Riffle)
1148	27	0.134	0.031	22	6(Riffle)
1149	30	0.467	0.077	22	6(Riffle)
1150	24	0.123	0.096	22	6(Riffle)
1151	5	0.001	0.027	22	6(Riffle)
1152	2	n.m	n.m	23	6(Riffle)
1153	16	0.147	-0.053	23	6(Riffle)
1154	22	0.367	-0.39	23	6(Riffle)
1155	23	0.237	-0.342	23	6(Riffle)
1156	20	0.146	-0.128	23	6(Riffle)
1157	14	0.033	-0.38	23	6(Riffle)
1158	5	n.m	n.m	23	6(Riffle)

Slope (%)	6
Unit Area(m2)	91.1
Max Velocity In the X direction (m/s)	0.649
Max Velocity In the Y direction (m/s)	0.096
Max Depth(m)	39
Mean velocity in the X direction(m/s	0.192
Mean velocity in the Y direction(m/s	-0.089
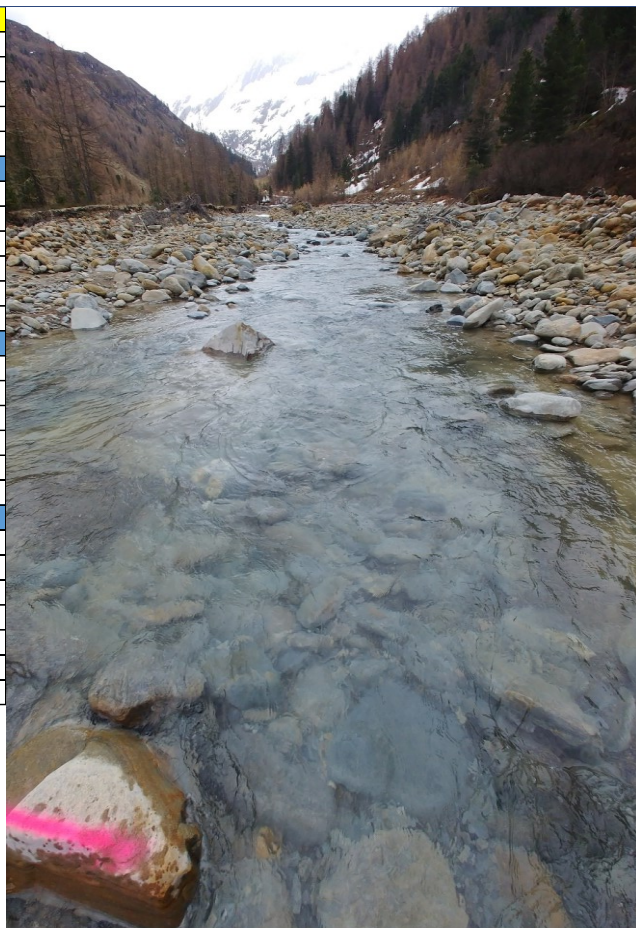
Figure 79. Data measurements for flow depth and velocities in the longitudinal and transversal direction form geomorphic unit 6

Point	Depth [cm]	Vx [m/s]	Vy[m/s]	C-S	Unit
1159	3	n.m	n.m	24	7(Rapid)
1160	16	0.147	-0.053	24	7(Rapid)
1161	28	0.817	-0.05	24	7(Rapid)
1162	12	0.126	-0.071	24	7(Rapid)
1163	16	0.043	-0.402	24	7(Rapid)
1164	7	n.m	n.m	25	7(Rapid)
1165	18	0.624	-0.196	25	7(Rapid)
1166	28	3.329	0.212	25	7(Rapid)
1167	12	0.501	-0.0446	25	7(Rapid)
1169	10	0.178	-0.021	26	7(Rapid)
1170	21	0.253	-0.106	26	7(Rapid)
1171	31	0.507	-0.374	26	7(Rapid)
1172	2	n.m	n.m	26	7(Rapid)

Slope (%)	6.07
Unit Area(m2)	50.72
Max Velocity In the X direction (m/s)	3.329
Max Velocity In the Y direction (m/s)	0.212
Max Depth(cm)	31
Mean velocity in the X direction(m/s)	0.650
Mean velocity in the Y direction(m/s)	-0.111

Figure 80. Data measurements for flow depth and velocities in the longitudinal and transversal direction form geomorphic unit 7

Point	Depth [cm]	Vx [m/s]	Vy[m/s]	C-S	Unit
1174	27	0.117	-0.255	27	8(Glide)
1175	28	0.445	-0.195	27	8(Glide)
1176	35	0.075	-0.035	27	8(Glide)
1177	30	-0.089	0.057	27	8(Glide)
1178	3	n.m	n.m	27	8(Glide)
1180	10	0.14	-0.067	28	8(Glide)
1181	28	0.39	-0.21	28	8(Glide)
1182	32	0.208	-0.299	28	8(Glide)
1183	24	0.098	-0.24	28	8(Glide)
1185	4	n.m	n.m	29	8(Glide)
1186	26	0.217	-0.421	29	8(Glide)
1187	30	0.342	-0.239	29	8(Glide)
1188	25	0.383	-0.064	29	8(Glide)
1189	18	0.011	-0.031	29	8(Glide)
1190	9	0.298	-0.143	29	8(Glide)

Slope (%)	4.2
Unit Area(m2)	60.07
Max Velocity In the X direction (m/s)	0.445
Max Velocity In the Y direction (m/s)	0.212
Max Depth(cm)	35
Mean velocity in the X direction(m/s)	0.203
Mean velocity in the Y direction(m/s)	-0.111

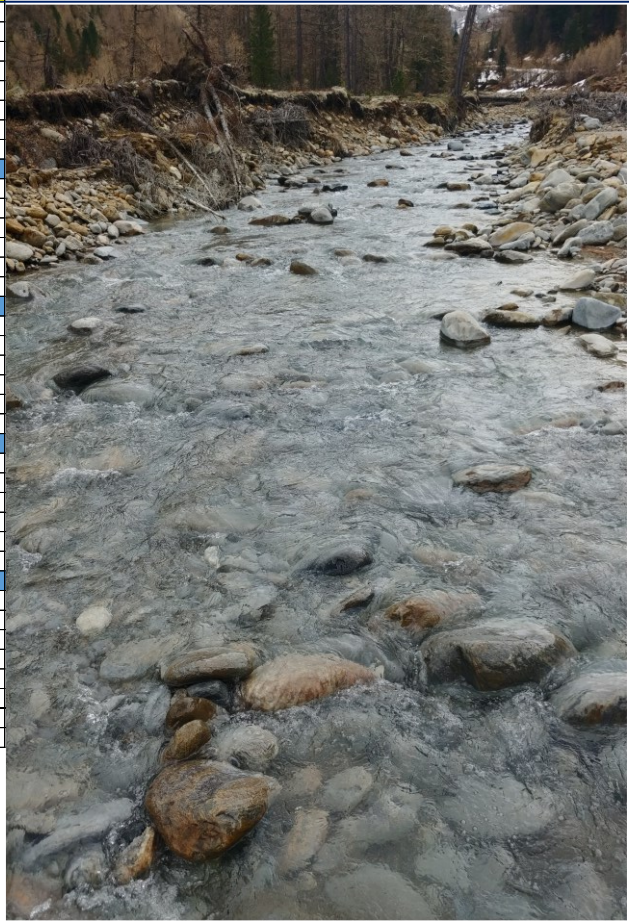Figure 81. Data measurements for flow depth and velocities in the longitudinal and transversal direction form geomorphic unit 8

Point	Depth [cm]	Vx [m/s]	Vy [m/s]	C-S	Unit
1192	4	n.m	n.m	30	9(Rapid)
1193	16	0.496	-0.212	30	9(Rapid)
1194	8	0.491	-0.057	30	9(Rapid)
1195	10	0.468	-0.374	30	9(Rapid)
1196	10	0.29	-0.318	30	9(Rapid)
1197	12	0.181	-0.13	30	9(Rapid)
1198	17	0.121	-0.314	30	9(Rapid)
1199	24	0.15	-0.334	30	9(Rapid)
1202	26	0.204	-0.348	31	9(Rapid)
1203	14	0.129	-0.145	31	9(Rapid)
1204	10	-0.039	-0.042	31	9(Rapid)
1205	18	0.402	-0.181	31	9(Rapid)
1206	8	0.749	0.3	31	9(Rapid)
1207	13	0.141	-0.334	31	9(Rapid)
1208	3	n.m	n.m	31	9(Rapid)
1210	18	0.383	-0.171	32	9(Rapid)
1211	19	0.122	-0.632	32	9(Rapid)
1212	22	0.121	-0.342	32	9(Rapid)
1213	9	0.304	-0.103	32	9(Rapid)
1214	18	0.218	-0.148	32	9(Rapid)
1215	10	0.182	-0.194	32	9(Rapid)
1216	4	n.m	n.m	32	9(Rapid)

|	
Slope (%)	4.6
Unit Area(m2)	207
Max Velocity In the X direction (m/s)	0.749
Max Velocity In the Y direction (m/s)	0.3
Max Depth(cm)	26
Mean velocity in the X direction(m/s)	0.269
Mean velocity in the Y direction(m/s)	-0.215

Figure 82. Data measurements for flow depth and velocities in the longitudinal and transversal direction form geomorphic unit 9

Point	Depth [cm]	Vx [m/s]	Vy[m/s]	C-S	Unit
1218	18	0.277	-0.814	33	10(Rapid)
1219	18	0.369	-0.167	33	10(Rapid)
1220	30	0.723	-0.322	33	10(Rapid)
1221	8	0.738	-0.199	33	10(Rapid)
1222	3	n.m	n.m	33	10(Rapid)
1224	14	0.387	0.165	34	10(Rapid)
1225	20	0.443	-0.19	34	10(Rapid)
1226	28	0.227	-0.204	34	10(Rapid)
1227	15	0.399	-0.339	34	10(Rapid)
1228	3	n.m	n.m	34	10(Rapid)
1230	21	0.49	0.306	35	10(Rapid)
1231	21	0.856	-0.294	35	10(Rapid)
1232	18	0.151	-0.277	35	10(Rapid)
1233	20	0.59	-0.139	35	10(Rapid)
1234	2	n.m	n.m	35	10(Rapid)
1236	12	0.456	-0.473	36	10(Rapid)
1237	22	0.171	-0.055	36	10(Rapid)
1238	18	0.437	-0.343	36	10(Rapid)
1239	18	-0.018	0.019	36	10(Rapid)
1240	4	n.m	n.m	36	10(Rapid)

| Slope (%)	5.4
Unit Area(m2)	149
Max Velocity In the X direction (m/s)	0.856
Max Velocity In the Y direction (m/s)	0.306
Max Depth(cm)	30
Mean velocity in the X direction(m/s)	0.419
Mean velocity in the Y direction(m/s)	-0.208
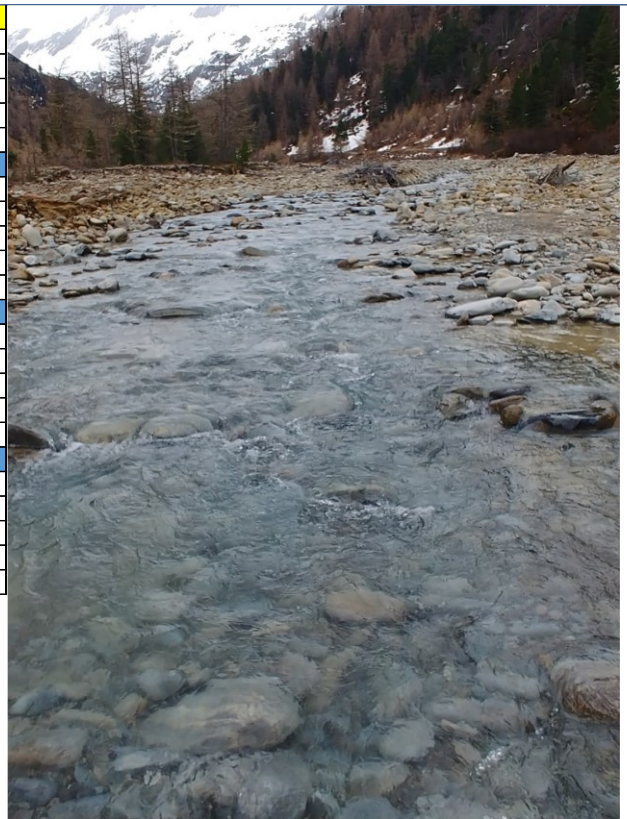
Figure 83. Data measurements for flow depth and velocities in the longitudinal and transversal direction form geomorphic unit 10

Point(GPS)	Depth [cm]	Vx [m/s]	Vy[m/s]	C-S	Unit
1241	10	0.609	-0.271	37	11(Glide) 2nd Channel
1242	18	0.028	-0.019	37	11(Glide) 2nd Channel
1243	14	0.967	-0.558	37	11(Glide) 2nd Channel
1244	3	n.m	n.m	37	11(Glide) 2nd Channel
1245	2	n.m	n.m	38	11(Glide) 2nd Channel
1246	14	0.16	-0.247	38	11(Glide) 2nd Channel
1247	15	0.478	-0.015	38	11(Glide) 2nd Channel
1248	3	n.m	n.m	38	11(Glide) 2nd Channel
1250	22	0.029	0.003	39	11(Glide) 2nd Channel
1251	26	0.431	-0.295	39	11(Glide) 2nd Channel
1252	22	0.048	-0.017	39	11(Glide) 2nd Channel
1253	3	n.m	n.m	39	11(Glide) 2nd Channel
1255	19	0.415	-0.217	40	11(Glide) 2nd Channel
1256	26	0.274	-0.234	40	11(Glide) 2nd Channel
1257	20	0.034	0.013	40	11(Glide) 2nd Channel
1258	2	n.m	n.m	40	11(Glide) 2nd Channel

Slope (%)	4.3
Unit Area(m2)	22.7
Max Velocity In the X direction (m/s)	0.967
Max Velocity In the Y direction (m/s)	0.013
Max Depth(cm)	26
Mean velocity in the X direction(m/s)	0.316
Mean velocity in the Y direction(m/s)	-0.169

Figure 84. Data measurements for flow depth and velocities in the longitudinal and transversal direction form geomorphic unit 11
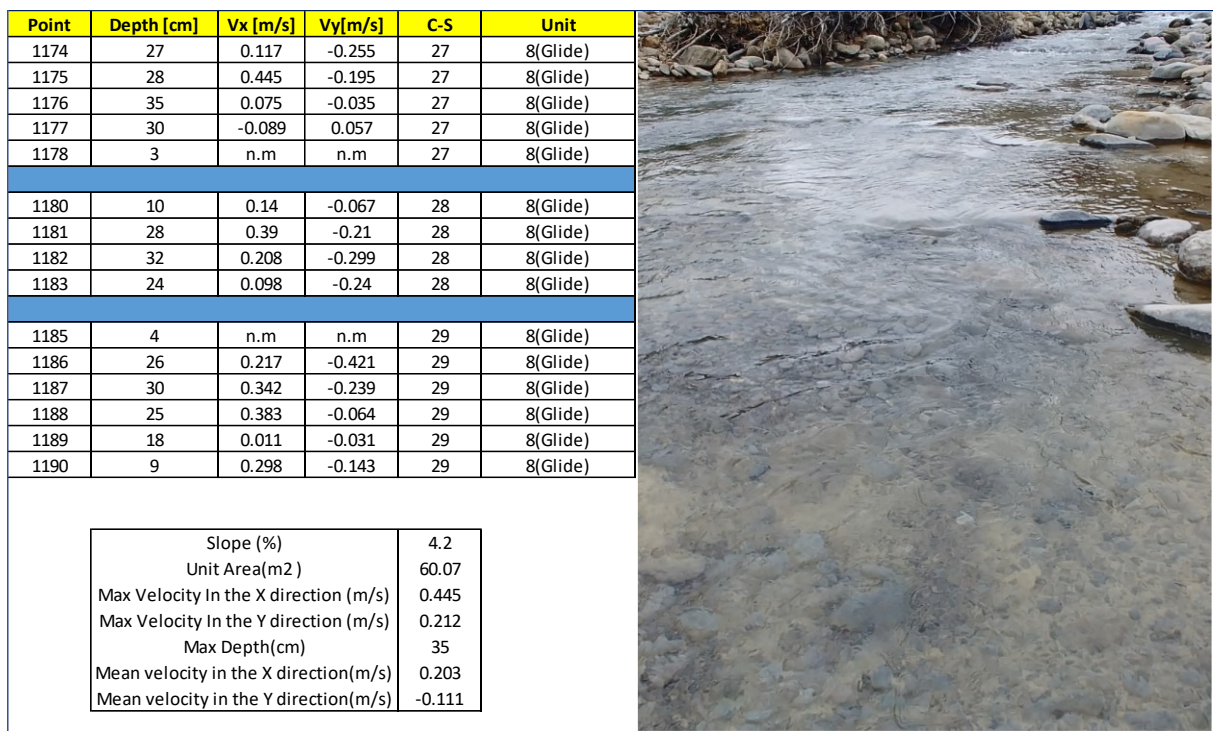
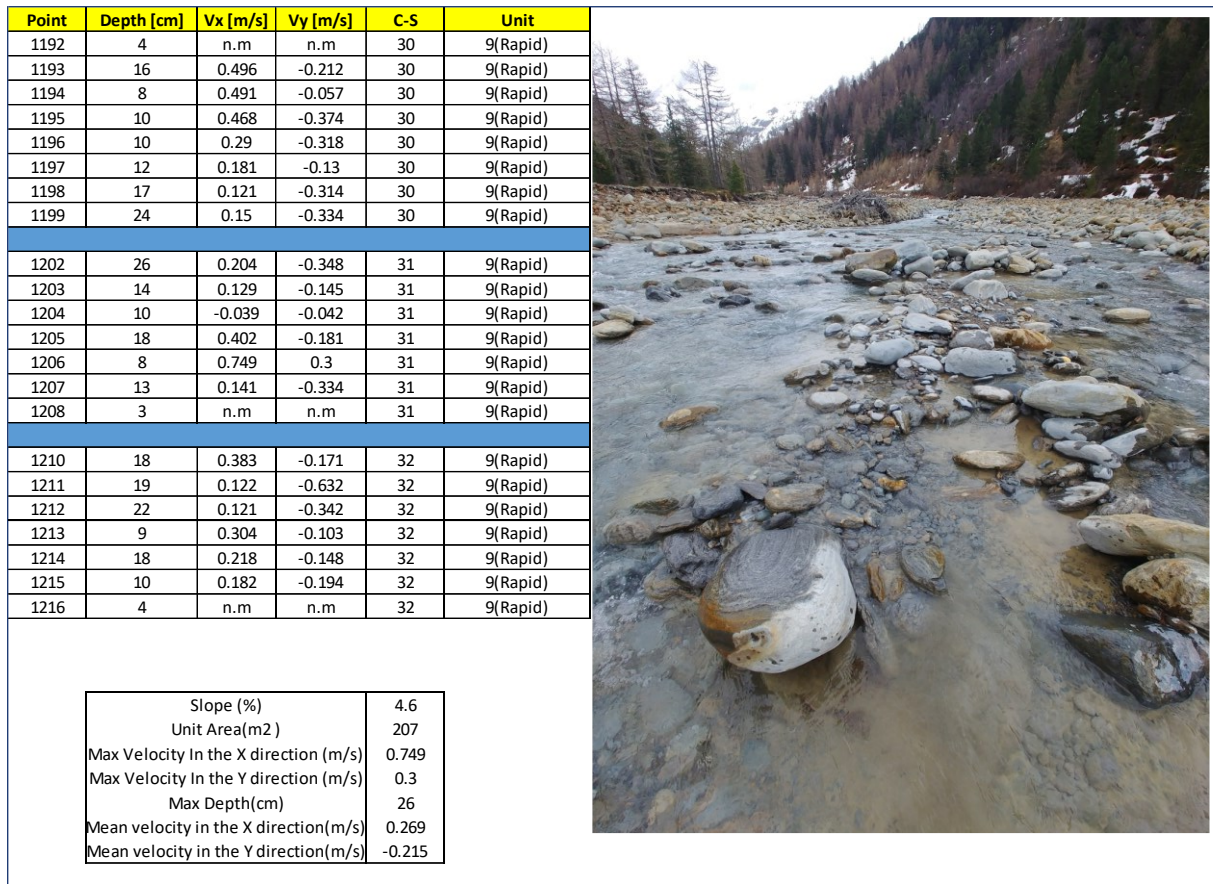*GRAIN SIZE DISTRIBUTION ANALYSIS FROM THE LABORATORY FOR ALL THE EXCTRACTION SITES*

Concessione Ministeriale nr. 8013, prove geotecniche (settore a), Circolare 7618/STC anno 2010
Sistema di gestione ISO 9001/2015 n. 9175.GEOL

Pag. 2 di 2
VERBALE ACCETTAZIONE NR: 38/13.05.2022

Geo-Labor s.a.s.
Via del Garda, 46L - tel. 0464913102
38068 - Rovereto (TN)

KORNGROSSENANALYSE (GEMÄß: UNI CEN ISO/TS 17892-4)
ANALISI GRANULOMETRICA (NORMA: UNI CEN ISO/TS 17892-4)

TABELLA RIASSUNTIVA

AUFTRAG./COMMIT.:	Ingenieure Patscheider & Partner GmbH
BEZUG/RIFERIMENTO:	Sig. Florian Lico
ORT/LOCALITA':	Ova dal Fuorn - Parco Nazionale Svizzero – Canton Grigione
PROJEKT/PROGETTO:	Masterarbeit F. Lico
BOHRUNG/SONDAGGIO:	09:54 - Retrieveo at the bank (right)
PROBE/CAMP.:	1 - 05.05.22
TIEFE/PROF. m:	Banco di ghiaia
BESCHREIBUNG/DESCRIZIONE:	ghiaia e ciottoli subarrotondati calcarei in matrice sabbiosa color grigio

SIEBUG/SETACCIATURA

Sieb / Setaccio	Durchmesser Diametro (mm)	Rückstand Trattenuto (g)	Rückstand Trattenuto (%)	Durchgang Passante (%)
3, 1/2"	90,000	1001,4	5,4	94,6
2, 1/2"	63,000	0,0	#N/D	#N/D
2, 1/4"	56,000	0,0	#N/D	#N/D
1, 3/4"	45,000	1864,7	15,4	84,6
1, 1/4"	31,500	4403,1	39,2	60,8
7/8"	22,400	2622,6	53,3	46,7
5/8"	16,000	2253,9	65,4	34,6
7/16"	11,200	1652,1	74,3	25,7
5/16"	8,000	1067,0	80,1	19,9
3,50	5,600	662,2	83,7	16,3
5	4,000	357,4	85,6	14,4
10	2,000	245,2	86,9	13,1
18	1,000	163,9	87,8	12,2
35	0,500	354,9	89,7	10,3
60	0,250	661,2	93,3	6,7
120	0,125	505,2	96,0	4,0
230	0,063	294,0	97,6	2,4
	< 0,063	453,0		2,4

Trockenmasse (g)		18561,7	Peso secco iniziale (g)	
Steine/Ciottoli	5,4	%	D10 mm =	0,460
Kies/Ghiaia	81,5	%	D30 mm =	14,000
Sand/Sabbia	10,7	%	D60 mm =	30,50
Schluff/Limo+Ton	2,4	%	Cu coeff.uniformità	66,3
			Cc coeff. curvatura	14,0

BESCHEINIGUNG/CERTIFICAZIONE NR.: 38/240
ANNAHMEDATUM/DATA ACCETTAZIONE: 13/05/2022
VERSUCH DATUM/DATA PROVA : 16/05/2022

SPERIMENTATORE
R. Mattozzi

DIRETTORE LABORATORIO
dr.F. Sforzs

Figure 85 Detailed grain size analysis from the laboratory for the location 1 from Ova dal Fuorn site 1

Concessione Ministeriale nr. 8013, prove geotecniche (settore a), Circolare 7618/STC anno 2010
Sistema di gestione ISO 9001/2015 n. 9175.GEOL

Pag. 2 di 2

VERBALE ACCETTAZIONE NR: 38/13.05.2022

Geo-Labor s.a.s.

Via del Garda, 46L - tel. 0464913102
38068 - Rovereto (TN)

KORNGROSSENANALYSE (GEMÄS: UNI CEN ISO/TS 17892-4)
ANALISI GRANULOMETRICA (NORMA: UNI CEN ISO/TS 17892-4)

TABELLA RIASSUNTIVA

AUFTRAG/COMMIT.:	Ingenieure Patscheider & Partner GmbH
BEZUG/RIFERIMENTO:	Sig. Florian Lico
ORT/LOCALITA':	Ova dal Fuorn - Parco Nazionale Svizzero – Canton Grigione
PROJEKT/PROGETTO:	Masterarbeit F.Lico
BOHRUNG/SONDAGGIO:	11:30 - Right Bank (Pol 6) F.L.
PROBE/CAMP.:	2 - 05.05.22
TIEFE/PROF. m:	Banco di ghiaia
BESCHREIBUNG/DESCRIZIONE:	ciottoli e ghiaia subarrotondata calcarea e rara sabbia color grigio

SIEBUG/SETACCIATURA

Sieb Setaccio	Durchmesser Diametro (mm)	Rückstand Trattenuto (g)	Rückstand Trattenuto (%)	Durchgang Passante (%)
3. 1/2"	90,000	0,0	0,0	100,0
	80,000	3039,2	10,7	88,3
2. 1/2"	63,000	12011,2	53,0	47,0
2. 1/4"	56,000	2312,2	61,2	38,8
1. 3/4"	45,000	2852,0	71,2	28,8
1.1/4"	31,500	4146,0	85,9	14,1
7/8"	22,400	1405,0	90,8	9,2
5/8"	16,000	822,6	93,7	6,3
7/16"	11,200	544,6	95,6	4,4
5/16"	8,000	295,0	96,7	3,3
3,50	5,600	245,1	97,5	2,5
5	4,000	183,8	98,2	1,8
10	2,000	219,7	99,0	1,0
18	1,000	68,4	99,2	0,8
35	0,500	14,1	99,3	0,7
60	0,250	25,3	99,3	0,7
120	0,125	45,0	99,5	0,5
230	0,063	54,0	99,7	0,3
	< 0.063	87,7		0,3

Trockenmasse (g)			28371,6	Peso secco iniziale (g)	
Steine/Ciottoli	53,0	%		D10 mm =	23,800
Kies/Ghiaia	45,9	%		D30 mm =	46,000
Sand/Sabbia	0,7	%		D60 mm =	67,00
Schluff/Limo+Ton	0,3	%		Cu coeff.uniformità	2,8
				Cc coeff. curvatura	1,3

BESCHEINIGUNG/CERTIFICAZIONE NR.: 38/241
ANNAHMEDATUM/DATA ACCETTAZIONE: 13/05/2022
VERSUCH DATUM/DATA PROVA : 16/05/2022

SPERIMENTATORE
R. Mamani

DIRETTORE LABORATORIO
dti F. Sharra

Mi1 0019

Figure 86. Grain size distribution analysis from the laboratory for Ova dal Fuorn site 2

Pag. 2 di 2

VERBALE ACCETTAZIONE NR: 38/13.05.2022

Geo-Labor s.a.s.

Via del Garda, 46L - tel. 0464913102
38068 - Rovereto (TN)

KORNGROSSENANALYSE (GEMÄS: UNI CEN ISO/TS 17892-4)
ANALISI GRANULOMETRICA (NORMA: UNI CEN ISO/TS 17892-4)

TABELLA RIASSUNTIVA

AUFTRAG./COMMIT.:	**Ingenieure Patscheider & Partner GmbH**
BEZUG/RIFERIMENTO:	Sig. Florian Lico
ORT/LOCALITA':	Ova dal Fuorn - Parco Nazionale Svizzero – Canton Grigione
PROJEKT/PROGETTO:	Masterarbeit F.Lico
BOHRUNG/SONDAGGIO:	Left Bank (Poligan 11) F.L.
PROBE/CAMP.:	**3 - 05.05.22**
TIEFE/PROF. m:	Banco di ghiaia
BESCHREIBUNG/DESCRIZIONE:	ghiaia e ciottoli subarrotondati calcarei in matrice sabbiosa color grigio

SIEBUG/SETACCIATURA

Sieb Setaccio	Durchmesser Diametro (mm)	Rückstand Trattenuto (g)	Rückstand Trattenuto (%)	Durchgang Passante (%)
3. 1/2"	90,000	2637,0	8,7	91,3
2. 1/2"	63,000	3510,3	20,3	79,7
2. 1/4"	56,000	1305,6	24,6	75,4
1. 3/4"	45,000	3003,0	34,5	65,5
1.1/4"	31,500	3928,0	47,5	52,5
7/8"	22,400	2862,0	56,9	43,1
5/8"	16,000	2429,6	64,9	35,1
7/16"	11,200	2176,0	72,1	27,9
5/16"	8,000	1643,0	77,5	22,5
3.50	5,600	1533,9	82,6	17,4
5	4,000	973,6	85,8	14,2
10	2,000	1302,8	90,1	9,9
18	1,000	1031,3	93,5	6,5
35	0,500	604,5	95,8	4,2
60	0,250	381,8	97,1	2,9
120	0,125	243,0	97,9	2,1
230	0,063	251,3	98,7	1,3
	< 0,063	393,5		1,3

Trockenmasse (g)		30300,0	Peso secco iniziale (g)	
Steine/Ciottoli	20,3	%	D10 mm =	2,000
Kies/Ghiaia	69,8	%	D30 mm =	12,600
Sand/Sabbia	8,6	%	D60 mm =	39,50
Schluff/Limo+Ton	1,3	%	Cu coeff. uniformità	19,8
			Cc coeff. curvatura	2,0

BESCHEINIGUNG/CERTIFICAZIONE NR.: 38/242
ANNAHMEDATUM/DATA ACCETTAZIONE: 13/05/2022
VERSUCH DATUM/DATA PROVA : 16/05/2022

SPERIMENTATORE   DIRETTORE LABORATORIO
                          dr./F. Slkma

Figure 87. Grain size distribution analysis from the laboratory
for Ova dal Fuorn site 3

Geo-Labor s.a.s.

Via del Garda, 46L - tel. 0464913102
38068 - Rovereto (TN)

KORNGROSSENANALYSE (GEMÄß: UNI CEN ISO/TS 17892-4)
ANALISI GRANULOMETRICA (NORMA: UNI CEN ISO/TS 17892-4)

TABELLA RIASSUNTIVA

AUFTRAG./COMMIT.:	**Ingenieure Patscheider & Partner GmbH**
BEZUG/RIFERIMENTO:	Sig. Florian Lico
ORT/LOCALITA':	Rio Carlino - Vallelunga Curon Venosta (BZ)
PROJEKT/PROGETTO:	Masterarbeit F. Lico
BOHRUNG/SONDAGGIO:	Karlin Bach F.L.
PROBE/CAMP.:	**1 - 06.05.22**
TIEFE/PROF. m:	Banco di ghiaia
BESCHREIBUNG/DESCRIZIONE:	ciottoli e ghiaia arrotondata metamorfica (gneiss) e rara sabbia color marrone

SIEBUG/SETACCIATURA

Sieb Setaccio	Durchmesser Diametro (mm)	Rückstand Trattenuto (g)	Rückstand Trattenuto (%)	Durchgang Passante (%)
	100,000	7030,2	34,6	65,4
3. 1/2"	90,000	2419,0	46,5	53,5
2. 1/2"	63,000	3834,7	65,3	34,7
2. 1/4"	56,000	1671,2	73,6	26,4
1. 3/4"	45,000	817,5	77,6	22,4
1.1/4"	31,500	1722,4	86,0	14,0
7/8"	22,400	628,2	89,1	10,9
5/8"	16,000	431,0	91,3	8,7
7/16"	11,200	420,5	93,3	6,7
5/16"	8,000	251,1	94,6	5,4
3,50	5,600	160,6	95,3	4,7
5	4,000	136,0	96,0	4,0
10	2,000	189,2	96,9	3,1
18	1,000	161,7	97,7	2,3
35	0,500	140,9	98,4	1,6
60	0,250	138,1	99,1	0,9
120	0,125	97,2	99,6	0,4
230	0,063	39,6	99,8	0,2
	< 0.063	44,0		0,2

Trockenmasse (g)		20333,2	Peso secco iniziale (g)	
Steine/Ciottoli	65,3	%	D10 mm =	19,500
Kies/Ghiaia	31,6	%	D30 mm =	59,500
Sand/Sabbia	2,8	%	D60 mm =	96,50
Schluff/Limo+Ton	0,2	%	Cu coeff.uniformità	4,9
			Cc coeff. curvatura	1,9

BESCHEINIGUNG/CERTIFICAZIONE NR.:	38/243
ANNAHMEDATUM/DATA ACCETTAZIONE:	13/05/2022
VERSUCH DATUM/DATA PROVA :	16/05/2022

SPERIMENTATORE
R. Mattozzi

DIRETTORE LABORATORIO
dr.H. Stairs

Mod. 8.5.4.0

Figure 88. Laboratory grain size distribution analysis for
Rio Carlino site 1

Concessione Ministeriale nr. 8013, prove geotecniche (settore a), Circolare 7618/STC anno 2010
Sistema di gestione ISO 9001/2015 n. 9175.GEOL.

VERBALE ACCETTAZIONE NR: 38/13.05.2022

Geo-Labor s.a.s.

Via del Garda, 46L - tel. 0464913102
38068 - Rovereto (TN)

KORNGROSSENANALYSE (GEMÄ4: UNI CEN ISO/TS 17892-4)
ANALISI GRANULOMETRICA (NORMA: UNI CEN ISO/TS 17892-4)

TABELLA RIASSUNTIVA

AUFTRAG./COMMIT.:	**Ingenieure Patscheider & Partner GmbH**
BEZUG/RIFERIMENTO:	Sig. Florian Lico
ORT/LOCALITA':	Rio Carlino - Vallelunga Curon Venosta (BZ)
PROJEKT/PROGETTO:	Masterarbeit F. Lico
BOHRUNG/SONDAGGIO:	Karlin Bach F.L.
PROBE/CAMP.:	**2 - 06.05.22**
TIEFE/PROF. m:	Banco di ghiaia
BESCHREIBUNG/DESCRIZIONE:	ciottoli e ghiaia arrotondata metamorfica (gneiss) e rara sabbia color marrone

SIEBUG/SETACCIATURA

Sieb Setaccio	Durchmesser Diametro (mm)	Rückstand Trattenuto (g)	Rückstand Trattenuto (%)	Durchgang Passante (%)
	200,000	4164,0	21,3	78,7
	150,000	3160,8	37,5	62,5
	100,000	4821,0	62,6	37,4
3. 1/2"	90,000	1677,6	71,2	28,8
2. 1/2"	63,000	787,8	75,2	24,8
2. 1/4"	56,000	733,0	79,0	21,0
1. 3/4"	45,000	1672,5	87,5	12,5
1.1/4"	31,500	864,7	92,0	8,0
7/8"	22,400	508,7	94,6	5,4
5/8"	16,000	342,0	96,4	3,6
7/16"	11,200	256,1	97,7	2,3
5/16"	8,000	139,3	98,4	1,6
3,50	5,600	71,4	98,8	1,2
5	4,000	55,1	99,0	1,0
10	2,000	53,9	99,3	0,7
18	1,000	30,9	99,5	0,5
35	0,500	22,8	99,6	0,4
60	0,250	26,2	99,7	0,3
120	0,125	31,9	99,9	0,1
230	0,063	13,5	99,9	0,1
	< 0,063	10,1		0,1

Trockenmasse (g)		19583,1	Peso secco iniziale (g)	
Steine/Ciottoli	75,2	%	D10 mm =	36,500
Kies/Ghiaia	24,1	%	D30 mm =	90,500
Sand/Sabbia	0,6	%	D60 mm =	155,00
Schluff&Limo+Ton	0,1	%	Cu coeff.uniformità	4,2
			Cc coeff. curvatura	1,4

BESCHEINIGUNG/CERTIFICAZIONE NR.:	38/244
ANNAHMEDATUM/DATA ACCETTAZIONE:	13/05/2022
VERSUCH DATUM/DATA PROVA :	16/05/2022

SPERIMENTATORE
R. Martucci

DIRETTORE LABORATORIO
dr.F. Sforza

Mod. P.6.1.0

Figure 89. laboratory grain size distribution analysis for the Rio Carlino site 2